Spring 2019

Gypsum Karst Speleogenesis in Barber County, Kansas of the Permian Blaine Formation

Kaitlyn Gauvey
Fort Hays State University, kaitlyngauvey@gmail.com

GYPSUM KARST SPELEOGENESIS IN BARBER COUNTY, KANSAS

OF THE PERMIAN BLAINE FORMATION

being

A Thesis Presented to the Graduate Faculty

of Fort Hays State University

in Partial Fulfillment of the Requirements for

the Degree of Master of Science

by

Kaitlyn L. Gauvey

B.S., Sam Houston State University

Date 5/26/2019

Approved
Major Professor

Approved
Dean of the Graduate School

This thesis for

the Master of Science Degree

By

Kaitlyn L. Gauvey

has been approved

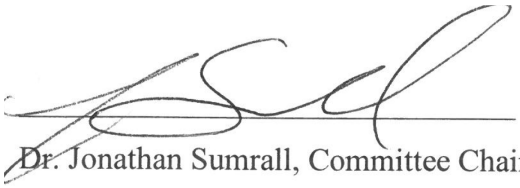

Dr. Jonathan Sumrall, Committee Chair

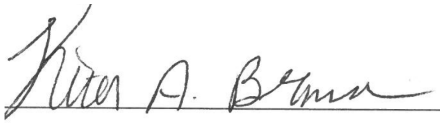

Dr. Keith Bremer, Committee Member

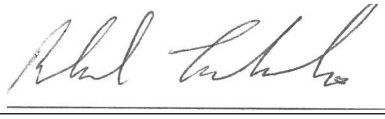

Dr. Richard Lisichenko, Committee Member

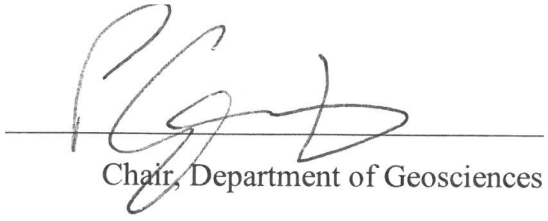

Chair, Department of Geosciences

ABSTRACT

Field reconnaissance examining the Permian Blaine Formation and the karst features within those rocks were conducted on two ranches in Barber County, Kansas. Karst features are developed dominantly in gypsum and include caves, sinkholes, losing streams, springs, and other surficial karst features. The Blaine Formation is known as a significant karst unit and major aquifer system in Oklahoma; however, little work has been conducted in Kansas. This study identifies the processes that lead to karst development in the Blaine Formation in Kansas and represents the first stage of a karst study to develop predictive karst models. This survey of caves and karst landforms adds significantly to the basic knowledge of the geology of this region. Known cave locations, provided by landowners, were used to determine particular areas to investigate. The location of each cave and karst feature was documented by a handheld GPS unit. When possible, each cave documented in this study was surveyed using standard cave survey techniques: compass, inclinometer, and tape (Dasher, 1994). The survey data and sketch produced for each surveyed cave were used to create a map using a computer graphics program. Field observations indicate cave formation is dependent on (1) the geologic contact between the Permian Medicine Lodge Gypsum and the underlying Flowerpot Shale, (2) the amount and type of surficial mantle material, and (3) fractures in the bedrock for subsurface flow. Future studies are necessary to develop karst management systems.

ACKNOWLEDGMENTS

I would like to express my very great appreciation to my Advisor, Dr. Jonathan Sumrall, for your guidance and commitment to your students. I owe all of my success to you. You have taught me so many valuable lessons in life and science. I hope to be as great of an educator as you have been to me. Thank you for dedicating every weekend to look for new caves. I look forward to future projects with you. I would also like to thank Dr. Jeanne Sumrall for her support both personally and professionally. All of my achievements would not have been possible without her support

My grateful thanks are also extended to Dr. Keith Bremer for his willingness to give his time and knowledge so generously. I appreciate his invaluable advice, encouragement, patience, and support in my academic journey and in developing my professional skills. To Dr. Richard Lisichenko, thank you for providing valuable insight and expertise in GIS. Thank you for your kind support and GIS wizardry.

I wish to acknowledge the help provided by Dr. James Murowchick from the University of Missouri-Kansas City for analyzing samples used in this study. I would also like to thank the property owners, Mr. and Mrs. Hinz, and Ted and Brian Alexander, for their assistance and allowing my research team to wander eleven thousand acres. I am particularly grateful for the assistance given by Mr. Alexander, without his guidance Garys' vehicle would have remained in a pasture.

I would like to offer my special thanks to, Jonathan Camelo and Gary Kelner. This research would not have been completed without your search efforts and collection of my data.

TABLE OF CONTENTS

Page

LIST OF TABLES

LIST OF FIGURES

LIST OF APPENDICES

CHAPTER I

INTRODUCTION

The objective of this study is to locate and document karst features in Barber County, Kansas to further understand the mechanics of karst formation within the Permian Blaine Formation. The Kansas Geological Survey lists the southcentral region of Kansas, containing over two-hundred caves, yet there has been no documented karst studies in southcentral Kansas (Young & Beard, 1993). This survey of caves and karst landforms adds significantly to the basic knowledge of the geology of this region. The primary method of data collection for this study was field reconnaissance to locate caves and physical survey to document the size and shape of each cave. *Google Earth* was used to determine possible karst landforms such as sinkholes, springs, and cave entrances. Known cave locations, provided by land owners, were used to determine particular areas to investigate. The location of each cave and karst feature was documented by a handheld GPS unit. When possible, each cave documented in this study was surveyed using standard cave survey techniques: compass, inclinometer, and tape (Dasher, 1994). The survey data and sketch produced for each surveyed cave were used to create a map using a computer graphics program.

CHAPTER II

DESCRIPTION OF STUDY AREA

2.1 Geographic Setting

Southcentral Kansas is dominated by red soil, red cedar trees, canyons, buttes, and mesas. The buttes are capped by pale blue-gray gypsum, and their slopes consist of highly friable red mudstone and fine red sandstone (Benison et al., 2015). The evaporites and associated red beds create a topography that does not fit the conventional portrayal of the Great Plains landscape of Kansas. This physiographic region, called the Gypsum Hills, is located in Clark, Comanche, Barber, and Harper counties of Kansas due to the vast deposits of gypsum. The National Gypsum Mine in Barber County mines the Medicine Lodge Gypsum Member of the Permian Blaine Formation (Benison et al., 2015). The Gypsum Hills are also referred to as the Red Hills due to the sparsely vegetated, iron-oxide rich soil, and the land in this region is mostly utilized as open rangeland (Kansas Geological Survey, 1997).

The Gypsum Hills are dominated by evaporite sedimentary deposits. Evaporite sedimentary deposits form by the precipitation of salts through the evaporation of water. Primary evaporate minerals include gypsum, anhydrite, and halite. Gypsum deposits underlie approximately 35-40% of the conterminous United States (Johnson, 1992). The midcontinent region of the United States is mostly composed of Mid-Permian red beds and evaporates as subsurface and surface deposits (Figure 1; Walker, 1967).

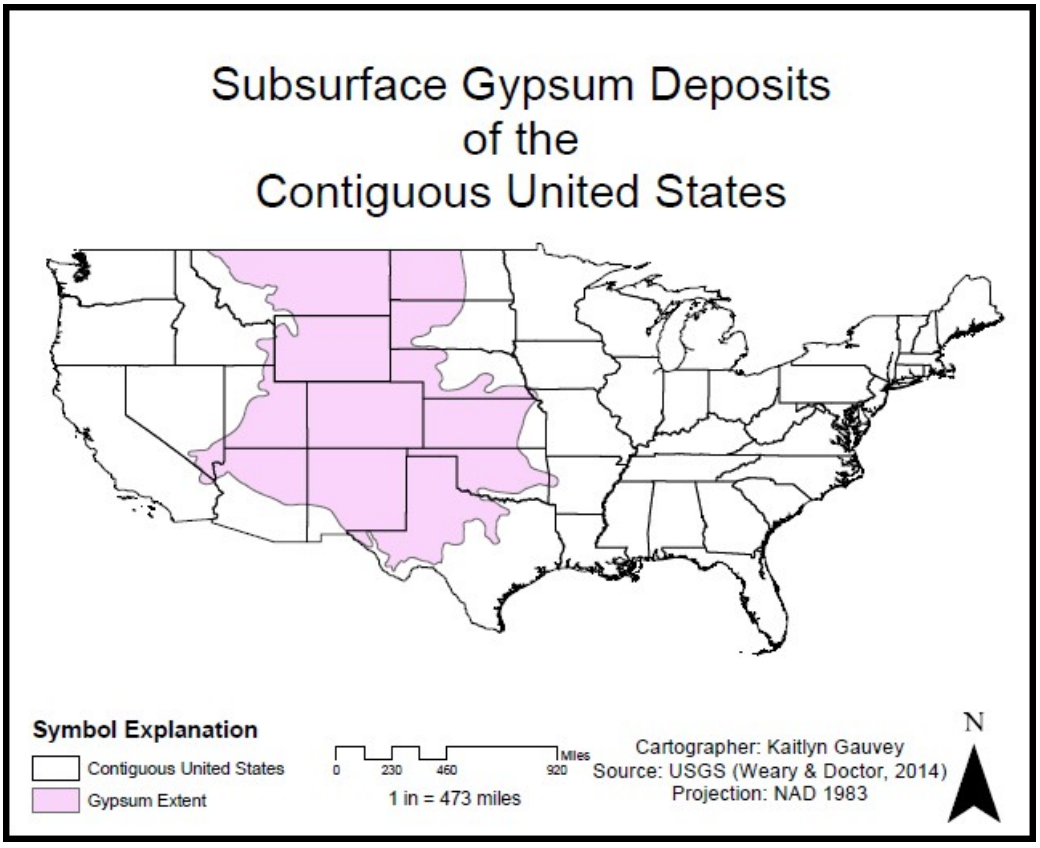

Figure 1. Subsurface gypsum deposit distribution within the United States (modified from Weary & Doctor, 2014)

2.2 Geologic Setting

Permian-aged red beds and evaporites are extensive across the midcontinent of North America, and include the Nippewalla, Quartermaster, Opeche, Chugwater, Spearfish, and Goose Egg strata (Tomlinson, 1916; Mudge, 1967; Walker, 1967; Holdoway, 1978; Turner, 1980; Glennie, 1987; Nance, 1988; Golonka & Ford, 2000; Benison & Goldstein, 2000, 2001; Zharkov & Chuakov, 2001; Roscher & Schneider, 2006; Benison et al., 2015). These sediments were deposited in the Permian Basin, which extends from west Texas and southeast New Mexico into western Oklahoma, western

Kansas, and southeastern Colorado (Figure 2). Many of these basins contain significant subsurface gypsum deposits (Figure 1).

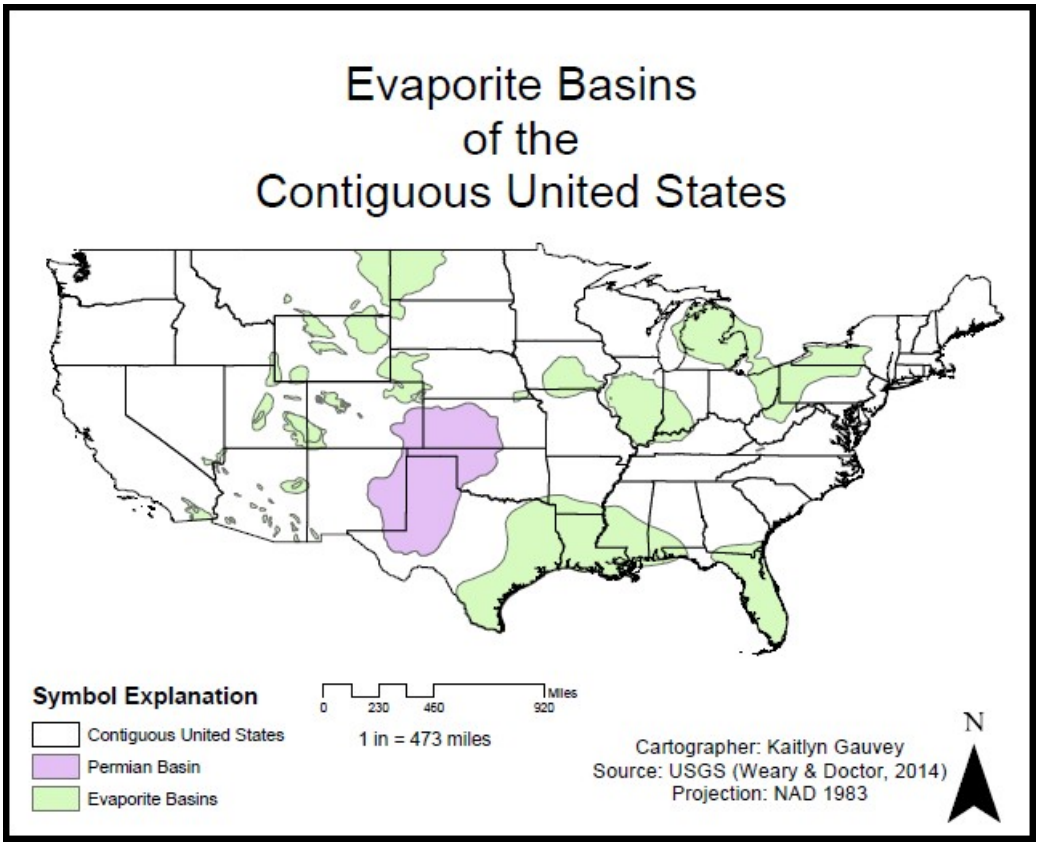

Figure 2. Evaporite Basins of the Contiguous United States (modified from Weary and Doctor 2014).

The mid-Permian Nippewalla Group in Kansas was deposited in a series of basins bounded by the Las Animas Arch to the west and the Nemaha Anticline to the east (Merriam, 1962b; Maughan, 1966; Mudge, 1967; Holdoway, 1978; Figure 3). The Nippewalla Group consists of alternating bedded evaporites (mostly gypsum and occasionally anhydrite), red bed mudstones, siltstones, and sandstones in outcrop. Much

of the Nippewalla Group is found in the subsurface and reaches thicknesses greater than 492 feet (150 m) (Merriam, 1963).

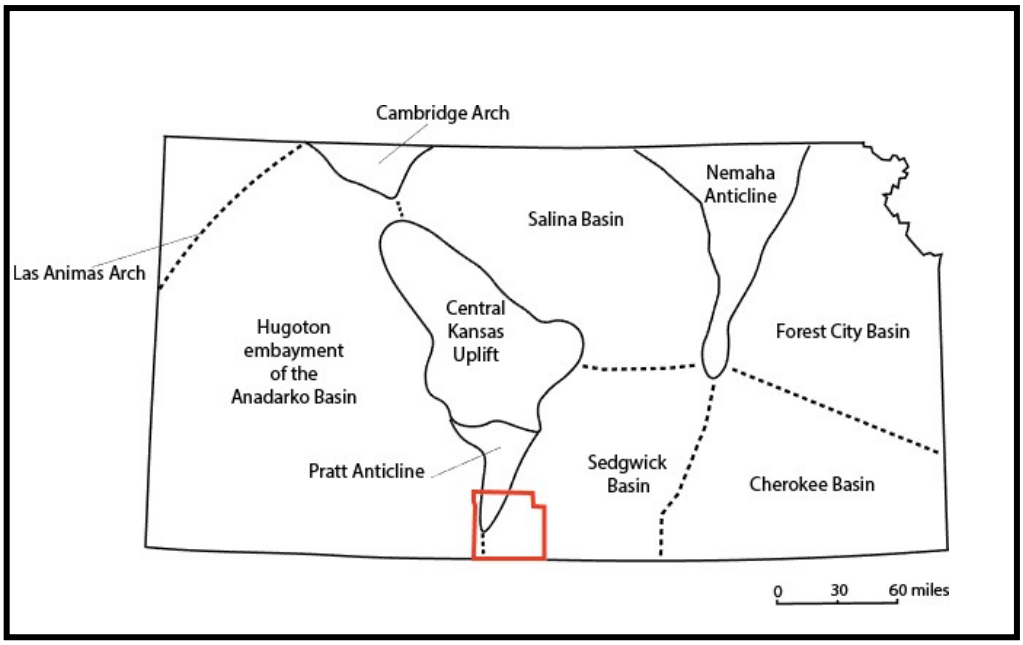

Figure 3. Major structural features of Kansas (modified from Lee and Merriam, 1954b).

Surficial outcrops in southcentral Kansas and northwestern Oklahoma are thinner due to salt (halite) dissolution (Benison & Goldstein, 2001; Benison et al., 2015). In southcentral Kansas, the beds are exposed where they strike approximately north and dip gently westward (Merriam, 1963). The Nippewalla Group is separated into six formations, listed in ascending order: Harper Sandstone, Salt Plain Formation, Flowerpot Shale, Blaine Formation, and Dog Creek Formation (Baars, 1990; Rascoe & Baars, 1972; Figure 4).

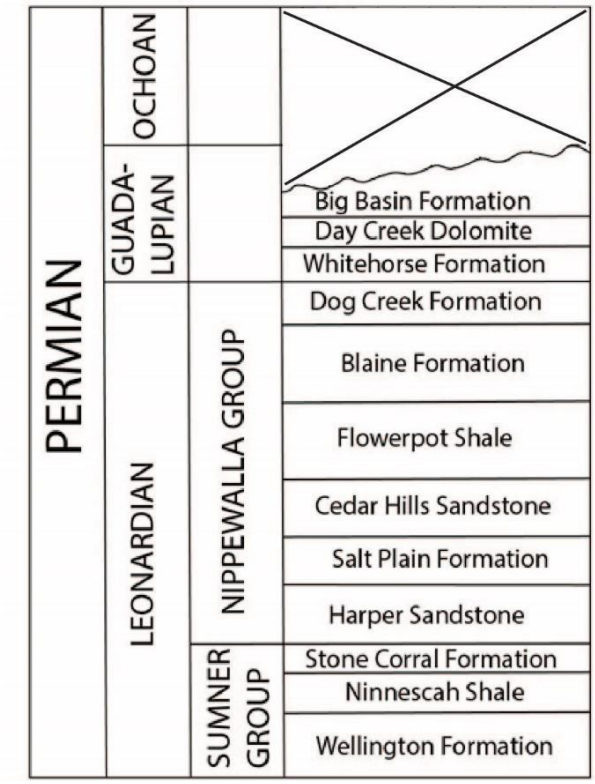

Figure 4. The stratigraphic position of the Permian Nippewalla Group in Kansas and northern Oklahoma (modified from Baars, 1990 and Rascoe & Baars, 1972).

Surficial outcrops of the Nippewalla that have been weathered, make correlation of core with outcrops by lithological association and/or thickness problematic (Benison et al., 2015). Surface outcrops of the Nippewalla Group in southcentral Kansas total 932 feet (284 m) thick; however, the six formations are very similar in lithology, and thickness estimates in the field area are controversial due to erosion and dissolution (Holdoway, 1978; Benison 1997a, 1997b; Benison et al., 2015; Figure 5).

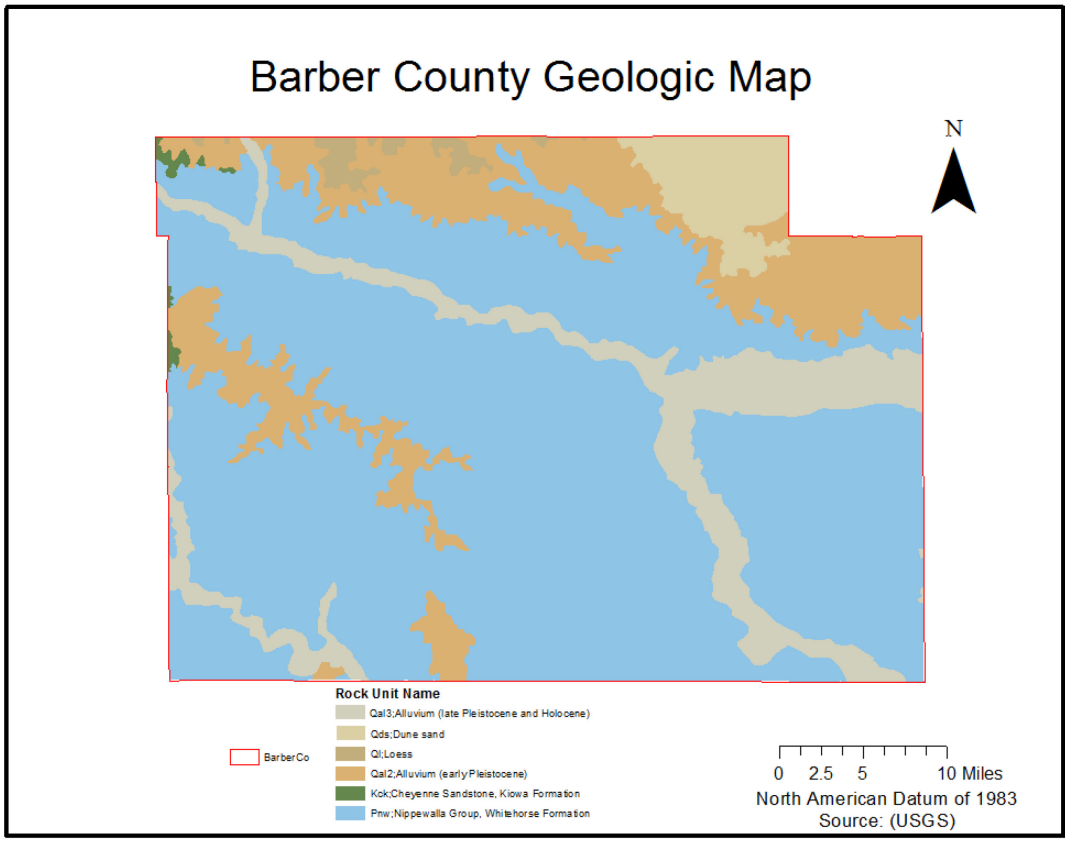

Figure 5. Surficial outcrop by lithology in Barber County, Kansas (modified from Weary & Doctor, 2014).

2.2.1 Permian Geology of Barber County, Kansas

The red bed–evaporite sequences in the Permian Nippewalla Group were classified in 1896 and further refined into individual units in 1939 due to the exploration of oil and gas (Cragin, 1896; Norton, 1939). The subsurface stratigraphy, regional stratigraphic correlations, and lithofacies maps of the Permian evaporites of the midcontinent region of the United States were studied by Merriam (1958b), Malone (1962), Campbell (1963), Schumaker (1966), Rascoe (1968), Rascoe and Baars (1972), and for the entire United States by McKee et al. (1967a; 1967b).

Further outcrop and subsurface studies on the Blaine Formation in Kansas and Oklahoma include: Kulstad et al. (1956), Ham (1960), Fay, (1964), and Johnson (1967). Equivalent-aged rock units to the Nippewalla Group of Kansas, Oklahoma, and the Texas Panhandle were described by Jordan and Vosburg (1963). Petrography of the sediments of the Nippewalla Group in southcentral Kansas was described by Swineford (1955). The Permian Strata in Barber County Kansas includes: the Sumner Group, Nippewalla Group, Whitehorse Formation, Day Creek Dolomite, and Big Basin Formation (Figure 4).

Whitehorse Formation

Gould (1905) characterized the Whitehorse Formation consisting of 270 feet (~82 m) of red friable sandstone, siltstone and shale, with minor dolostone. Outcrops are present in Barber, Kiowa, Comanche, and Clark counties. The formation overlies the Dog Creek Shale and underlies the Day Creek Dolomite. In Kansas, the formation is subdivided into four members: the Marlow Sandstone, the Relay Creek Dolomite, the Unnamed Member, and Kiger Shale Member (Norton, 1939).

Sawyer (1924) categorized the Marlow Sandstone and included beds between the Dog Creek Shale and Relay Creek Member. The Marlow Sandstone is approximately 110 feet (~33 m) thick and consists predominately of red, friable, massive, very fine-grained sandstone that is cross-bedded with large irregular areas of white to buff sandstone. The Relay Creek Dolomite was described by Evans (1931) as two beds of dolomite one-foot thick separated by 21 feet (6 m) of white to red fine-grained sandstone. In some areas, only one dolomite bed is present; in northern exposures, no dolomite beds are found. The

Even-Bedded Member contains approximately 100 feet (~30 m) of red, fine-grained, cross-bedded sandstones and siltstones with occasional red-brown shales. The Kiger Shale Member contains 38 feet (~11 m) of red-brown shale with minor beds of silty-shale, siltstone, and very fine-grained sandstone. Thin dolomite beds mark the base, and the top consists of green to gray argillaceous (muddy) sandstone.

Nippewalla Group

The Nippewalla Group consists mostly of red beds that were deposited on a broad, flat, arid alluvial-eolian plain bordering a shallow inland sea (Hills, 1942; Swineford, 1955). The group is primarily composed of siltstones and very fine-grained sandstones, with minor amounts of silty shale and gypsum. The Nippewalla Group is divided into six formations: Harper Sandstone, Salt Plain Formation, Cedar Hills Sandstone, Flowerpot Shale, Blaine Formation, and Dog Creek Shale.

Cragin (1896) describes the base of the Nippewalla Group as the Harper Sandstone. The Harper Sandstone ranges in thickness from 180–220 feet (54–67 m) of brown-red, argillaceous siltstones and silty shales. Cragin (1896) describes the Salt Plain Formation (above Harper Sandstone) as red-brown flaky siltstones, thin sandy siltstones, and very fine-grained sandstones that comprises a total thickness of about 265 feet (~80 m) (Moore et al., 1951). The Cedar Hills Sandstone (above the Salt Plain Formation) includes approximately 180 feet (~55 m) of brown-red, massive, very fine-grained sandstones and sandy siltstones separated by beds of argillaceous siltstone and silty shale. The top sandstone contains many white to pink “snowballs” of granular gypsum (Moore

et al., 1951). The Flowerpot Shale (above the Cedar Hills Sandstone) consists of about 180 feet of red-brown gypsiferous shale and thin layers of green-gray silty shale, gypsum, and dolomite. Eroded slopes commonly include selenite gypsum and satin gypsum spar crystals. Outcrops of the Flowerpot Shale are restricted to Barber County and the eastern part of Comanche County (Moore et al., 1951).

The Blaine Formation (above the Flowerpot Shale) consists of about 50 feet of massive gypsum, thin dolomite, and brown-red shale. The Blaine Formation is exposed in Barber, Comanche, and Kiowa counties and is divided into four members: Haskew Gypsum, Shimer Gypsum, Nescatunga Gypsum, and the Medicine Lodge Gypsum (Norton, 1939; Figure 6). The Blaine Formation is one of the most extensive and easily traced formations of the Permian red beds, reaching from Kansas across western Oklahoma and into Texas.

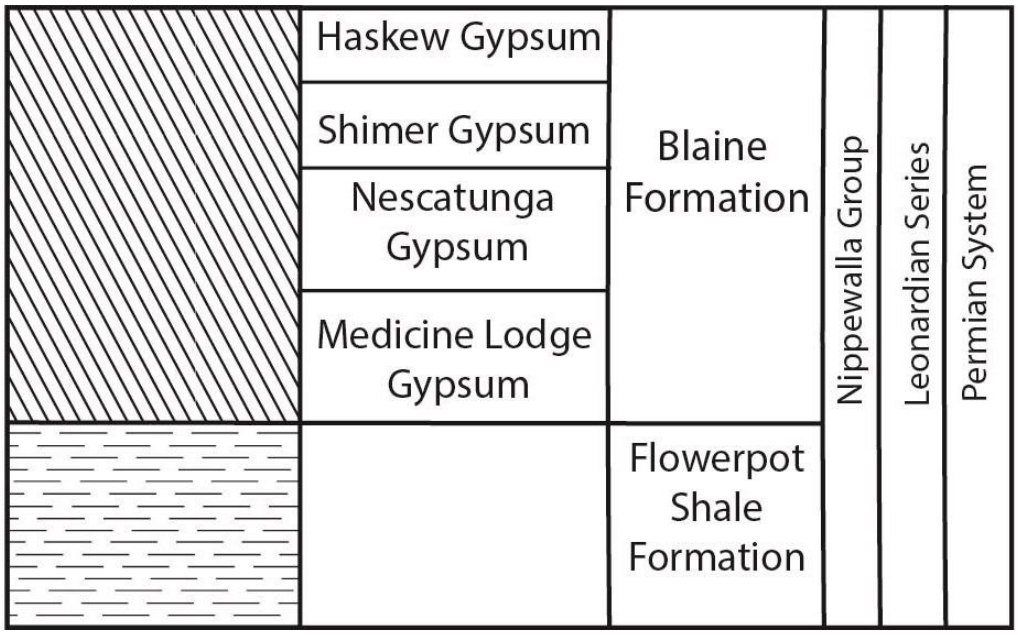

Figure 6. Stratigraphic position of the Blaine Formation and the four gypsum subdivisions (modified from Norton 1939).

The upper member of the Blaine Formation, the Haskew Gypsum, consists of less than one foot of gypsum underlain by about five feet of brown-red shale. The Haskew Gypsum has been removed by dissolution in many places, particularly north of the Kansas–Oklahoma line (Moore et al., 1951). The Shimer Gypsum underlies the Haskew member. This member consists of 13–23 feet (~4–7 m) beds of massive gypsum overlying approximately one foot of dolomite. Much of the Shimer Gypsum has been removed by solution (Moore et al., 1951). The Nescatunga Gypsum includes about eight feet (~2 m) of red shale overlying five feet (1.5 m) of gypsum, and eight feet (~ 2 m) of red shale underlying the gypsum. The Nescatunga and Shimer Gypsum beds pinch out in Comanche County and are not present in Barber County (Moore et al., 1951).The lowermost member of the Blaine Formation is the Medicine Lodge Gypsum. The

Medicine Lodge Gypsum is the thickest bed of gypsum in Kansas, measuring up to more than 30 feet (~9 m) (Moore et al., 1951). The Medicine Lodge Gypsum grades into a foot of oolitic/pellitic dolomite called the Cedar Springs Dolomite (Fay, 1964). Fay (1964) describes the gradational change of dolomite into the massive gypsum. Swineford (1955) reports anhydrite lenses measuring up to 12 inches thick at the base of the Medicine Lodge Gypsum (Swineford, 1955).

The Dog Creek Shale is commonly grouped with the Blaine Formation, as it lies between the uppermost gypsum of the Blaine and the base of the Whitehorse Sandstone. The thickness of the Dog Creek Shale is variable and is reported to range from 14 to 53 feet (Moore et al., 1951). The Dog Creek Shale consists of thin beds of dark-red silty shale, brown-red and green-gray siltstone, and very fine-grained sandstone, dolomite, dolomitic and gypsiferous sandstone, and gypsum (Swineford, 1955).

2.2.2 Depositional Environments of the Permian Geology of Kansas

Permian red beds and evaporites were deposited in extensive shallow brackish-saline inland seas that extended north and northeast of the marine carbonate platform that bordered the Midland Basin (located in western Texas) (Johnson, 1981, 1990b). These inland seas were subject to periodic influxes of marine water from the south (Hills, 1942). Evaporites were precipitated as layers or grew as coalescing crystals and nodules within the mud at the depositional surface as seawater evaporated from the basins (Johnson, 1992). Thick red bed shales, siltstones, and sandstones were deposited around the perimeter of the evaporative basin, and some of these also extended as blanket deposits across the basin (Johnson, 1992).

The Permian Salt Basin refers to sediments that were deposited throughout the region in southwestern Nebraska, western Kansas, western Oklahoma, western Texas, eastern Colorado, and eastern New Mexico (Bachman & Johnson, 1973). The seas were restricted by the Front Range to the west, a low-lying landmass was located to the north and northeast in Nebraska, the Ozark Mountains and Arbuckle Mountains to the east, and Wichita Mountains to the south (Mudge, 1967; Johnson, 1992; Figure 7). Erosion of the Arbuckle Mountains and Wichita Mountains delivered course-grained clastic sediment from the east and south (Swineford, 1955; Mudge, 1967). The Ozark Mountains and low-lying landmass in Nebraska delivered fine-grained clastic sediment from the north (Swineford, 1955; Mudge, 1967). Further restriction of the sea resulted in the deposition of halite (McKee et al., 1967a). In Kansas, the Nippewalla Group evaporites were deposited in the Hugoton Embayment of the Anadarko Basin (Hills, 1942; Maher & Collins, 1948; Figure 3).

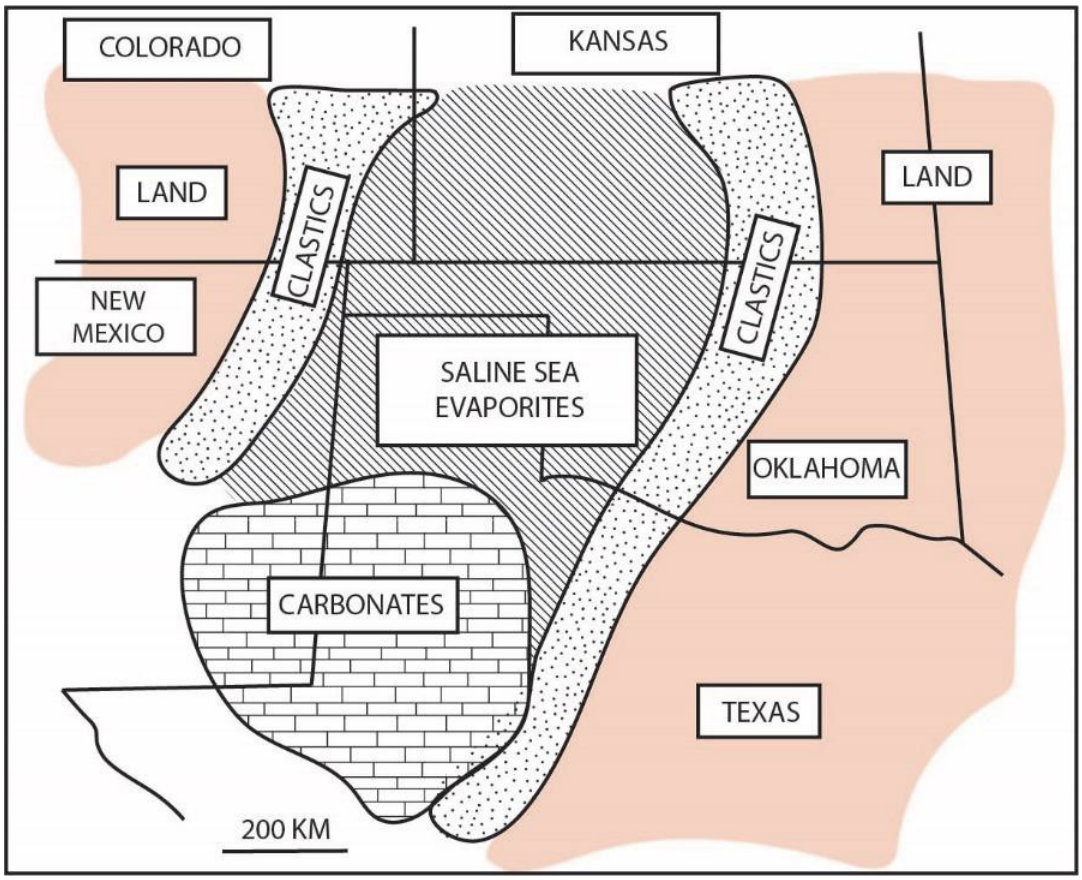

Figure 7. Permian paleogeography and principal facies during deposition of Blaine Formation evaporites in southwestern United States (modified from Johnson, 1981).

Southcentral Kansas was situated between 0°S and 5°S latitude during the mid-Permian (Golonka et al., 1994). The depositional environment of the Nippewalla Group was a series of extremely saline ephemeral lakes, mudflats, sandflats, paleosols, and eolian dunes (Benison et al., 1998, 2013; Benison & Goldstein, 2001; Sweet et al., 2013; Foster et al., 2014). The most direct chronological analysis by magnetostratigraphy of the Nippewalla Group suggests deposition during the Leonardian and Guadalupian (276-267 Ma) (Foster et al., 2014).

In central Oklahoma, the Blaine Formation contains bivalve-rich dolomite beds; however, in Kansas, the only carbonates reported are dolomitized mudstones or *Microcodium*-rich calcretes (Fay, 1964; Benison et al., 2001). Fay (1964) indicates one ft (0.30 m) of light gray oolitic/pelletic dolomite bed at the base of the Medicine Lodge Gypsum. Benison et al. (2001) does not identify an oolitic/pelletic dolomudstone, but a *Microcodium*-rich calcrete located in the red siliciclastics that does not contain dolomite. This *Microcodium*-rich calcrete suggests a pedogenic origin, or carbonate paleosol.

2.2.3 Structural and Diagenetic History of Permian Geology of Kansas

Barber County lies on the southern extent of the Pratt Anticline (Figure 3). The Pratt Anticline is a post-Mississippian extension of the Central Kansas Uplift and separates the Hugoton Embayment from the Sedgwick Basin (Strong, 1960; Merriam, 1962b). Cretaceous-aged strata unconformably overlie Permian-aged strata due to the post-Mississippian uplift and subsequent erosion of Triassic and Jurassic-aged strata during the Cretaceous (Western Interior Seaway) (McLaughlin, 1942; Merriam, 1955; Merriam, 1957). Quaternary glacial deposits unconformably overlie Cretaceous-aged

strata. Post-Pleistocene glacial and associated fluvial deposits mark a stark change in climate (Norton, 1939)

In the subsurface, the Nippewalla Group contains massively bedded and displacive halite, whereas surficial outcrops of the Permian Nippewalla Group have undergone late-stage dissolution of halite cement (Benison et al., 2015). Gypsum/anhydrite caprocks and slope forming siliciclastics are clues to past halite cement in the siliciclastics (Benison et al., 2015). Surface section measurements in central Kansas reveal depositional and early diagenetic halite such as pseudomorphs after displacive and chevron halite (Benison et al., 2015). Collapse structures in southcentral Kansas are evidence of dissolution of bedded halite close to the surface (Benison et al., 2015).

2.2.4 Other Permian Evaporites

Evaporite deposits corresponding in age to those of the Nippewalla Group in Kansas occur in Nebraska, Wyoming, and as far south as Oklahoma and Texas (Holdoway, 1978). Previous investigations postulate that basins in Nebraska and Wyoming were connected to the west and the basins in Oklahoma and Texas were connected to the south (Hills, 1942; Maughan, 1966). Kansas was connected to the inland sea by the Hugoton Embayment and the Anadarko Basin (Hills, 1942; Malone, 1962; Campbell, 1963; Schumaker, 1966). Quinlan et al. (1986) provides an overview of studies that include evaporite karst features in western Oklahoma and adjacent Texas (Jordan & Vosburg 1963; McGregor et al. 1963; Myers et al. 1969; Johnson 1972, 1981,

1986, 1990a, 1990b; Gustavson et al. 1980; Bozeman, 1987; Runkle & Johnson 1988; Hovorka & Granger 1988).

CHAPTER III

LITERATURE REVIEW

3.1 Karst Processes

Karst is defined as a terrain with distinctive hydrology and landforms that arise from a combination of high rock solubility and well-developed secondary porosity (Ford & Williams, 1989). Karst topography is defined as landscapes with closed depressions, integrated underground drainage with disappearing surface streams, and caves (White, 1988). Karst hydrology often does not reflect surface topography, as karst extends below the subsurface as a highly modifiable recharge system. Karst topography can develop on carbonates, evaporites, and silicate rocks, when dissolution rates are high enough. Chemical dissolution, rather than mechanical erosion, is the dominant process in karst regions.

Limestone Dissolution

Limestone is the dominant rock type that form karst features by dissolution. Limestone dissolution occurs by the reaction of carbonic acid with bedrock. Carbonic acid reacts with carbonate minerals to form bicarbonate ions and hydrogen ions that dissolve limestone. The reaction rate of carbonic acid dissolution is dependent on temperature and pressure. Carbonates (calcite) will readily dissolve at colder temperatures due to an increase in aqueous carbon dioxide in solution (Figure 8). This differs from simple ionic dissolution (i.e. salt dissociation in water) where the solubility rate generally increases with temperature (i.e. gypsum) (Figure 8).

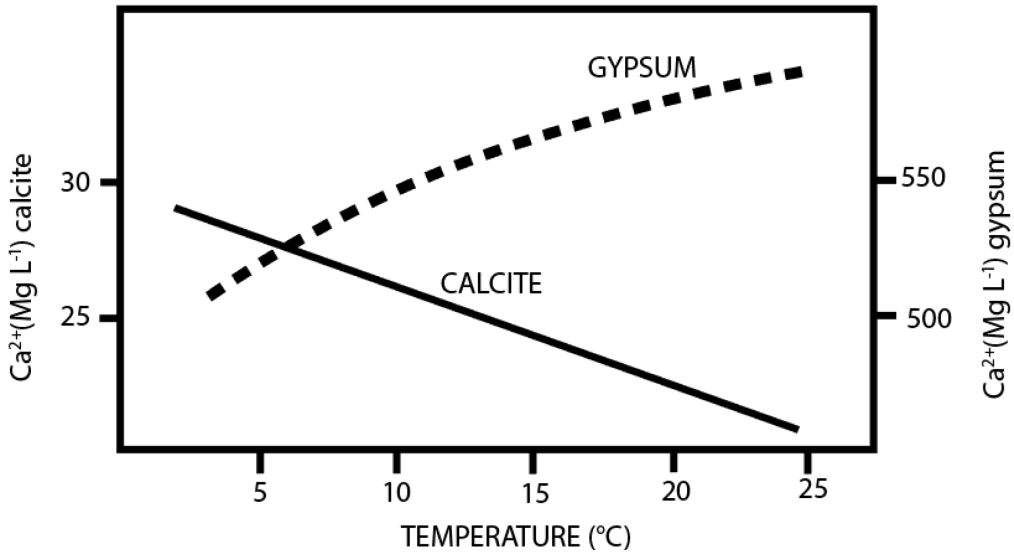

Figure 8. The solubility of calcite and gypsum in water and the standard atmosphere between 2 ºC and 25 ºC. Modified from Ford & Williams (1989).

Limestone Caves

Limestone is the most common lithology for caves and is dominantly composed of the mineral calcite ($CaCO_3$) (Palmer, 1991). Metamorphosed carbonates (e.g. marble) or magnesium-rich carbonates (dolostone) are composed of calcium and magnesium. These rocks are dissolved by carbonic acid dissolution and are grouped as carbonate caves.

Cave formation is typically dependent on mechanical weaknesses (faults or joints) or heterogeneities (bedding planes) to allow an undersaturated water to dissolve rock (Palmer, 1991). Rocks with high solubility and well-developed secondary (fracture) porosity preferentially form caves (Ford & Williams, 1989). Caves will not readily form in soluble rock without a primary or secondary porosity to form a connection through pore spaces for dissolution.

Primary porosity is the porosity developed during a rocks formation. Limestone with a low primary porosity and permeability will not allow fluid to migrate through pore spaces. Secondary porosity is any pore space in a rock that occurs after lithification. Secondary porosity includes joints, faults, and any chemical alteration that produces pore space. Cave development is controlled by the structure and lithology of the host rock. The best developed caves form in a pure, dense, massive, coarsely fractured rock, whereas, poorly developed karst will form in soluble rocks with negligible primary porosity (Ford & Williams, 1989).

Evaporite Dissolution

Evaporite rocks include rock salt, rock gypsum, and rock anhydrite. The most common rock salt types are sodium chloride (NaCl, the mineral halite) and potassium chloride (KCl, the mineral sylvite). Gypsum ($CaSO_4 \bullet 2H_2O$) and anhydrite ($CaSO_4$) are chemically true salts but are not grouped with rock salt; instead they are termed "rock gypsum" and "rock anhydrite" to differentiate them from mineral deposits. Salt dissolves in water by simple ionic dissociation resulting in two charged ions (Na^+ and Cl^-) in solution. Gypsum and anhydrite dissolve in a similar fashion, but they dissolve more slowly, in smaller amounts, and are highly temperature dependent (Equation 1):

Gypsum: $CaSO_4 \bullet 2H_2O \rightleftharpoons Ca^{2+} + SO_4^{2-} + 2H_2O$ (Equation 1)

Anhydrite: $CaSO_4 \rightleftharpoons Ca^{2+} + SO_4^{2-}$ (Equation 2)

Gypsum and anhydrite are the most common varieties of calcium sulfate. These minerals are commonly deposited in shallow lagoons and inlets of seas with a high evaporation (termed evaporites). Gypsum is stable at the Earth's surface, except under

very dry conditions, and anhydrite is more stable at high pressures and temperatures (Hardie, 1967; Blount & Dickson, 1973). Rock gypsum is mined as an ingredient for construction materials such as portland cement, construction plasters, and wallboard panels. Anhydrite, being harder, resists dissolution more than gypsum.

Gypsum dissolves by a two-phase dissociation that depends on the temperature, pressure, and concentration of dissolved salts (Blount & Dickson, 1973; Figure 9). The solubility of gypsum reaches a maximum at 43°C; however, as the temperature of the solution rises to 58°C at 1 atm, crystalline gypsum reverts to anhydrite by losing its water of crystallization (White, 1988; Figure 9). Gypsum may still precipitate from higher temperature waters; however, it often requires higher pressures (Blount & Dickson, 1973).

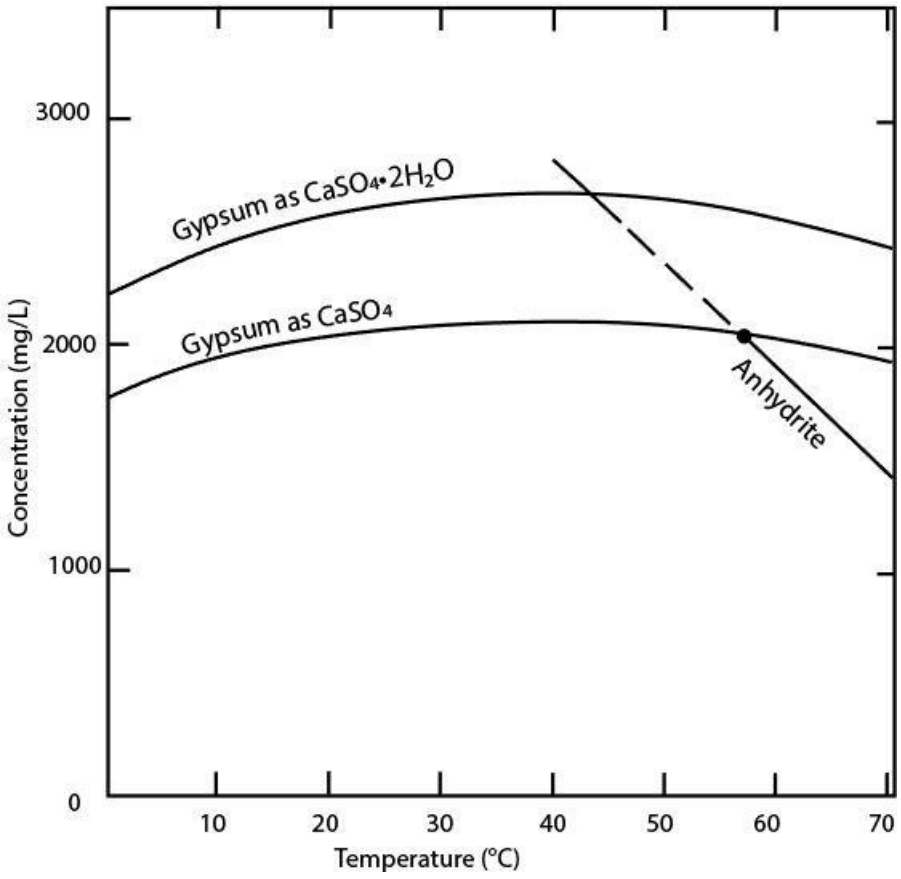

Figure 9. Solubility curves for gypsum and anhydrite based on experimental data of Blount and Dickson (1973). The upper curve is calculated as gypsum and pertains for the mass loss of gypsum rock in solution. The lower curve is calculated as $CaSO_4$ and displays the invariant point at 58°C, where gypsum, anhydrite, and liquid coexist (after White, 1988).

Evaporite rocks (gypsum, anhydrite, and rock salt) dissolve more rapidly than other rock types in pure water (Navas, 1990). Gypsum is structurally weaker (low mechanical strength) and more ductile than carbonate rocks (Gutierrez & Cooper, 2013). Rapid dissolution of gypsiferous rocks may structurally weaken the overlying rock mass at a human timescale (Gutierrez & Cooper, 2013). Gypsum karst is described by

Klimchouck et al. (1996), Calaforra (1998), and Klimchouk and Aksem (2005). Gypsum karst of the U.S. is described by Johnson and Neal (2003). Gypsum karst does not differ from karst of carbonate rocks except for the timescale of its formation (Gutierrez & Cooper, 2013).

3.2 Geomorphology of Karst Terrain

Most caves and surface karst features are related spatially due to growing in close proximity with one another. Water that forms caves first flows through karst depressions (sinkholes and sinking streams) and eventually emerges at springs overflowing through a cave. These features may serve as cave entrances and are indications to the presence and patterns of caves (Audra & Palmer, 2011; Figure 10).

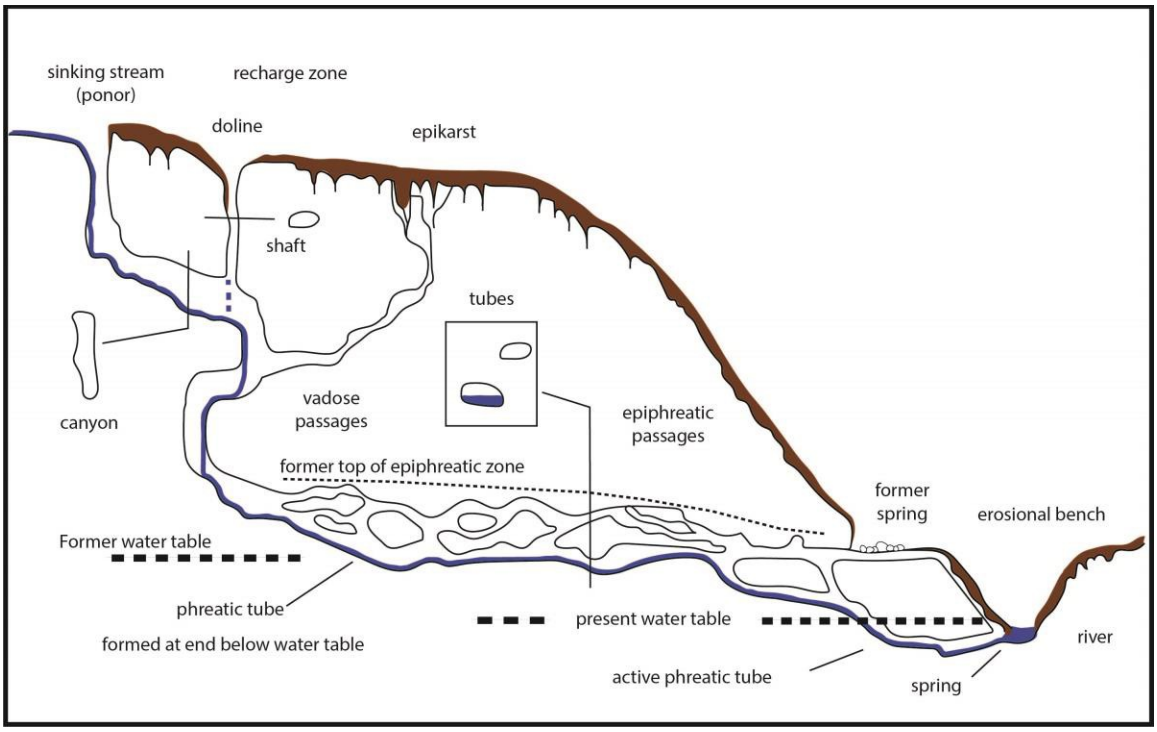

Figure 10. Generalized cross section through a typical multi-stage karst system from Audra & Palmer (2011).

Sinkholes (Dolines)

Sinkholes, or dolines, are relatively shallow, bowl-shaped depressions ranging in diameter from a few feet to more than 3000 feet (~1000 m) (White, 1988). Sinkholes contain a drain, a solutionally modified zone below the bedrock surface, and a cover of unconsolidated material that covers the surface (White, 1988). Drains permit high permeability pathways through the zone above the water table (vadose zone) (White, 1988). Permeability pathways include concentrations of fractures, fracture intersections, and bedding parting planes in steeply dipping soluble rock (White, 1988).

There are three mechanisms of developments for drain systems of closed depressions: 1) a solutionally widened fracture zone with enough permeability to permit

soil transport to the subsurface; 2) a solution chimney, which is essentially a vertical cave developed by selection of one pathway through the fracture system; and 3) a vertical shaft (White, 1988) Solution chimneys are structurally controlled and irregular in shape and ground plan with a cross-section resembling a fissure (White, 1988). Vertical shafts are right circular cylinders whose vertical walls cut the bedding regardless of the inclination of the beds. The shape is dependent on the hydraulics of fast-moving water films and independent of structure and bedding (White, 1988).

Sinking Streams

Streams that lie above the water table lose water through openings in the underlying rock to form sinking streams. Streams may travel underground vertically through their beds or laterally into their banks (White, 1988). The sink points are called swallow holes, or insurgences (to contrast with resurgences, where water emerges at springs) (Monroe, 1970). Some sinking streams do not disappear into visible openings but instead seep through a bed of sediment, which behave like a sieve. Swallow holes come in a variety of morphologies such as pits, cave entrances, and some are completely filled with sediment (choked) without a macroscopic "hole" (White, 1988). Water flows at full discharge upstream from the sinking stream and becomes dry downstream unless a resurgence exists (White, 1988).

Springs

Springs (resurgences) are found when ground water eventually resurges at the surface. Karst springs are either fed by a cave or other conduit system, and water usually emerges from the ground as a stream. Karst springs are classified by lithology, water

temperature, discharge rate, and variation in seasonal discharge rates (Ford & Williams, 1989).

Caves

Caves form where there is enough chemically aggressive subsurface water flow to dissolve bedrock and keep undersaturated water (with respect to a mineral phase) in contact with the soluble walls (Palmer, 1991). A cave system is a network of conduits that connect recharge and discharge areas. Solutionally enlarged caves contain a variety of passages that interconnect in distinctive patterns (Figure 11). The four types of solutional caves are: A) branchwork pattern, B) anastomotic, C) network (maze) and D) spongework (ramiform) (Palmer, 1991).

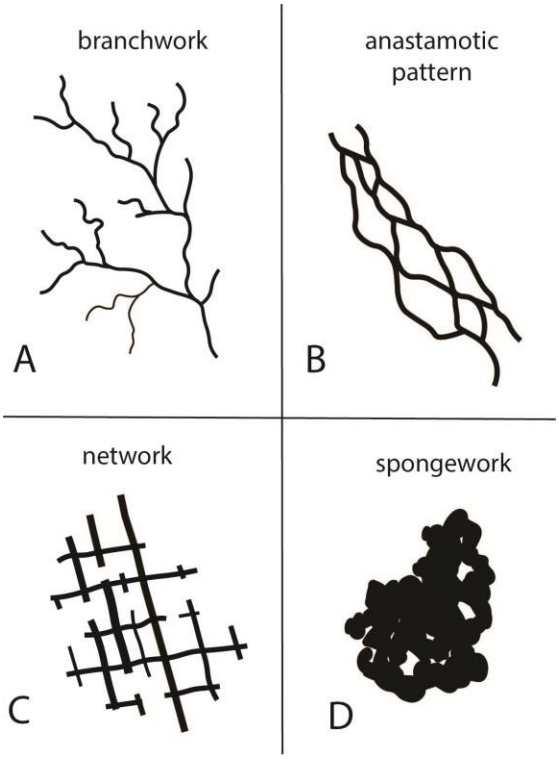

Figure 11. Common solutional cave patterns in plan view from Palmer (1991).

Branchwork caves consist of stream passages that converge as tributaries and are the underground equivalent of surface streams forming a dendritic pattern (Palmer, 1991; Figure 11A). Each major water source contributes to a single solution conduit, or occasionally more than one. Anastomotic caves are composed of curving tubes that intersect in braided patterns (Palmer, 1991; Figure 11B). Nearly all anastomotic caves are formed by flood waters fed by sinking streams or by rapid infiltration through a karst surface (Palmer, 1991). Network caves contain many closed loops and are grouped as either anastomotic or network caves (Palmer, 1991). Network caves are angular grids of intersecting fissure passages formed by the enlargement of fractures (Palmer, 1991; Figure 11B). Spongework caves consist of interconnected solution cavities that produce a three-dimensional pattern like the pores in a sponge (Palmer, 1991; Figure 11B). Ramiform caves, a type of spongework, are composed of irregular rooms and galleries in three-dimensional arrays with branches that extend outward from the central portions (Palmer, 1991; Figure 11B). They are most commonly produced by sulfuric acid from the oxidation of rising hydrogen sulfide (Palmer, 1991).

Pseudokarst

Pseudokarst consists of karst-like features that form either by processes other than dissolution or by slow, lengthy dissolution of rocks that are ordinarily not soluble to form karst (i.e. granite caves and the dissolution of quartzite) (Monroe, 1970; Lowe & Waltham, 2002). Most caves that do not have a solutional origin are considered pseudokarst (e.g. lava tubes or sea caves).

3.3 Speleogenesis

Speleogenesis refers to cave formation. Caves can form in a variety of lithologies and by different dissolutional processes. Cave passage patterns and morphologies may indicate the role of groundwater and its interaction with its environment (Klimchouk, 2000).

Petrographic Controls

Rock type plays an important role in the formation of caves. Rock gypsum is ten times more soluble than limestone in typical groundwater. The dissolution rate of gypsum slows abruptly at about 95% saturation (Dewers & Raines, 1997; Jeschke et al., 2001). Evaporite caves require enough water to form by dissolution but not too much to be lost to surface denudation. This balance point of formation/ preservation is favored in arid climates.

Beds of insoluble strata, such as shale, sandstone, or chert, act as barriers to cave formation. If thick, insoluble beds are sandwiched between soluble rocks, aggressive water must utilize fractures to move through insoluble rocks. Gypsum is often interbedded with carbonates and other soluble salts (e.g. halite, sylvite, and glauberite). The dissolution of interbedded salts produces fractures and breccias in the overlying sequence, providing pathways for groundwater flow (Gutiérrez & Cooper, 2013). In a mixture of carbonate and sulfate rocks, the various rock types interact with one another as they dissolve. For example, calcite is forced to precipitates as dolomite and sulfates dissolve, which allows more gypsum and dolomite to dissolve than if each rock type were isolated from the others (Palmer, 2007). This is due to the common ion effect.

Structural Controls

The next control after host rock petrology is the presence of structural features that control secondary porosity. Caves are preferentially influenced by geologic structures more than surface streams because groundwater can follow these irregularities and fractures, dissolving the host rock as it flows (Palmer, 1991). Cave passage patterns reflect the influence of bedding-plane partings and by fractures (joints and faults) that cut across rock strata. Bedding-plane partings and joints guide the initial cave development (Palmer, 1991). Cave passages in rocks with structural features have angular patterns composed of high, narrow, and straight segments that intersect at various angles, most commonly at the regional joint/fracture set (Palmer, 1991).

Faults can influence cave development in massive rocks by substantially redirecting fluid flow or providing extremely high permeability pathways for fluid flow. Normal faults are more preferential for cave development than reverse or lateral faults due to the recrystallization process that occurs with higher stress compression/shear conditions. Faults can determine passage orientation, and conversely, present barriers to cave formation by terminating and blocking passages (Kastning, 1977).

Hydrologic Controls

The most important control on cave formation is recharge. The vadose zone, or undersaturated zone, is the portion of the subsurface above the groundwater table (Monroe, 1970). Karst groundwater recharge occurs via sinking streams, sinkholes, and through epikarst to form tributaries of a branching cave system and are formed above the water table. Vadose cave passages are shaped by the gravitational flow of water downward along available openings (Palmer, 1991).

The phreatic zone, or saturated zone, is the portion of the subsurface below the groundwater table (Monroe, 1970). Phreatic passages originate along routes of greatest hydraulic efficiency (least expenditure of hydraulic head per unit discharge). These routes enlarge solutionally over their entire perimeter and usually acquire a rounded or lenticular cross section (Palmer, 1991). Phreatic passages will lower the local water table because they are so efficient at transmitting water, acting as an open pipe. As the fluvial base level drops relative to local strata, water in a phreatic passage will entrench the passage floor to form a keyhole-shaped cross section that reflects the transition from phreatic to vadose conditions. The epiphreatic zone is the zone of water table fluctuation. Complex looping overflow routes form in the epiphreatic zone during floods because the phreatic passages may be unable to transmit all the incoming water (Audra & Palmer, 2011). Phreatic passages tend to drain through diversion routes as the base level drops. Old phreatic passages give evidence of the former base level (Audra & Palmer, 2011).

Source for Karst Recharge

Karst terranes can have multiple sources of recharge that vary in terms of amount of water within the conduit network and the residence time. Sources of karst recharge are categorized as either autogenic or allogenic, depending on whether the recharge originates as precipitation falling on karstic or non-karstic terrane (Gunn, 1983). Allogenic recharge is defined as recharge from neighboring or overlying non-karst rocks that drains into a karst aquifer (Monroe, 1970). Allogenic water has the potential to be highly aggressive towards soluble rock due to the lack of soluble minerals in the neighboring/overlying rocks. Recharge derived from precipitation directly onto the karst

landscape is defined as autogenic recharge (Monroe, 1970). Autogenic water flowing through karst conduits and other small networks is described as diffuse autogenic recharge. Recharge (that is saturated with respect to a mineral phase) that flows into large fractures, sinkholes, and streams is defined as concentrated autogenic recharge.

Hydrologic Classification of Caves

Epigenic caves are formed by near-surface or surface processes, such as CO_2 production in the soil that makes aggressive waters with respect to limestone. Most solution caves are epigenic in origin and are produced by the flow of shallow meteoric water (Palmer, 2011). Infiltrating water flowing directly at the surface or beneath a soil cover follows all available openings where soluble rock is exposed. The water is highly aggressive (undersaturated with respect to a mineral phase) near the surface, having no prior contact with soluble rock, which rapidly enlarge the openings (Palmer, 2011).

Hypogenic caves are formed by fluids that are not tied directly to surface processes (Palmer, 1991, 2007a; Klimchouk, 2007; Ford & Williams, 2007). Hypogenic caves have several possible origins, but the most popular involve the interaction of rising fluids with the surrounding rock (i.e. Carlsbad Caverns). Floor slots, wall grooves, ceiling channels, complex wall tubes, and cupolas are features that may indicate the morphologic suite of rising flow in hypogenic caves (Klimchouk, 2007; 2009). Most hypogene caves have network or spongework patterns and certain speleothem and mineral types are diagnostic in regional settings (Klimchouk, 2007; 2009).

3.4 Karst Bearing Formations in the United States

The distribution of surface karst in the contiguous United States is dependent on the presence of soluble rocks near the land surface and mean annual precipitation above 30 inches (76 centimeters) (Weary & Doctor, 2014). The distribution of karst and potential karst areas in Kansas is shown in Figure 12.

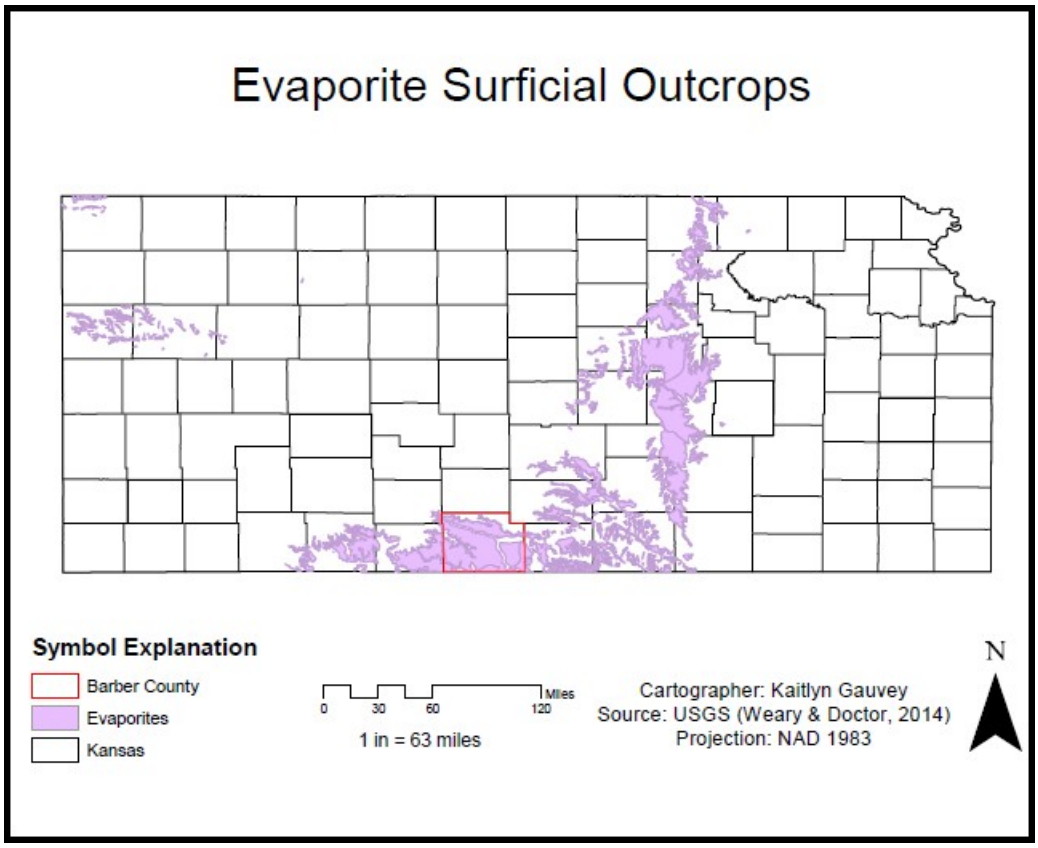

Figure 12. Karst bearing formations in Kansas (modified from Weary & Doctor 2014).

Most karst features occur in carbonate rocks in the humid parts of the United States. Evaporite rocks are rarely found near the surface in humid regions due to their high solubility. In the semi-arid to arid regions of the western United States, evaporite karst features are more common. Carbonates located in arid regions are more resistant to erosion due to the lower precipitation. Hypogenic processes tend to be preserved and less

likely to be modified by epigenic processes in dry climates due to the lack of precipitation and surficial waters (Palmer, 2004; Auler & Smart, 2003).

3.5 Permian Basin Evaporite Karst

Extensive outcrops of gypsum are found in the Permian Basin due to the arid climate. The east flank of the Permian Basin contains a major gypsum-karst region where gypsum beds are 10 –100 feet (3–30 m) thick (Johnson, 2002). The Permian Basin climate has transitioned into an arid to semi-arid desert within the last 10,000 years, (Hill, 1996). Current average precipitation ranges from 6–16 inches (150 – 400 mm) with an average annual temperature of 75 °F (24°C) and average summertime high of 104°F (40°C) (Johnson, 1991).

There are two well-known cave systems and a major fresh-water aquifer in the Permian Basin: the J.C. Jester Cave, Alabaster Caverns State Park, and the Blaine aquifer (Johnson, 2002). J.C. Jester Cave of southwestern Oklahoma is one of the longest gypsum caves in the world (> 6 miles or >9 km) and is located within the Permian Blaine Formation (Bozeman & Bozeman, 2002). The cave system drains the bluffs/escarpments and normally end in karst spring resurgences (Bozeman & Bozeman, 2002). Alabaster Caverns State Park of northwestern Oklahoma includes approximately 200 acres of karst features such as caves, sinkholes, disappearing streams, springs, and (previously) a natural bridge (Johnson, 2011). The caverns are mostly comprised of massive rock gypsum of the Permian Blaine Formation, largely composed of large selenite gypsum crystals instead of the alabaster variety (Johnson, 2011). The karst Blaine aquifer is located in southwestern Oklahoma and northcentral Texas. Extensive outcrops of the

Permian Blaine Formation include interbedded gypsum, shale, and dolomite that cover benches and buttes (Johnson, 2011). The red-brown Flowerpot Shale that underlies the Permian Blaine Formation forms steep-sided slopes and acts as an impermeable layer below the Blaine aquifer (Johnson, 2011).

CHAPTER IV

METHODS

4.1 Site Descriptions

Two privately-owned ranches located west of Medicine Lodge were used in this study. Property owners have asked not to have their exact geographic location revealed for privacy. Specific cave locations have been removed to protect these features. Property One includes 4000 acres (16 km^2) of mostly open rangeland. Bedrock at Property One is mantled with a thin veneer of clay loams up to ~<0.5 ft (0.15 m). Property Two includes over 7000 acres (28 km^2) of mostly open range pasture land. The bedrock at Property Two is highly mantled up to ~3 ft (1 m) with sandy loam and marks a stark contrast to the thinly mantled Property One just 6 miles (10 km) southeast.

4.2 Field Methods

Cave surveying and rock sampling was conducted from April to September of 2018. Previous exploration and documentation of southcentral Kansas have been done by members of the Kansas Speleological Society (KSS). The KSS has not explored Property One. Rock samples were collected from key locations within caves to distinguish petrographic controls on passage morphology. Twelve samples were obtained from cave ceilings (proto-conduits), “ledges”, and walls (Figure 13). These bulk samples were large enough to create one by two inch (2.5 cm by 5 cm) thin sections and leave enough material for mineralogical and geochemical analyses.

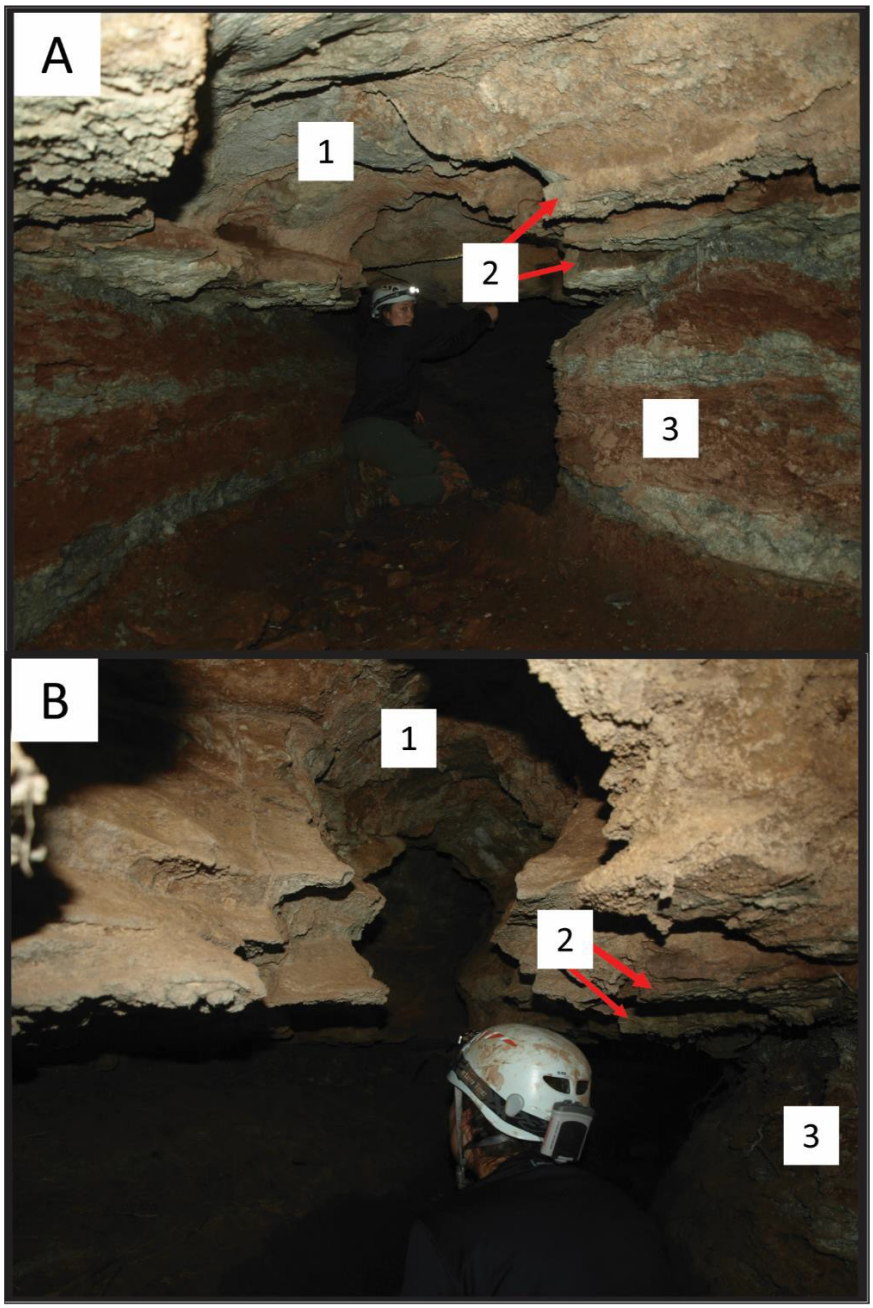

Figure 13 Cave passage morphologies.
Left (A) shows 1) Proto-conduit, 2) Cave Ledge, 3) Cave wall. Right (B) depicts 1) Proto-channel (tube-shaped), 2) Cave Ledge, 3) Cave wall.

Most cave and karst features located were surveyed using standard cave survey techniques (compass, inclinometer, and tape) as documented by Dasher (1994). Plan sketches and cross sections of each cave were created to document cave passage morphology and passage orientation. The locations of karst features were documented with a handheld Global Positioning System (GPS) unit, recorded as UTM coordinates, and stored in a relational database to be used within a Geographical Information System (GIS) to generate maps. Georeferenced satellite data were used to correct erroneous points (Access, 2011).

4.3 Laboratory Methods

Twelve samples were made into standard petrographic thin sections. Several thin sections were stained with alizarin red-S to distinguish the presence of dolomite and calcite (Dickson, 1966). Samples were powdered for X-ray diffraction (XRD) using a low-speed dental drill and sieved through 250 μm, 125 μm, and 63 μm sieves for routine qualitative evaluation of mineral components. Bulk mineralogy was analyzed using a Rigaku x-ray diffractometer with Cu Kα radiation and internal quartz standard at the University of Missouri-Kansas City.

4.4 Cave Data Processing

The survey data from each cave were reduced using the Compass Project Manager computer program (Compass, 2018). The line plot of each cave produced by Compass Project Manager was imported into the Sketch Editor drawing program. The sketch map of the cave was scanned and converted to a digital file that was then imported to Sketch Editor. The line plot and sketch were scaled and oriented so that a map of the

cave could be drawn. Field sketches were digitized into Adobe Illustrator for a final cave map drafting. The cave and the features within it were depicted using the symbols adopted by Dasher (1994). Additional symbols were incorporated as needed to properly depict the features discovered in various caves. The cave maps produced are included in Appendix B. Cave volume was determined by CaveXO software, using the cave volume tool. Cave dimensions were determined by the use of ImageJ software (Schneider, Rasband, & Eliceiri, 2012). Cave maps were uploaded into the software and outlined using a "straight line" tool to calculate cave area. The map scale was set in the software to calculate the number of pixels per unit foot. The software calculated the distance in pixels of the segment. The cave outline was created using the "polygon selections" tool and the area in squared feet was calculated using the software. Cave length was determined by ImageJ by using the "segmented selections" tool and tracing the survey lines with the computer mouse. In cases where the survey shots were "zig-zagged", a straight-line segment was measured through survey shots and given in feet (Figure 14). Cave dimensions are listed in Table One.

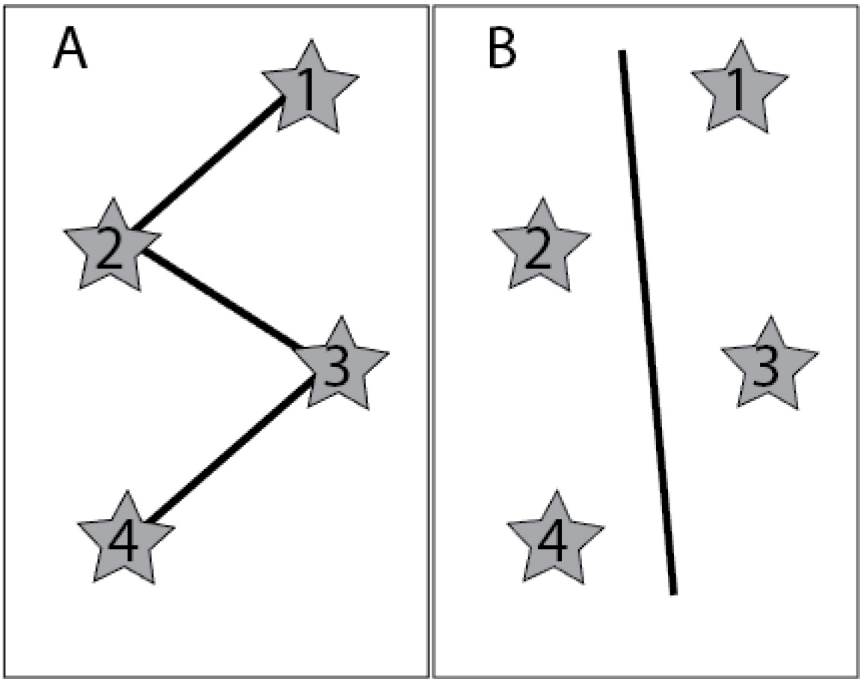

Figure 14. A) “Zig-zag” patterned survey stations (stars). B) Straight-line segment approximating cave length through the survey shots.

4.5 Spatial Distribution

Karst features were inventoried by handheld GPS and added to a GIS Geodatabase in ArcMap 10.6.1. Karst features include: caves, sinkholes, ponded sinkholes (water-filled), swallow holes (insurgence points), springs (resurgence points), microkarst, and pseudokarst. Microkarst features are defined as karst features such as small (<0.5 ft (<0.15 m)) diameter conduits within gypsum beds. Pseudokarst included shelter caves. Shelter caves contain the same features as caves but are too small to consider a cave. Shelter caves in this area have a drip line that animals can use to shelter out of the weather.

GIS layers were collected from the State of Kansas GIS Data Access and Support Center. The karst inventory geodatabase was created in ArcCatalog and maintained in

ArcMap 10.6.1, both of which are applications included in the ESRI ArcGIS software package. Cave survey data was converted from Compass plot files to ESRI shapefiles format and georeferenced based on GPS locations of surface survey stations.

When encountered, specific biota were documented and these data are included in Table Two.

4.6 Sample Collection and Preparation of Thin Sections

Rock samples were collected from the cave ceilings, ledges, and walls. Sample collection involved a rock hammer, chisel, and sledge hammer depending on the hardness and nature of the rock.

Six samples were cut using a water-cooled diamond saw into rectangular prism-shaped rocks called billets. The billets were polished using silicon carbide grit and mounted to a glass slide using UV curing epoxy (Norland Optical Adhesive). The excess billet was trimmed using a trim saw and ground incrementally until reaching a final thickness of approximately 30 microns.

Optical petrographic analyses were performed using a Leica DM 750 P microscope with LAS EZ imaging software to collect the bulk of the data for this project. One hundred-point point counts were performed on each thin section. A randomized grid pattern was used to ensure the one hundred-points were not biased. One-hundred point counts ensure an 85 % confidence interval (V.D Plas, & Tobi, 1965). The petrographic feature present at each point was documented to determine the relative abundance in each thin section.

4.7 X-Ray Diffraction

Samples were powdered for X-ray diffraction (XRD) using a low-speed dental drill and analyzed for mineralogy using a Rigaku Miniflex 600 diffractometer at Missouri State University-Kansas City. XRD patterns were obtained as follows: continuous mode, 0.002º per step, 4º 2θ per minute, 3º -70º 2θ CuKα radiation. Mineral percentages were estimated from relative intensities of peak heights of XRD lines. The most abundant minerals include tall peak heights of XRD lines.

CHAPTER V

RESULTS

Descriptions of the individual named cave features are listed alphabetically in Appendix A. Cave maps generated by this project are included in Appendix B. Individual other karst features (springs, sinkholes, swallow holes) are listed numerically by property in Appendix C.

5.1 Field Results

Field reconnaissance identified 62 karst features, including 18 open sinkholes (i.e., caves or smaller solutional conduits that connect directly to sinkholes), nine filled sinkholes, 14 caves with no associated sinkhole, and 13 springs. Ten of the 18 sinkholes contained caves that were large enough for humans to enter. Sinkhole complexes and associated caves were primarily on Property One where the gypsum is exposed or thinly mantled with clay loam. Filled sinkholes were generally found in the sandy loam mantled material on Property Two. Average cave passage length measures 76 ft (23 m) with vertical extents of 14 ft (4 m). The average cave volume was 1,245.25 ft^3 (380 m^3) with the average cave area being 1119 ft^2 (341 m^2).

5.1.1 Cave Morphology

On both properties, cave entrances are found near cover-collapse sinkholes or where surface denudation has breached the cave. Entrances typically contain a solutionally enlarged fracture in the gypsum. Cave passages follow joint sets; and where these joint sets meet, passages extend vertically, in some cases up to 14 ft (4 m) (Figure 16). Passage survey shots are short (ranging from to 4.8 to 17 ft (1.5–5 m), straight to

slightly sinuous, and are oriented along joints that have sharp, orthogonal bends at joint intersections (Figure 16). In some cases, cave passage length measures up to 1232 feet (325 m). The average passage orientation is 134º (Figure 17). Several caves are "through caves" that have two entrances (one collection sink and one resurgence) (Jennings 1971; Klimchouk, 1996b). Cave entrances are typically found near the upstream portion of erosional valleys and some caves are found along canyon walls. Cave entrance elevations were sorted in ascending order (Figure 18). Cave classifications are included in Table Three.

Ceiling tubes measure less than one foot to two feet (0.3–0.6 m) in diameter, and follow ceiling joints (Figure 13). Carbonate ledges occur between the overlying gypsum and the shale. The ledges form resistant beds that protrude out into the cave passage (Figure 16). The underlying shale is friable and contains abundant satin spar gypsum stringers, masses of selenite gypsum, and laminations of bleached-gray shale. The shale portion of the cave passage is often wider than the passage developed in overlying strata. Cave passages formed in the gypsum unit are often short in height (<3 feet), and wide (<6 feet) and form elliptical shaped cross sections. Passages that are entrenched into the underlying shale unit are often square in shape and vary in height (<3 feet to >5 feet).

Active water seeps are commonly seen at the contact between the carbonate ledge and the shale, and most caves contain standing pools of water year round (personal testimony of ranch owners). Solutional features related to flowing water, called scallops, were observed on gypsum passage walls and on recent breakdown blocks (Figure 19).

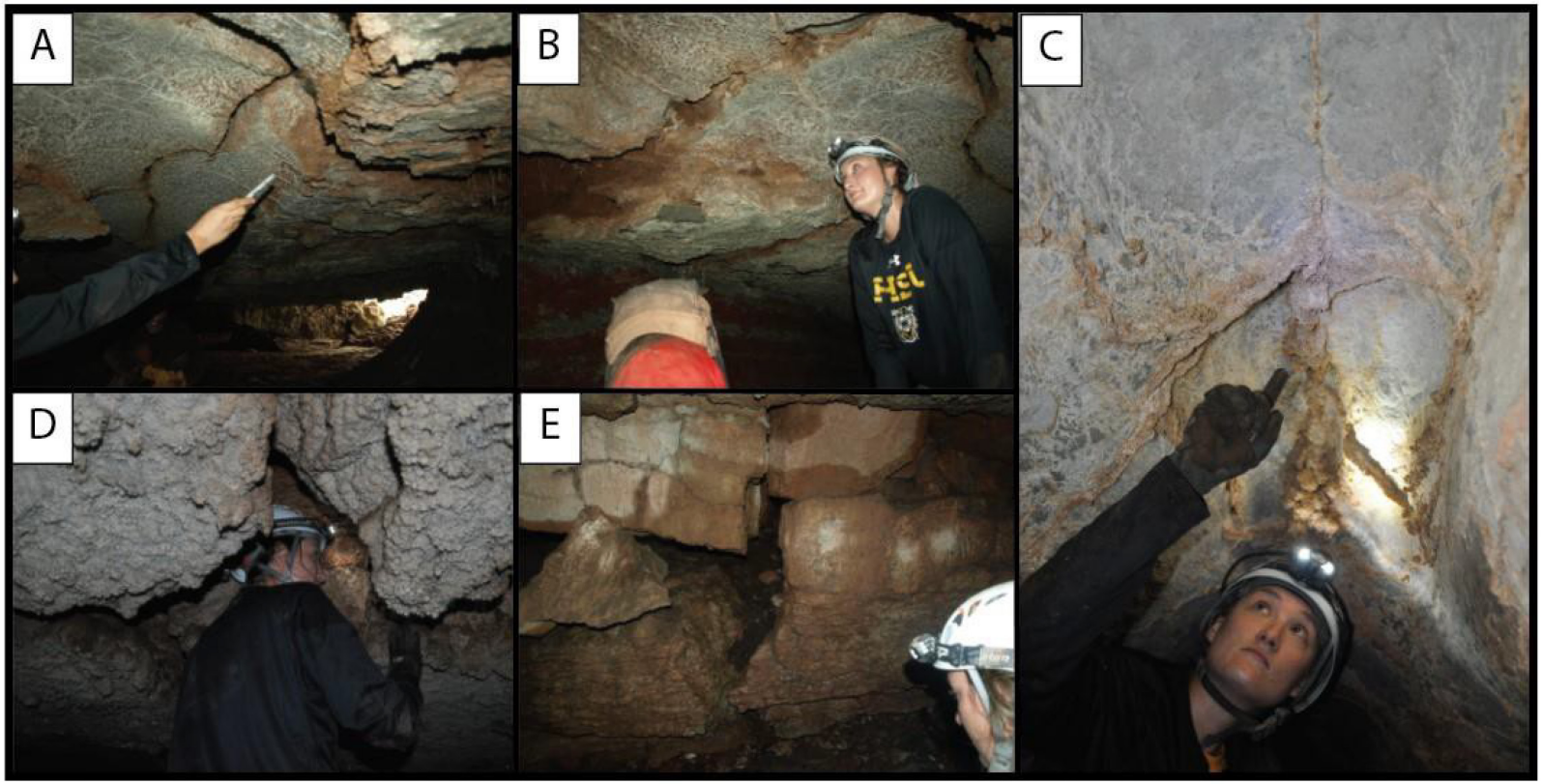

Figure 16 A) and B) Ceiling channel in Medicine Lodge Gypsum following ceiling fracture. C) Ceiling channel in the Medicine Lodge Gypsum following a ceiling fracture. Scallops are observed on the wall. D) Joint set intersection in the Medicine Lodge Gypsum that extends 14- feet vertically. E) Joint set intersection where water is seeping into the cave towards a standing pool of water. Scallops are observed on the walls.

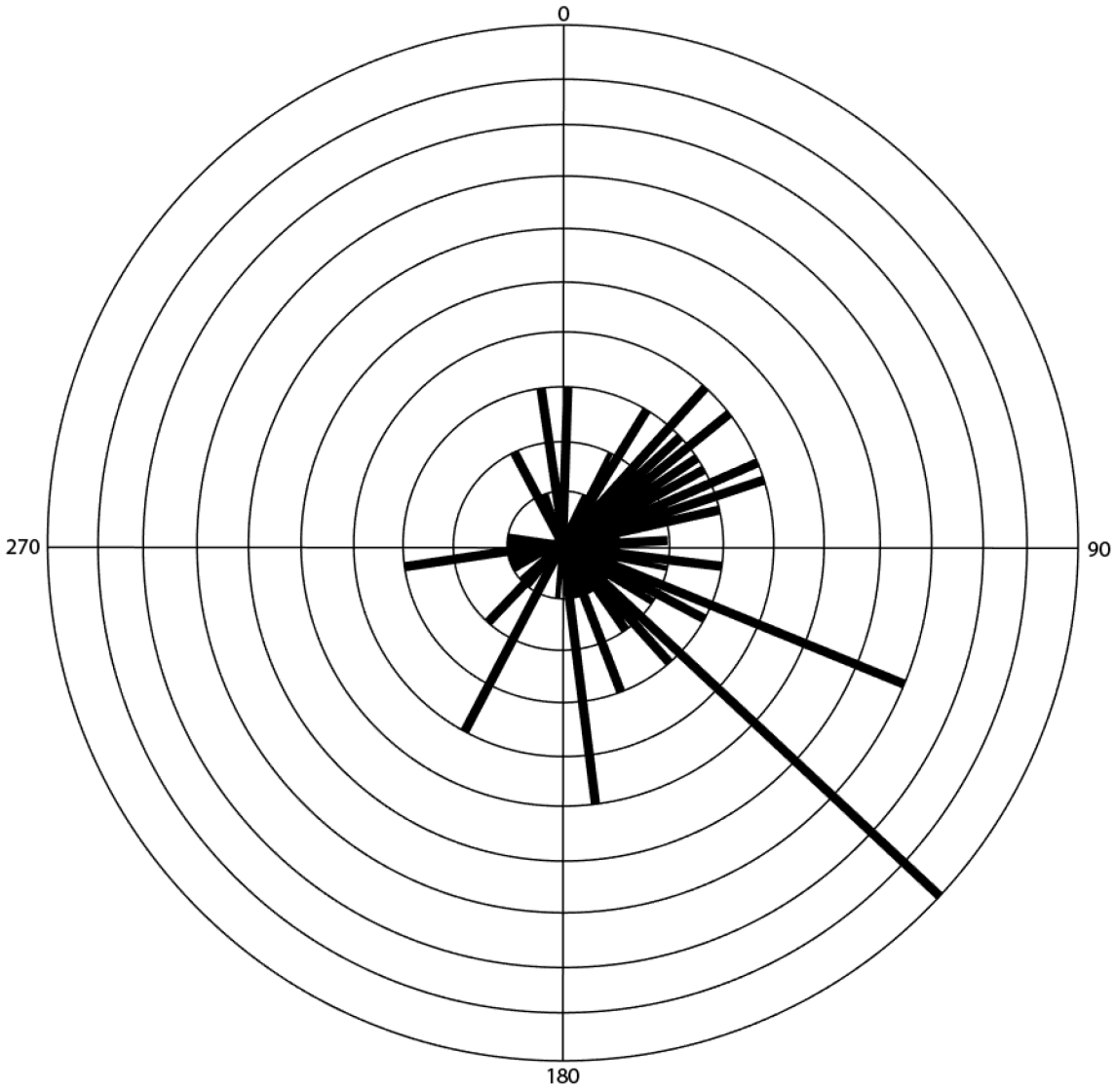

Figure 17. Rose diagram for all cave passage orientations. Each ring represents one occurrence. There are a total of 110 passage shots. The average passage orientation is 13

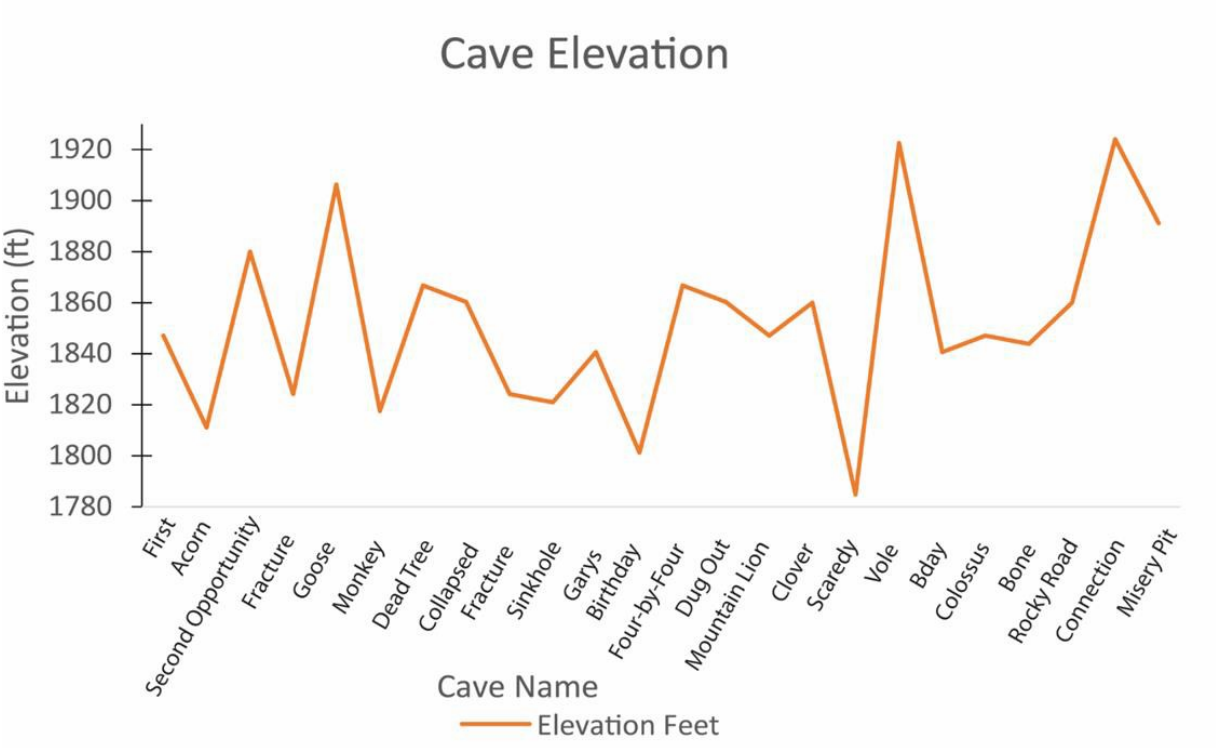

Figure 18. Cave entrance elevation in feet. Caves' entrance elevation were ordered to delineate controls on elevation. There are possibly some elevation horizons; however, more data is required for a valid generalization.

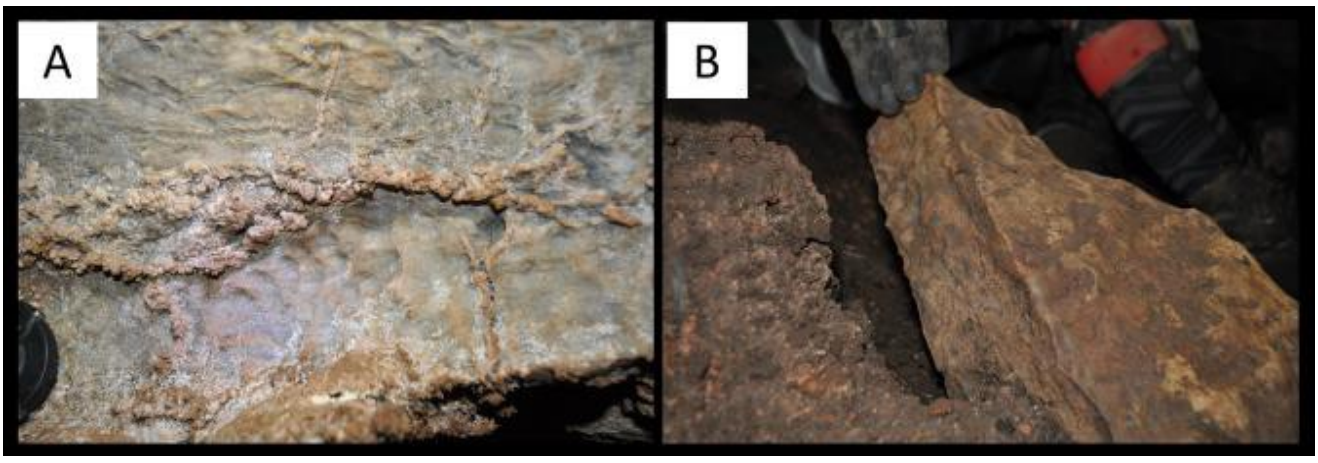

Figure 19. A) Scallops in the Medicine Lodge Gypsum member. Scallops are located in the wall of the ceiling channel. Camera lens cap for scale. B) Scallops in the Medicine Lodge Gypsum. Scallops are located on a recent breakdown block in the center of the cave passage.

5.1.2 Sinkhole Morphology Observations

Solutional sinks are found atop the buttes and mesas within the Medicine Lodge Gypsum. Sinkholes on Property One are expressed differently than those on Property Two. On Property One, the bedrock is exposed with a thin veneer of loamy soil, creating sinkhole complexes that are not easily identified from aerial photographs as sinkholes due to their dendritic shape (Figure 20). Sinkhole complexes form in the upper valley, where slightly mantled material is funneled into solutionally enlarged surface joints (Figure 20). On Property Two, sinkholes are highly mantled with a sandy aggregate, creating an easily identifiable depression on aerial photographs (Figure 21).

5.1.3 Surficial Karst Development

The Blaine Formation has been heavily modified by surficial processes where gypsum bedrock is exposed. Small karren, microkarst features, and sinkholes develop on the plateaus. Rillenkarren, or rills, are often found near cave entrances and atop exposed breakdown blocks. These features are shallow and separated by sharp ridges (<1/3 inch apart). Solutionally enlarged surface joints, typically follow the same trend as cave passages (Figure 22).

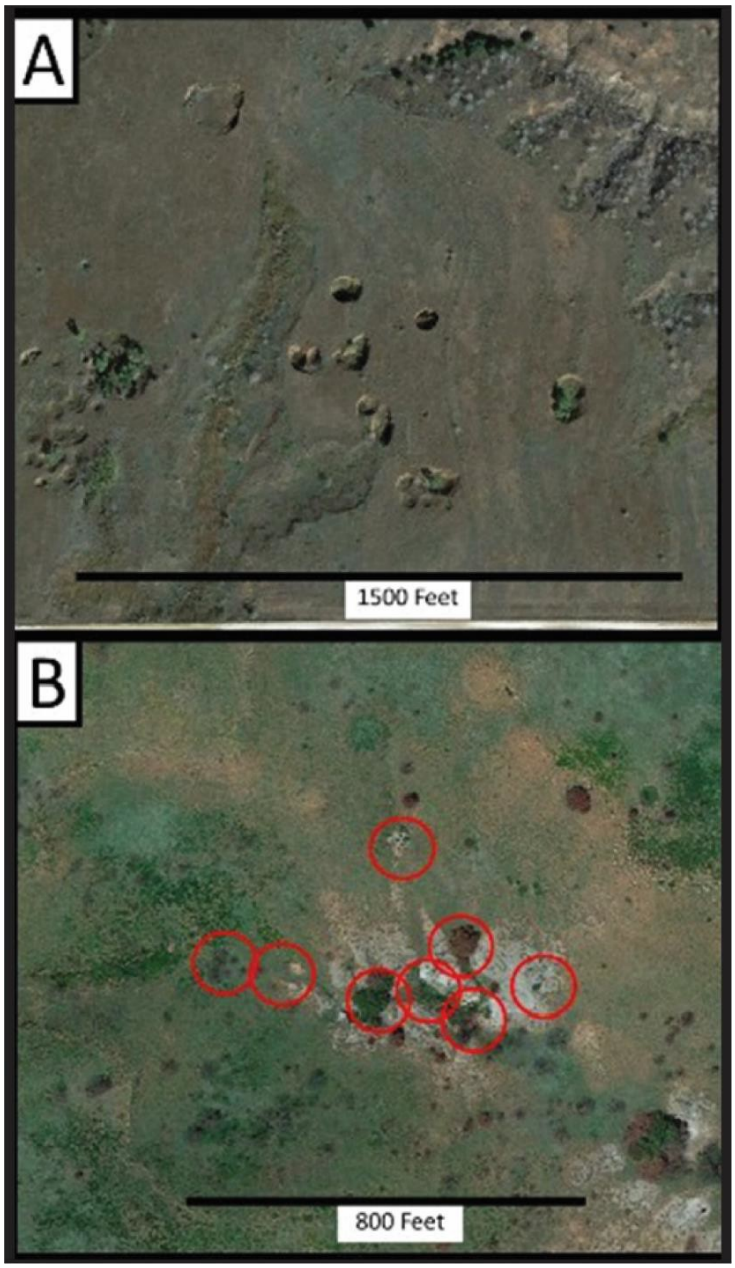

Figure 20. Sinkhole complexes in the two regions of the study area. A) Northern portion of the study area where mantled material is thicker produces more distinct sinkholes. Notice the two generations of sinkholes. The first generation represents collapse and reworking to form a dendritic pattern. The second generation represents recent collapse due to mining activities in the area. B) Southern portion of the study area when mantled material is thin or lacking. Sinkholes are less noticeable, so their locations have been circled.

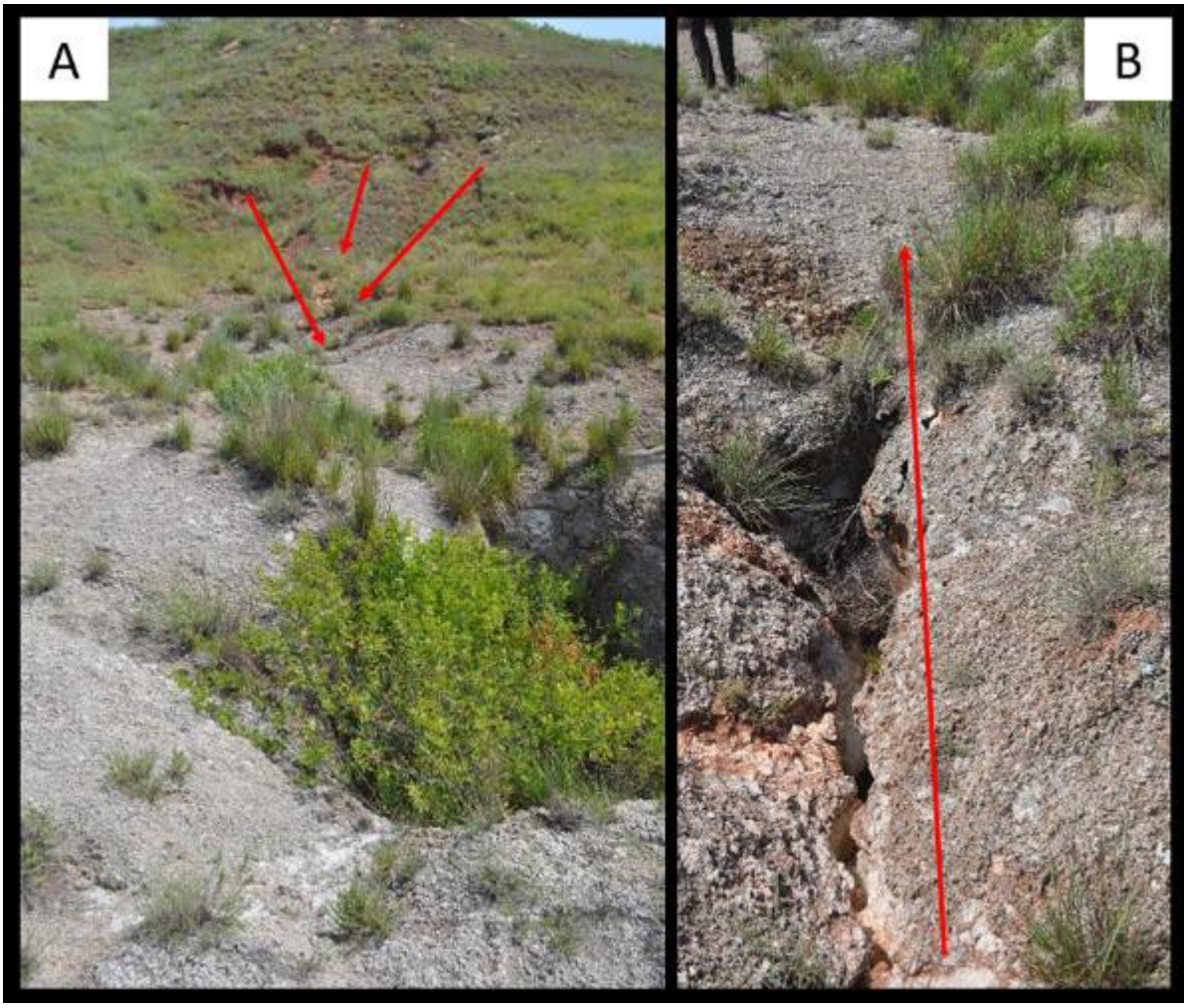

Figure 21. Epikarst surface. A) Mantled material is eroded into solutionally enlarged fractures and vadose into a cave system below. B) Solutionally enlarged fracture that acts as a funnel for mantled material. Surface fractures follow the same trend as cave ceiling fractures.

Figure 22. Various sinkholes from Barber County. A) Sinkhole complex in a thicker sand loam mantled sinkhole complex from Property Two. These sinkholes do not have bedrock exposed in the bottoms. B) Slightly mantled sinkhole complex with exposed bedrock from Property One. Mantled material is a clayey loam. C) Exposed bedrock cover collapse sinkhole from Property One. The mantle material has been stripped by surface erosion by the adjacent stream. There is a cave entrance in the bottom of this sinkhole that feeds a stream passage.

5.2 Spatial Distribution

Karst features were inventoried by handheld GPS and added to a GIS Geodatabase in ArcMap 10.6.1 (Figure 23). The properties were subdivided into reconnaissance sections, where property owners knew of cave locations and other karst features. Property One is divided into three sections: the Northeast, the Southwest, and the Southeast (Figure 24). The Northeast section includes four caves, nine sinkholes, and

two microkarst features (Figure 25). All of the caves in the Northeast section are associated with nearby sinkholes. Caves are located at the upstream portion of canyons. A sinkhole complex is also present near the upstream end of a canyon. The Southeast section contains six caves, one sinkhole, four microkarst features, and three pseudokarst (Figure 26). This region does not show a sinkhole–cave relationship. The Southwest section contains 11 caves, two swallow holes, three sinkholes, and two microkarst features (Figure 27). There is a sinkhole–cave relationship in the center of the section, and most caves are located at the upstream end of canyons.

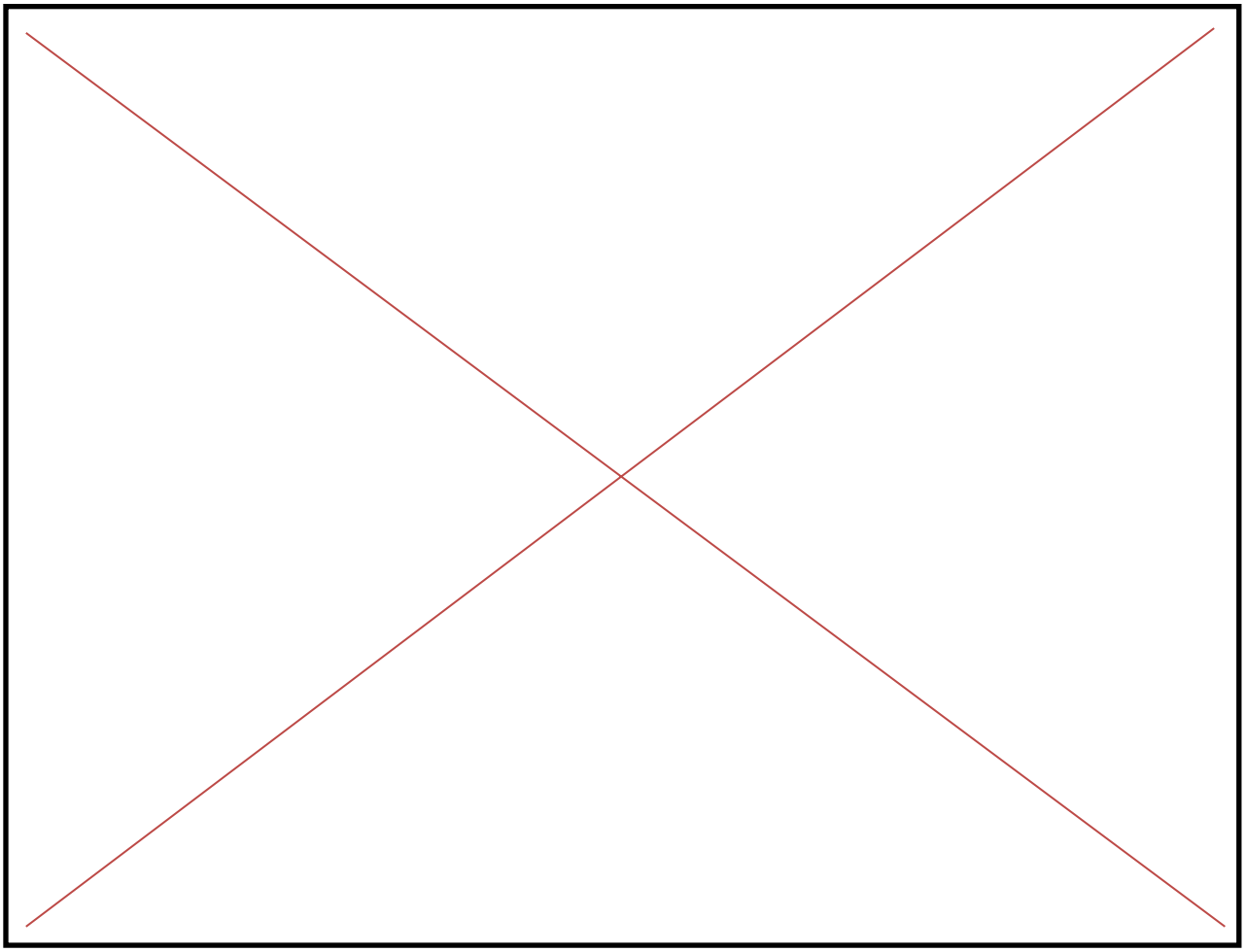

Figure 23. Karst feature locations for Property One and Property Two. Medicine Lodge, the nearest small town, is shown to the east.

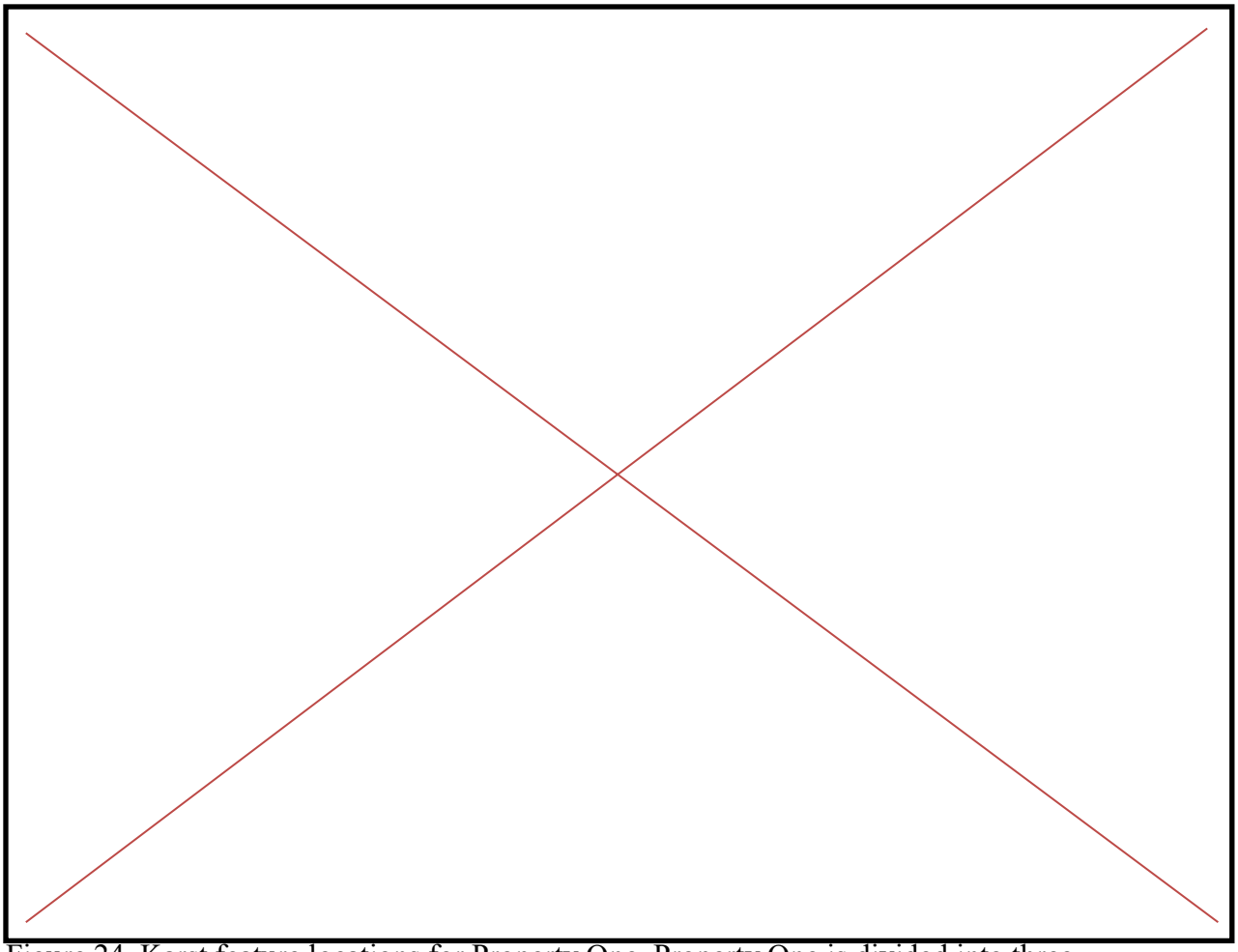

Figure 24. Karst feature locations for Property One. Property One is divided into three sections: the Northeast (green), the Southwest (yellow), and the Southeast (red).

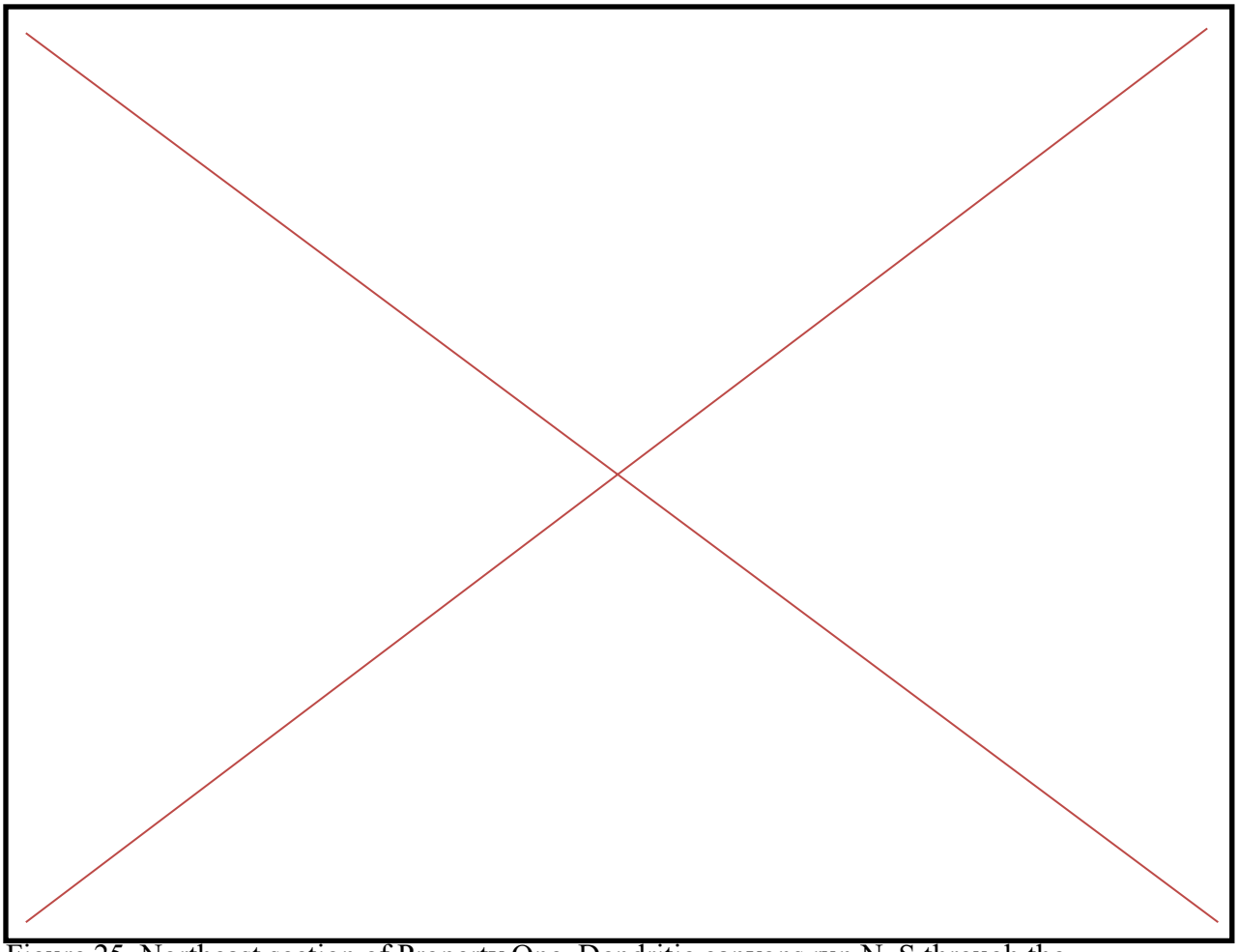

Figure 25. Northeast section of Property One. Dendritic canyons run N–S through the section. Caves are associated with nearby sinkholes and are located at the upstream portion of canyons. A large sinkhole complex is found in the Northeast portion of the Northeast section (circled in green).

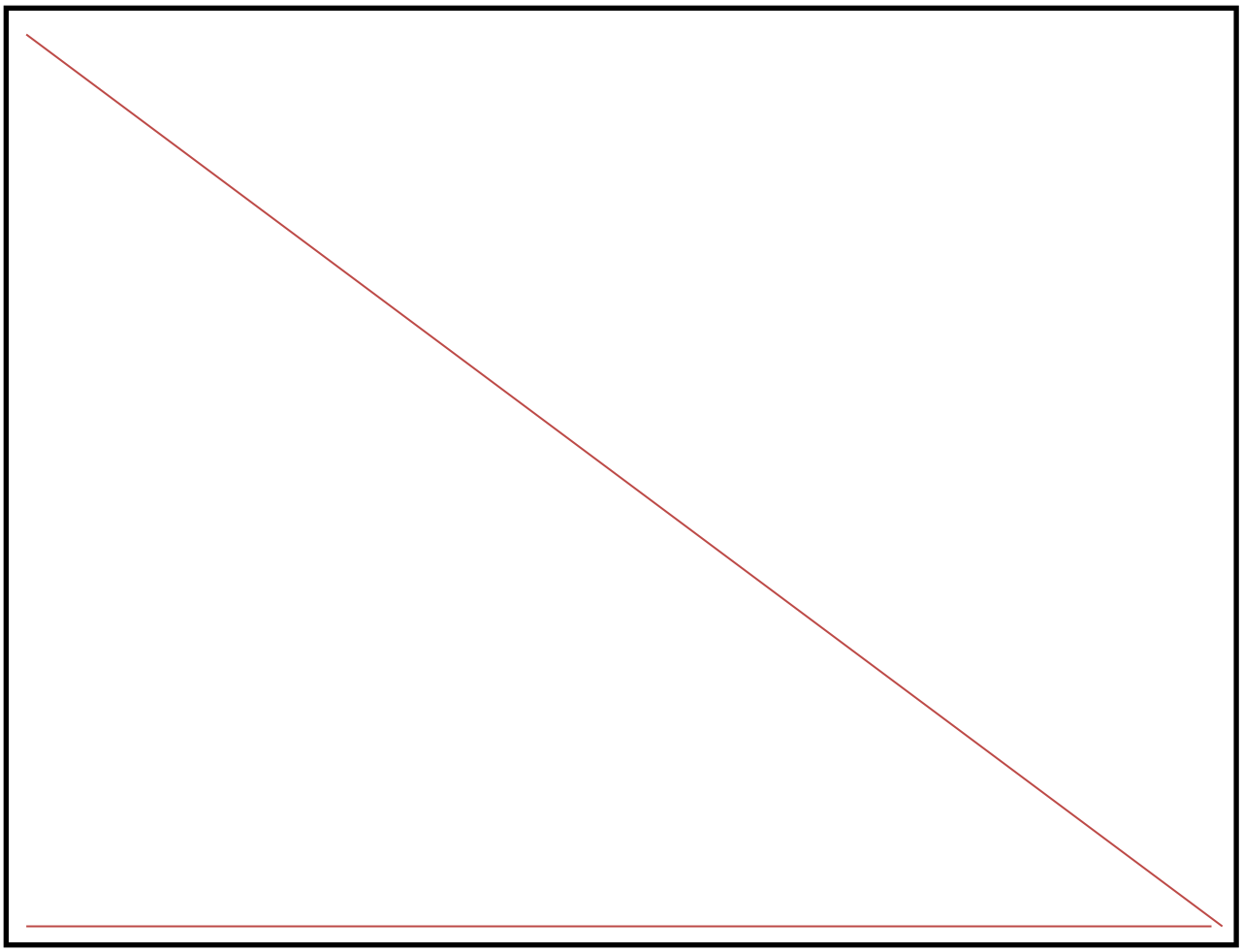

Figure 26. Southeast section of Property One. One large canyon runs through the center of the section. Caves are located either at the upstream end of canyons or near the rim of the canyon walls. Pseudokarst (shelter caves in this case) line the canyon walls.

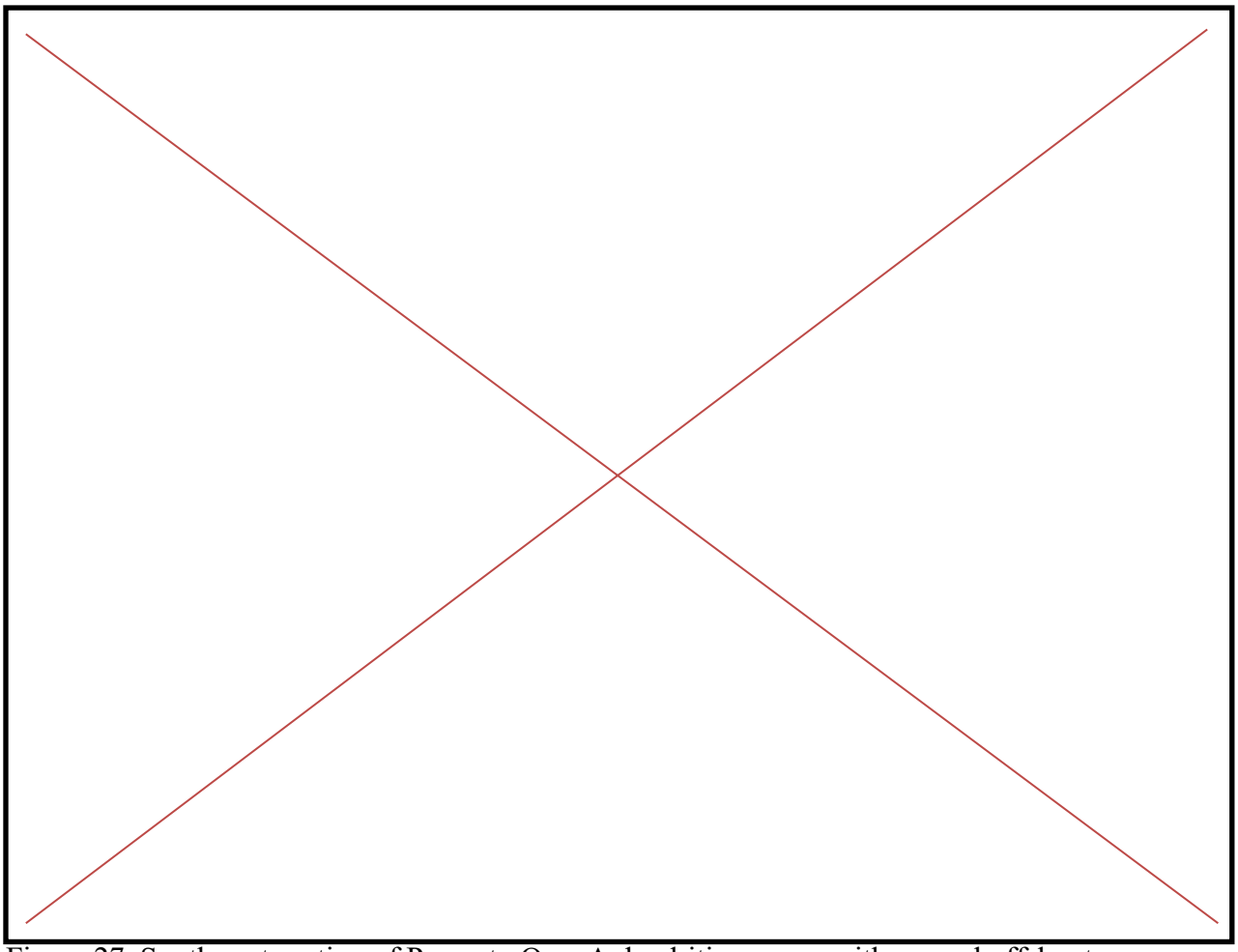

Figure 27. Southwest section of Property One. A dendritic canyon with several offshoots can be observed in this section. Several caves are found at the upstream portion of the canyon. In one area (circled in yellow) there is a sinkhole that empties into a cave. A swallow hole also lies in front of the entrance of the cave. Caves are found at the upstream end of the canyons.

Property Two mostly contains ponded sinkholes and mantled sinkholes that are located on valley floors (Figure 28). In the Northwestern section of Property Two, there includes a through cave that connects to a sinkhole complex on the other side of the canyon wall (Figure 29). In the Northeast section, the valley floor is far more vegetated with red cedar trees and willow trees. There are three ponded sinkholes that are filled with vegetated debris. Nearby, there are four non-ponded sinkholes that are nearly filled

by debris (Figure 30). In the southeast section of Property Two there includes highly mantled sinkholes that dot the valley floor as well as lining the rim of a nearby canyon (Figure 31).

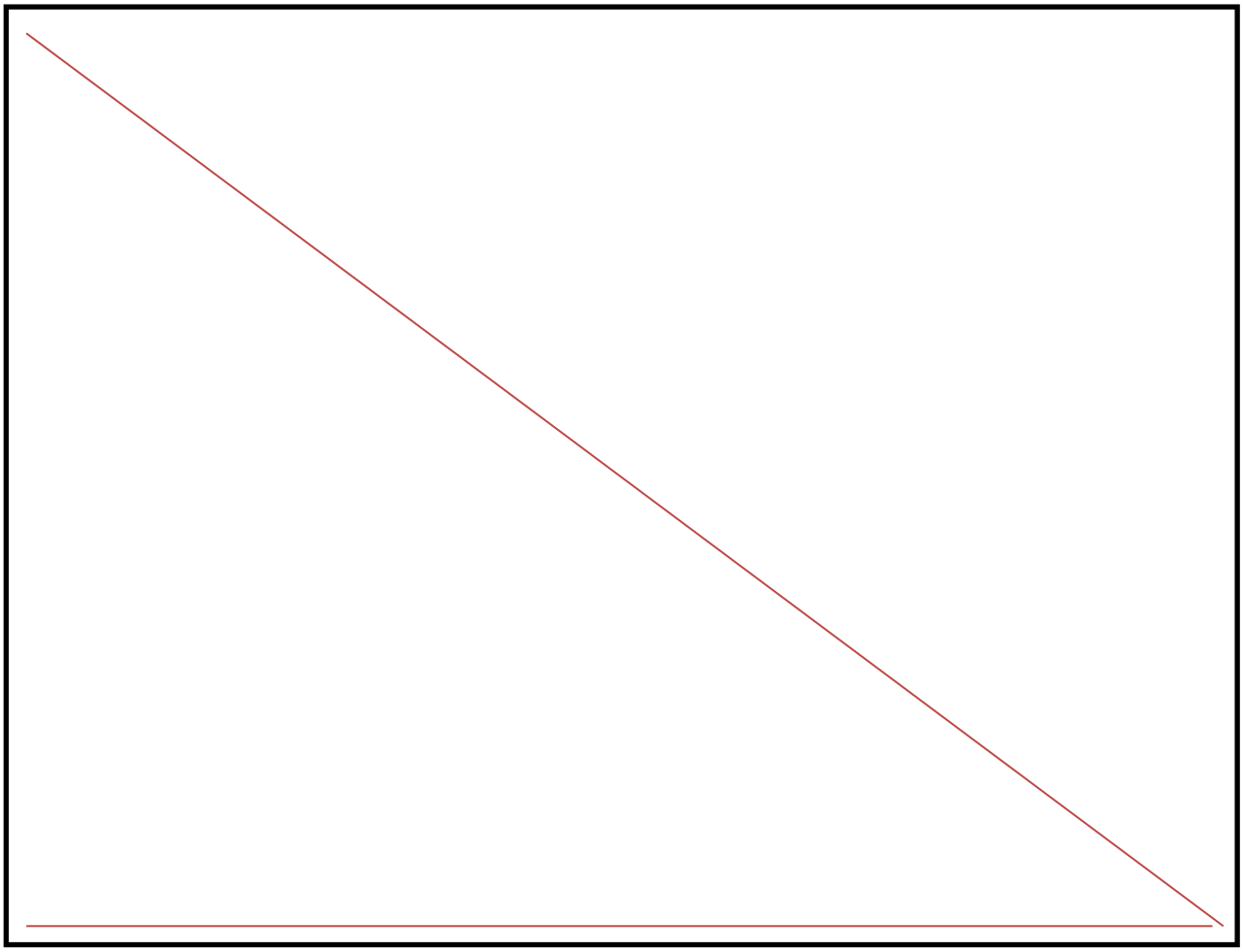

Figure 28. Property Two Karst Features are divided into three sections: The Northwest (orange), the Northeast (red), and the Southeast section (yellow).

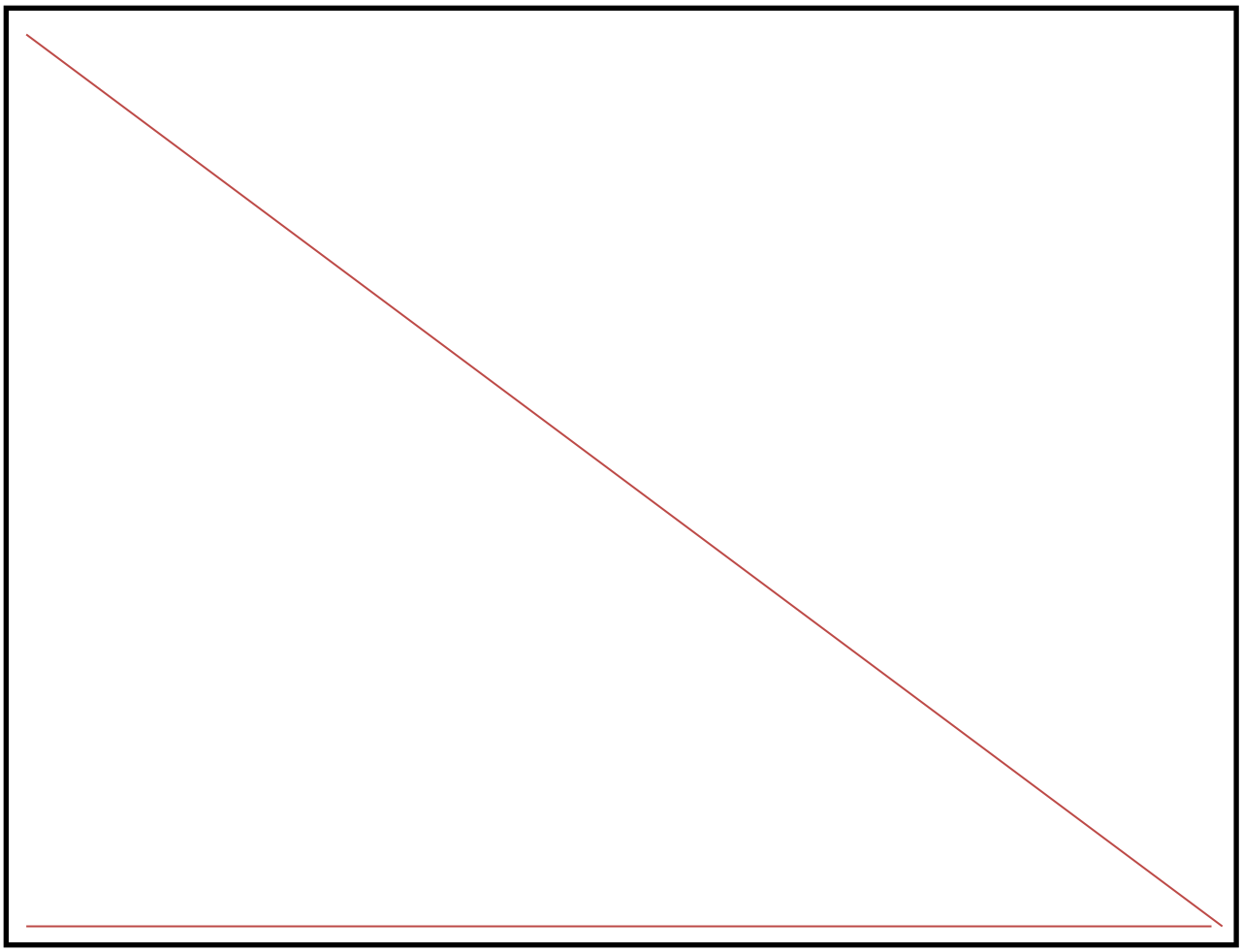

Figure 29. A sinkhole complex is spread along the valley floor of a wide canyon. This canyon is highly vegetated with red cedar trees and willow trees. Ponded sinkholes are filled with vegetated debris. A through cave with an associated sinkhole complex is circled in red. This cave (Bone Cave) runs through a 30 foot tall canyon wall towards another canyon.

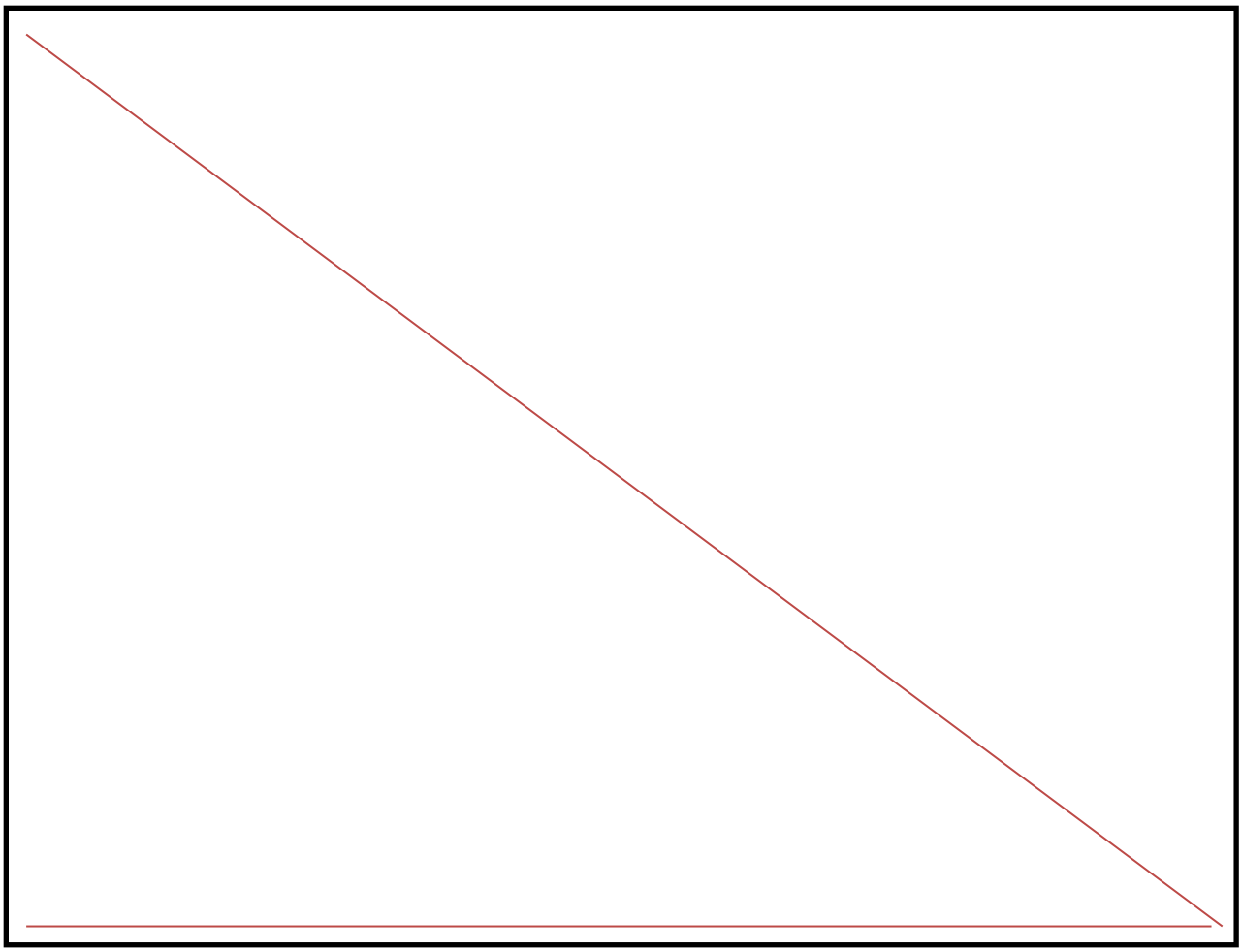

Figure 30. A large sinkhole complex is found on the valley floor of a canyon. Two ponded sinkholes are also associated with this canyon and are filled with vegetated debris.

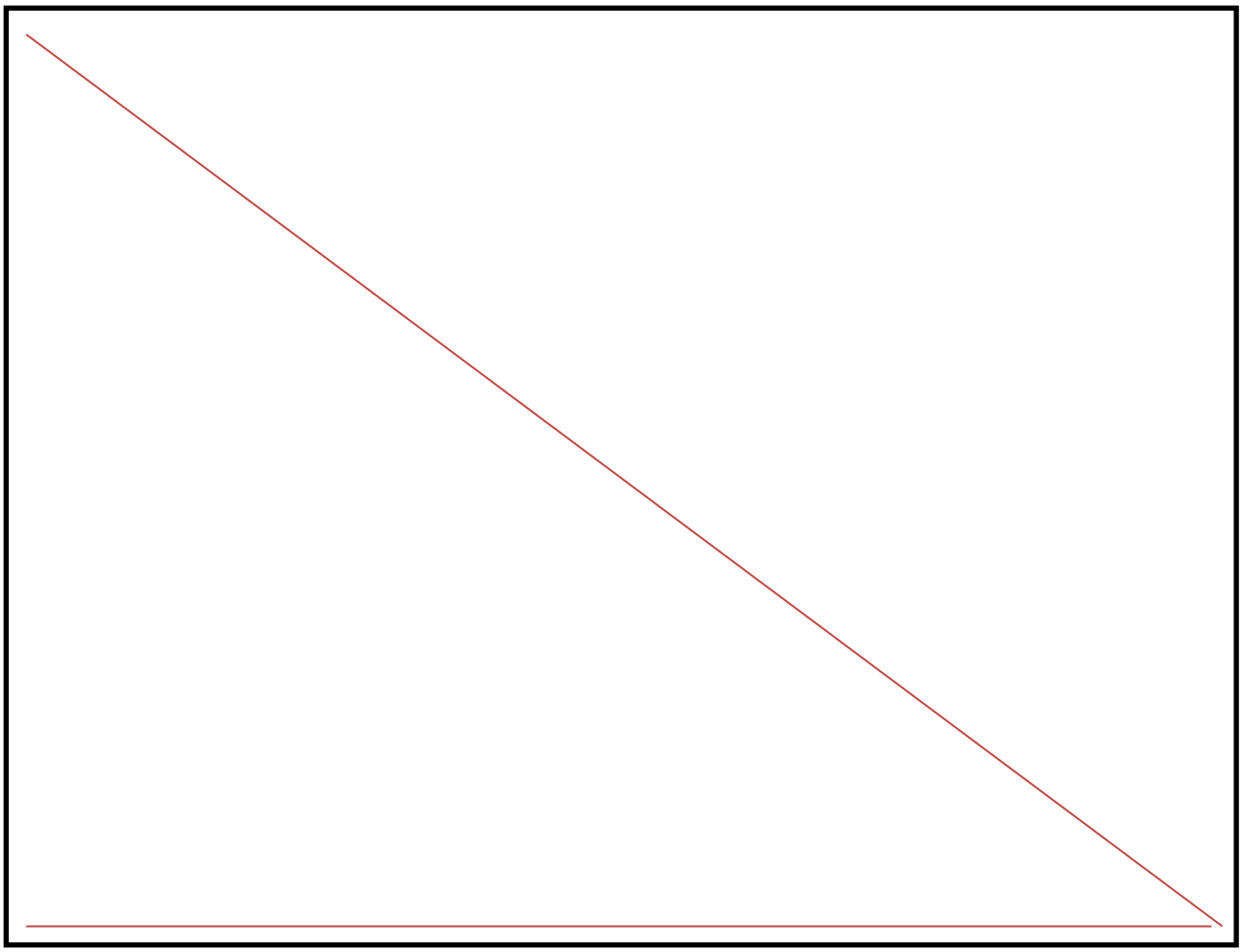

Figure 31. A sinkhole complex is present on the valley floor and further along the edge of the canyon.

5.3 Petrographic and Mineralogic Results

Cave Ceiling

Megascopically, the gypsum is soft, buff to gray, and microcrystalline. Anhedral secondary granular gypsum replacement crystals are abundant in all cave ceiling/proto-channel samples (Figure 32A). These crystals range in size from 0.05 to 5 mm. Subhedral to anhedral gypsum laths measuring up to 2 mm are scattered throughout (Figure 32A).

Anhedral dolomite inclusions are present measuring up to 2 mm (Figure 32A). Patchy iron oxide staining is common; however, anhydrite was not identified in any of the samples. XRD analysis indicates the ceiling rock of most caves is composed of mostly gypsum with minor dolomite (Figure 33).

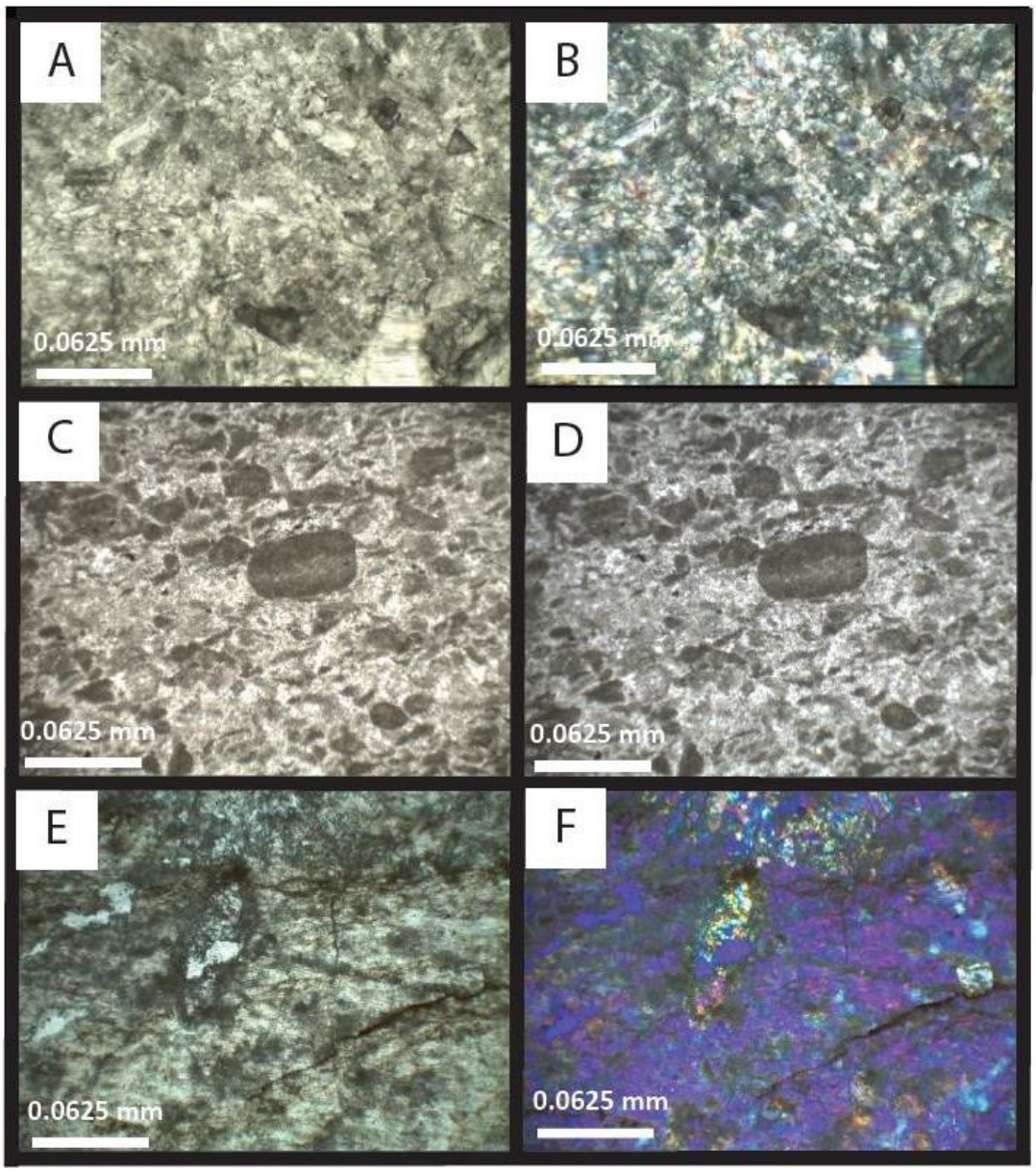

Figure 32. A) Cave ceiling sample in plane polarized light. Secondary granular gypsum matrix with euhedral dolomite inclusions. B) Cave ceiling sample in cross polarized light. C) Cave ledge sample in plane polarized light. Pelloids are laminated and are completely dolomitized with a sucrosic texture. D) Cave ledge sample in cross polarized light. E) Cave wall sample in cross polarized light. A euhedral anhydrite ghost can be observed in the center. The cave wall is mostly composed of selenite gypsum, satin spar gypsum, and fe-oxide rich clay. Fe-oxides commonly fill fractures. F) Cave wall sample in cross polarized light with the gypsum plate inserted. An anhydrite ghost is replaced with secondary granular gypsum.

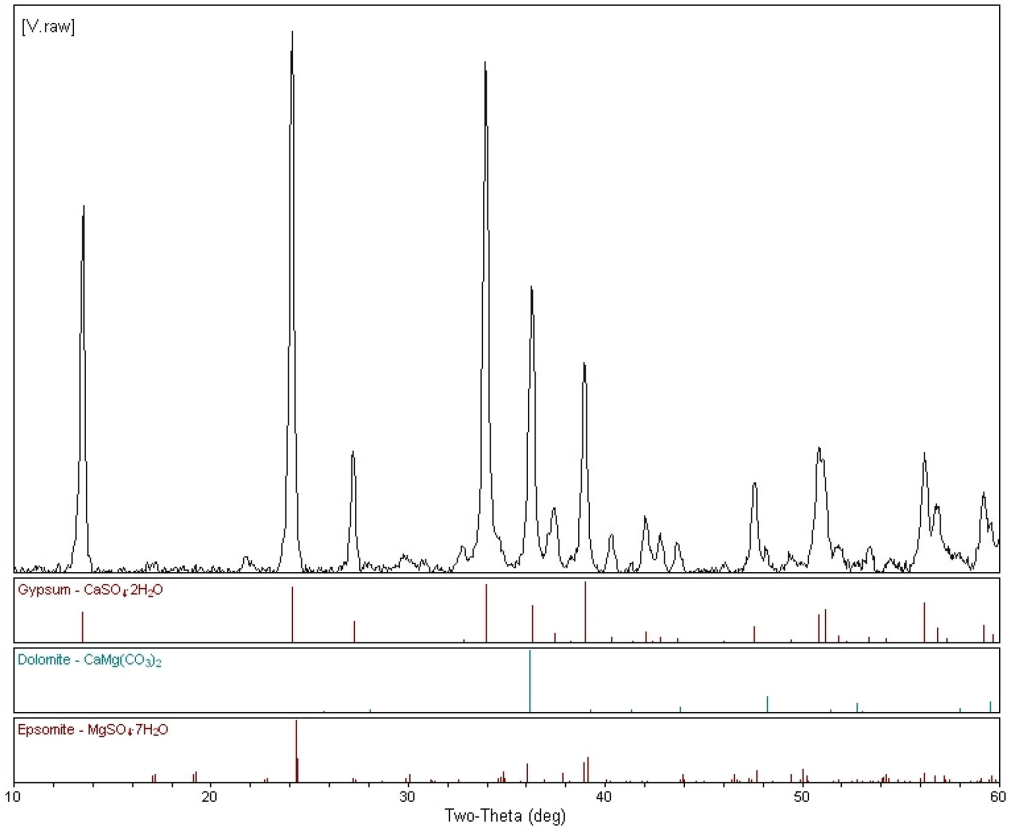

Figure 33. Vole Cave Ceiling XRD Results. This sample mostly contains gypsum indicated by the 14º 2Θ, 22º 2Θ, and 34º 2Θ peaks. Traces of dolomite (~36º 2Θ peak) are found and perhaps epsomite (~22º 2Θ peak).

Cave "Ledge"

Megascopically, the carbonate layer is dark gray mudstone. The "ledge" lithology ranges from dolomicrite to laminated peloidal dolomicrite (Figure 32B). The matrix is composed of anhedral dolomite crystals measuring up to 1 mm and composes > 90% of the samples. These crystals are sucrosic near the base and progressively increase in secondary granular gypsum and iron-oxides moving stratigraphically upward. Euhedral

dolomite cements measuring up to 1 mm commonly fill pores. Staining indicates the presence of dolomite, which is confirmed by XRD analysis (Figure 34).

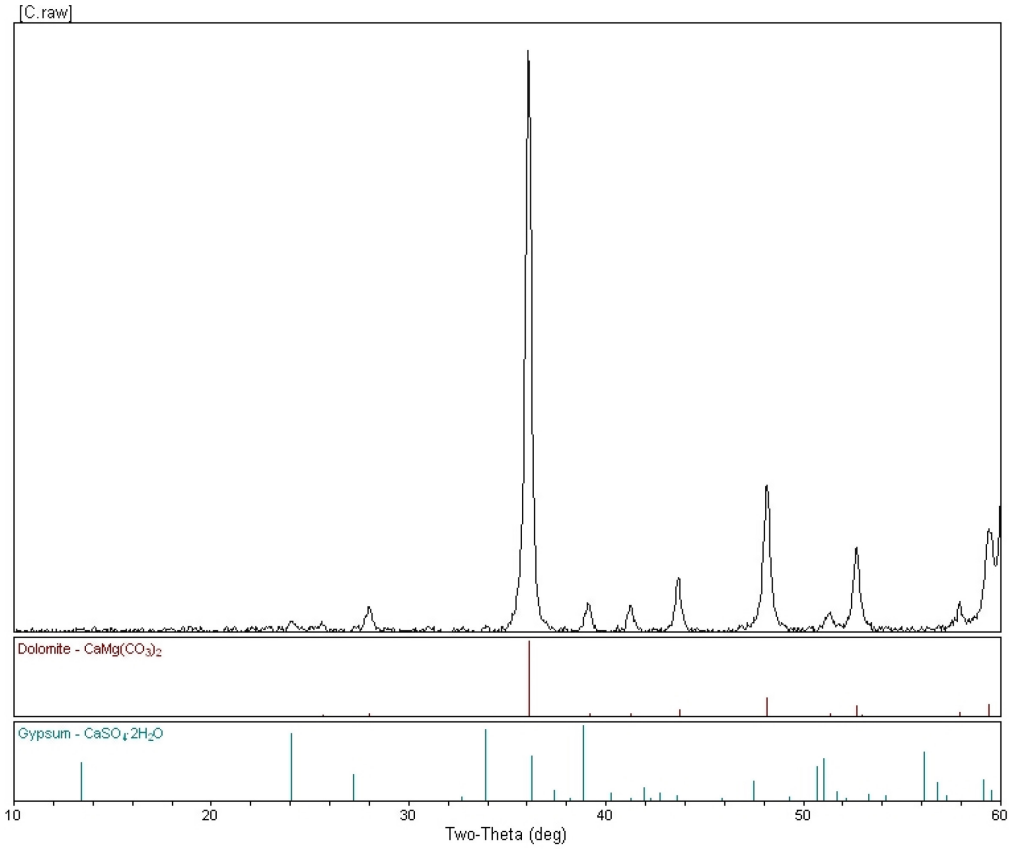

Figure 34. Colossus Cave "Ledge" XRD Results. This sample mostly contains dolomite indicated by the 36º 2Θ peak. Traces of gypsum (~34º 2Θ, 36º 2Θ, and 39º 2Θ peaks) are also found.

Cave Wall

Megascopically, the cave wall is composed of red to bleached gray shale interbedded with satin spar gypsum stringers and selenite gypsum crystals. Samples were obtained from more indurated shale units within the cave passage. Sampling was biased due to poor induration and friability. In thin section, secondary granular gypsum

composes > 90% of the bulk mineralogy. Subhedral satin spar gypsum laths measuring up to 2 mm are found. Subhedral to anhedral dolomite (1 mm) are found. Euhedral anhydrite ghosts are replaced with secondary granular gypsum (Figure 32C). Insoluble iron-oxides commonly fill fractures. XRD analysis indicates the cave wall is mostly composed of dolomite and gypsum with the presence of quartz, calcite, and possibly epsomite (Figure 35).

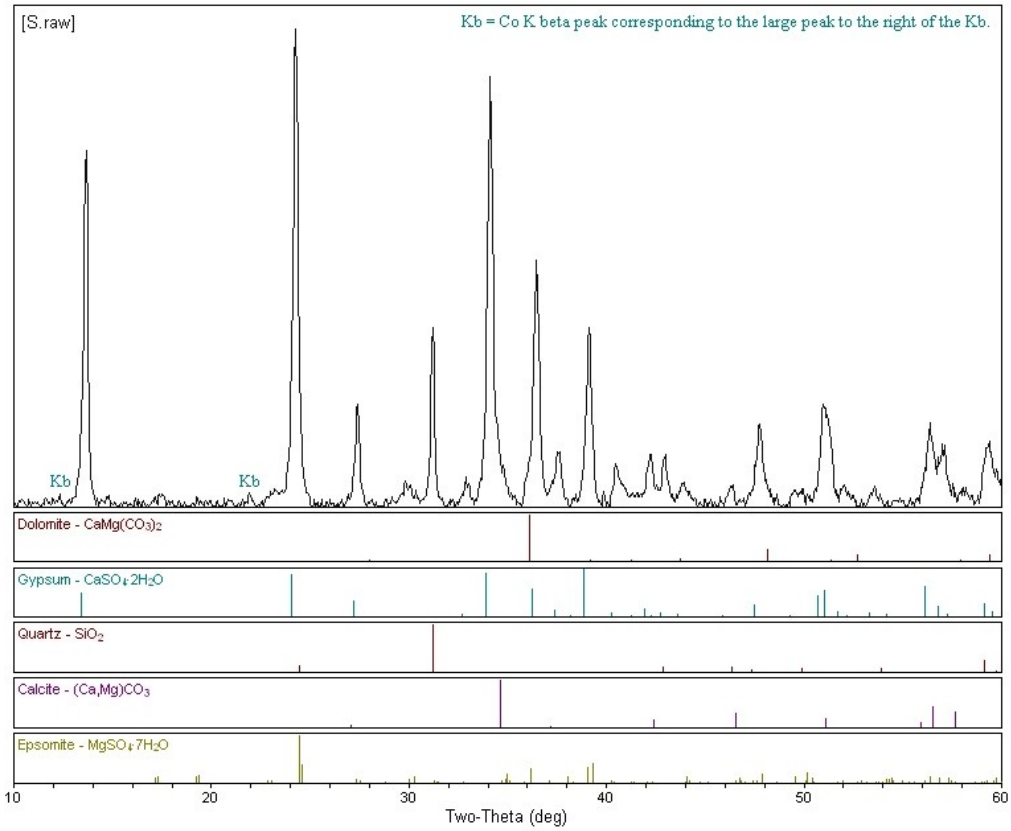

Figure 35. Cave Wall XRD Results. This sample mostly contains dolomite indicated by the 36 2Θº peaks. Traces of gypsum (~34 2Θº, 36 2Θº, and 39 2Θº peaks), quartz (32 2Θº peak), and calcite (34 2Θº peak) are found and perhaps epsomite (~22 2Θº peak).

CHAPTER VI

DISCUSSION

6.1 Speleogenesis

Cave formation in these study areas in Barber County is primarily the result of aggressive waters infiltrating through joints in the gypsum and encountering an impermeable boundary layer (shale). Speleogenesis appears to be controlled by the geologic contact between the Medicine Lodge Gypsum and Flowerpot Shale, which prevents infiltrating waters from moving vertically downward. Water begins moving along higher permeable joint networks within the Medicine Lodge Gypsum. Solutionally enlarged joints observed on the surface follow the same trend as jointing observed within cave passages (Figure 16). Proto-conduits can be seen in the Medicine Lodge Gypsum/Flowerpot Shale contact outcrops where a conduit develops as surface water can no longer move downward (Figure 14). In these locations, surface water is pirated (diverted) through solutionally enlarged joints and forms conduits within the Medicine Lodge Gypsum (Figure 21). As this process continues, larger voids develop, forming the caves observed today in the study areas.

The conduit entrenches into the underlying carbonate layer (Figure 14). This carbonate layer forms a resistant ledge that is present in every cave. Further entrenchment into the underlying Flowerpot Shale widens the cave passage, creating the “ceiling channel” appearance.

6.1.1 Petrographic Controls on Cave Formation

XRD and petrographic observations of the carbonate layer agreed with Fay's (1964) observations of dolomite and gypsum in the region. Fay (1964) described the basal dolomite layer as the Cedar Springs Dolomite, which is an oolitic dolomudstone grading into a pelletoid dolomitized mudstone. Petrographic observations did not support the presence of ooids; however, pelloids were observed (Figures 32C, D). For these sites, this basal carbonate unit is established as the Cedar Springs Dolomite based on XRD and petrographic observations. Benison et al. (2015) reports XRD and petrographic observations of the Cedar Springs Dolomite as lacking dolomite, but instead the "dolomite" contained calcite-rich *Microcodium* structures. The petrographic findings of this study suggest that Benison et al. (2015) were not at the geologic contact between the Medicine Lodge Gypsum and Flowerpot Shale or that there were significant diagenetic differences between outcrops and core between Benison et al's (2015) study and this study. Overall, the stratigraphy of southcentral Kansas is difficult to correlate due to the high solubility of the gypsum and underlying gypsiferous shale coupled with subsurface variations between thickness and lithology across the region of the Red Hills. Caves in this study are interpreted to dominantly form at the geologic contact between the Medicine Lodge Gypsum and Flowerpot Shale. The presence of such karst features may be a key observation in determining the stratigraphic position of strata within the region.

6.1.2 Other Speleogenetic Controls

It appears that the dominant control on cave formation is the geologic contact between the Medicine Lodge Gypsum, Cedar Springs Dolomite, and Flowerpot Shale.

The relationship between cave formation and cave elevation cannot be determined at this time due to the lack of precise cave elevations and the limited number of caves in the sample set (Figure 19). Larger sample sizes can delineate if a relationship between cave elevation and cave formation exists. It is likely that a relationship between elevation and cave formation will not exist due to the dip of the geologic contact that is proposed to control cave formation. The regional dip of this geologic contact is approximately 11º to the southwest. The combination of dipping geologic strata and irregular surface denudation will likely produce no significant elevation control on cave formation (or an elevation where one would expect to find cave entrances).

All cave passages surveyed in this study had a strong influence of joints, indicating a control on passage morphology. The average passage orientation is 134º. Cave passages do not follow the regional dip and are largely controlled by joint sets oriented along 040º and 080º (Figure 17). The regional strike is 169º and also appears to have control on some passage orientation. This is a common phenomenon in joint controlled karst systems where water dissolves along dip within joints and then turns to follow strike when encountering the local water table (Palmer, 1991). Currently, there have been no documented studies on joint sets in Barber County and future work should document these structural features of the area.

6.2 Speleogenetic Model for the Study Area

Young and Beard (1993) propose a simplistic model for Kansas gypsum speleogenesis (Figure 36). In this model, surface streams are partially robbed of flow by surficial joints in the exposed gypsum. A simplistic model for this area's gypsum

speleogenesis is proposed (Figure 36). Cave passage morphology is controlled by solutionally enlarged joints that transmit the overlying mantled material and allogenic water into conduits. Proto-conduits develop at the base of the Medicine Lodge Gypsum and reach the resistant Cedar Spring Dolomite as seen in outcrops (Figure 22). Vadose entrenchment through the Cedar Springs Dolomite forms a resistant ledge (Figure 14). Further entrenchment into the Flowerpot Shale results in mechanical erosion of the shale layers and dissolution of interstratal gypsum stringers. Cave passage morphology is influenced by the differential erosion between the Flowerpot Shale and the Cedar Springs Dolomite.

This study agrees with, and builds upon Young and Beard's (1993) model for Kansas gypsum speleogenesis and resulting geomorphology of the area based on field observations. Surface streams are partially pirated by surficial joints in the exposed gypsum and fully pirated into enlarged joints that flow through caves and exit into the walls of a canyon. In the field, sinkholes and caves form at the upstream end of dendritic canyons and appear to pirate surface water and mantled soil.

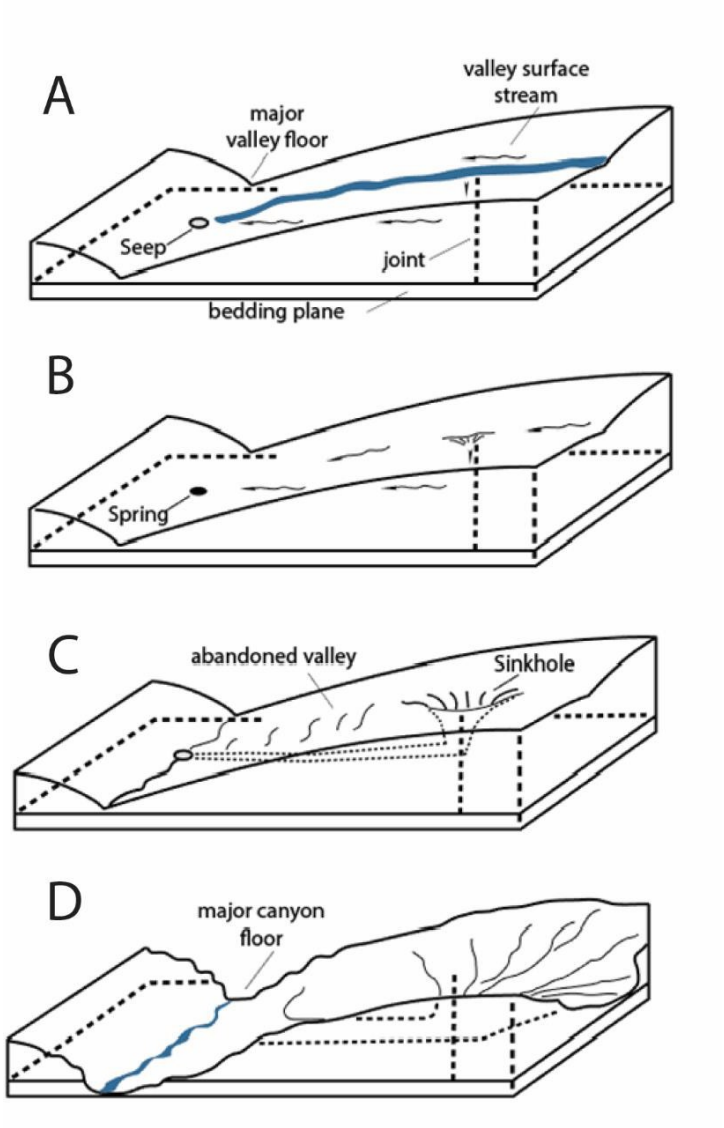

Figure 36. Kansas gypsum speleogenesis model by Young and Beard, 1993. Where (A) shows where a surface stream is partially robbed of flow by joint in gypsum. (B) More surface water is pirated as joints and bedding plane are enlarged. (C) All water is pirated by enlarged joint- determined sinkhole. (D) Cave as seen today.

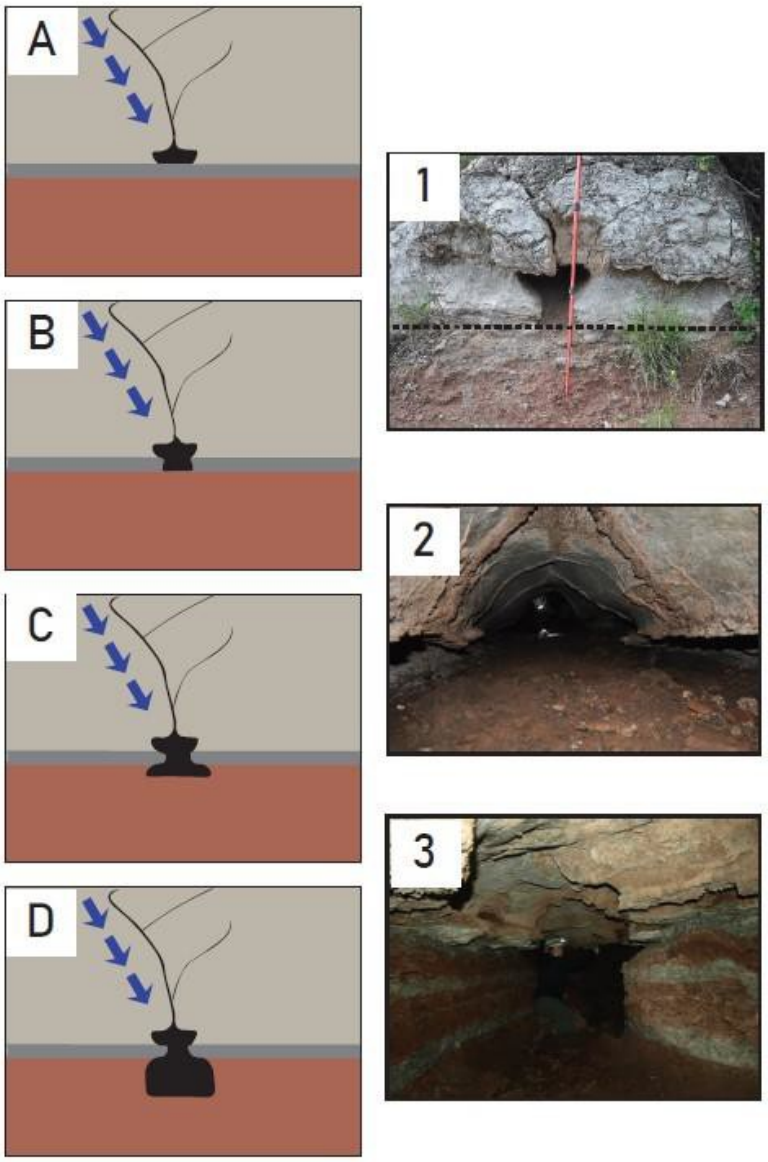

Figure 37. Simplistic model depicting gypsum speleogenesis in Barber County. A) Surface fractures and solutionally enlarge joints. Shown in 1. A proto-channel develops at the geologic contact between the Medicine Lodge Gypsum and Flowerpot Shale (approximate contact in dashed line). B) Vadose entrenchment into the underlying Cedar Springs dolomite layer. The dolomite forms a resistant ledge seen in 2. C) Further vadose entrenchment into the underlying Flowerpot shale mechanically erodes the shale nearest the dolomite ledge. D) This erosion widens the passage. Erosion and dissolution of gypsum further entrenches the passage seen in 3.

Field reconnaissance also determined that the upstream end of every erosional valley did not reveal a new cave as Young and Beard (1993) proposed. Exposed outcrops of gypsum in the Southwestern portion of Property One did not contain caves. This area has been interpreted to be higher in the Blaine stratigraphic section, too high above the geologic contact for cave formation. Aerial imagery shows an abundance of exposed gypsum bedrock in the Southwest region (Property One); however, the geologic contact between the Medicine Lodge Gypsum, Cedar Springs Dolomite, and Flowerpot Shale was also not present. As documented in this study, cave formation is heavily dependent upon this geologic contact between bedding planes, and no cave features are found without this geologic contact.

The visualization of karst feature locations by the use of GIS determined caves are typically positioned near the upstream end of erosional valleys where gypsum bedrock is exposed. Multiple insurgence points found on the plateaus likely drain into these solutional features and into cave systems below (Figures 24-29). Remnant caves, or shelter caves, are often found along the walls of steep sided canyons (Figure 26).

Cave entrances were initially spotted during reconnaissance where red cedar trees would cluster. Red cedar trees are great indicators of water in the semiarid terrain of southcentral Kansas. Caves drain the plateaus as rainfall is funneled into the caves and ends in karst-spring resurgences.

6.3 Specific Features Inside Caves

All of the cave passages are oriented along ceiling fractures (Figure 15). Dead-end cross-passages enlarged along ceiling fractures are also common. Bedding plane

anastomoses are observed in Mountain Lion Cave, where a section of the passage is devoid of fractures. Anastomoses indicate episodes of flood waters being injected into joints and bedding planes. These features indicate a phreatic phase of interstratal dissolution before stream entrenchment and vadose overprinting.

Field reconnaissance in the first section of Property One revealed three cave systems: Acorn Cave, Second Opportunity, and a collapsed cave that likely represents an extension of Second Opportunity Cave (Figure 38). Second Opportunity has two entrances located within a sinkhole. Most of the overlying gypsum has since collapsed. This sinkhole represents a larger cave system that has since been unroofed. It is believed that Second Opportunity was once connected to the collapsed cave where water drained into the canyon.

Many of the caves found within sinkholes have features that suggest ceiling collapse. Many of these caves have ceiling fractures that extend upward and breaches the surface resulting in a collapse sink. Multiple caves have been segmented by cave collapse.

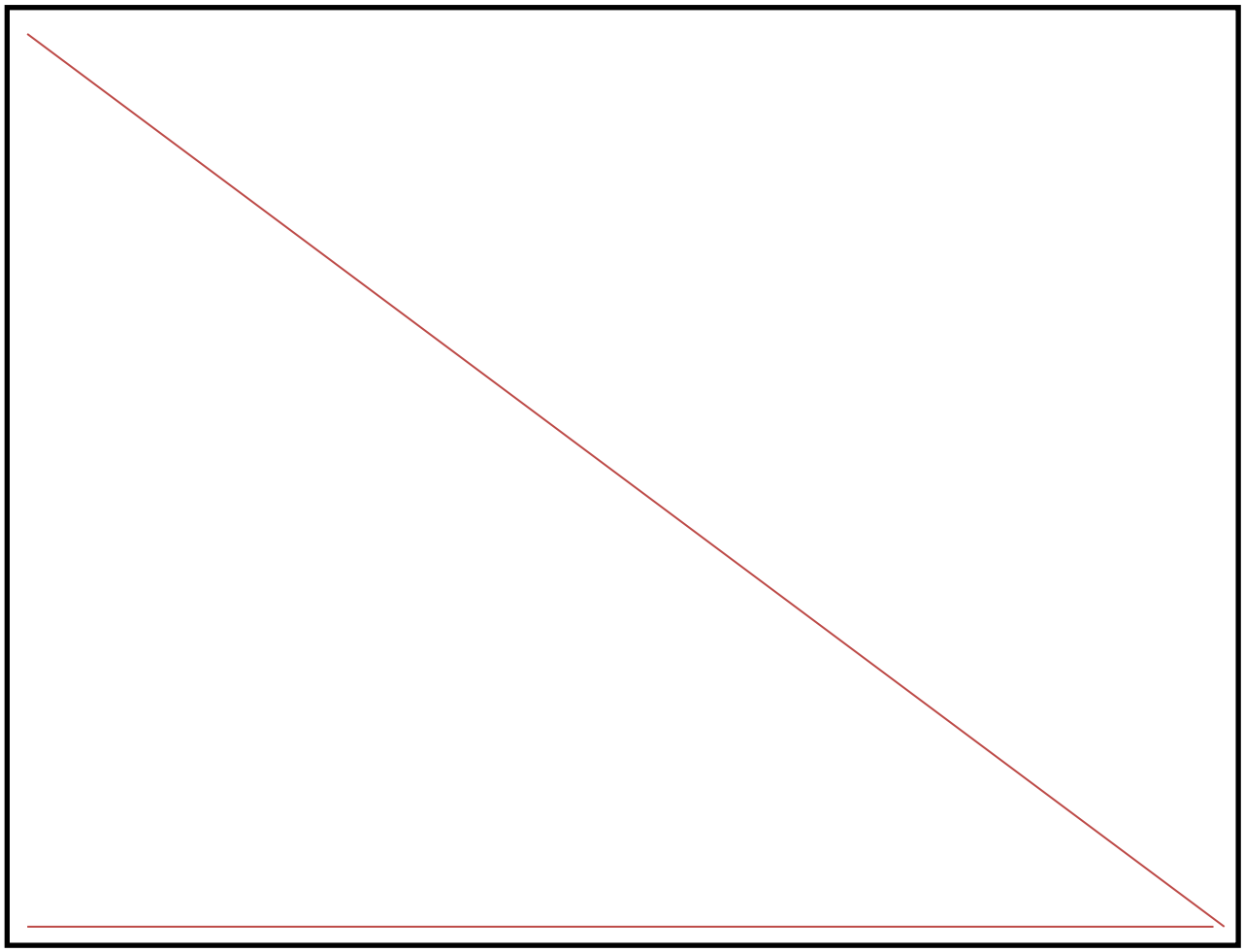

Property One contains a major sinkhole complex that includes up to four known caves: Misery Pit, Mountain Lion, Rocky Road, and Connection. This cave complex was once likely connected as a single cave system and was later exposed at the surface by collapse and surface denudation. Mountain Lion Cave contains a vadose shaft that connects to the surface via solutionally enlarged fractures. Additionally, Mountain Lion Cave appears to pirate surface water that flows toward Monkey Cave, where it empties into the canyon (Figure 39). This suggests a possible hydrological connection between these caves. Future studies are necessary to determine whether a hydrological connection exists, and if other sinkhole complexes in the area behave in the same manner.

This region, and particularly its sinkhole complexes, may serve as a real-time example of how the landscape evolves over time, especially considering that gypsum cave formation can be observed over a human's lifetime (Gutierrez & Cooper, 2013). After a sinkhole complex forms, mantled soil material sloughs off the hillslope and is funneled into the complex (Figure 20). All of the caves in the sinkhole complex are heavily choked with sediment. For example, Mountain Lion Cave was excavated another 300 feet (91 m) during exploration with a continuing survey lead. Mountain Lion Cave continues for another 100 feet (30 m) until the cave passage becomes too tight for humans to continue without further sediment excavation.

6.4 Cave Passage Morphology

Almost all caves contain similar passage features such as proto-conduits in the ceilings formed within the gypsum, a resistant carbonate ledge protruding out into the passage, and an underlying red shale bed with multiple satin spar stringers and selenite crystals (Figure 38). Three of the most notable caves containing these features include: Mountain Lion Cave, Monkey Cave, and Vole Cave (Figure 14). These caves contain keyhole passages within the gypsum, carbonate, and shale and represent different stages of cave development. Sections of cave passage through the gypsum member are narrow (<2 feet) and canyon-like with scallop marks indicating vadose down-cutting of aggressive meteoric waters. Flood waters increase the hydraulic head and sediment load that corrade (corrosion by abrasion) and widen the passage walls. Evidence of corrasion can be seen in every cave where sections of Flowerpot Shale are calving away from the wall.

The ceiling height of Mountain Lion Cave ranges from less than one foot up to greater than six feet (where the vadose shaft is located). Ceiling proto-conduits are observed in the gypsum where the underlying carbonate protrudes out into the passage. The exposed thickness within caves of the underlying Flowerpot Shale ranges in thickness from one inch to one foot where water has further entrenched the passage. This downward entrenchment represents a change in cave formation from dissolution to the combination of dissolution and mechanical erosion (Figure 39). Cave passages are often wider than the ceiling height due to the corassion of the shale. In many caves, the majority of the ceiling is flat and consists of the basal dolomite unit except where the passage is cut by

the ceiling proto-conduit (Figure 40). This unit is typically thin (<2 inches up to 5 inches) and results in ceiling collapse.

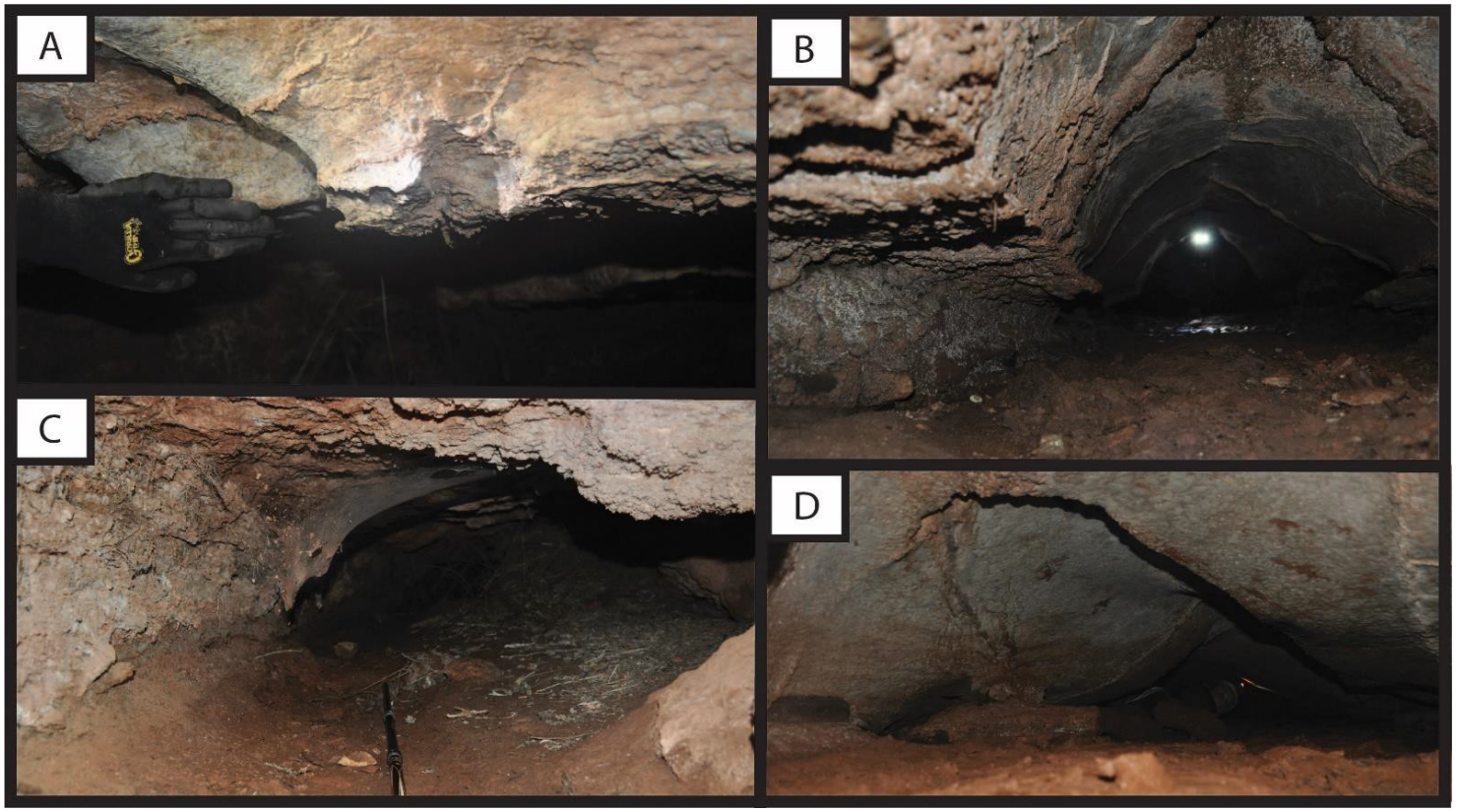

Figure 39. Distinctive cave features. A) Vole Cave. Anastomoses within gypsum. B) Mountain Lion Cave. Ceiling conduit following a ceiling fracture. The carbonate ledge can be seen protruding out into the cave passage. C) Gary's Tube. The ceiling is composed of carbonate with no noticeable fractures or joints observed. D) Mountain Lion Cave. Meandering ceiling conduit following intersecting joint sets in the ceiling.

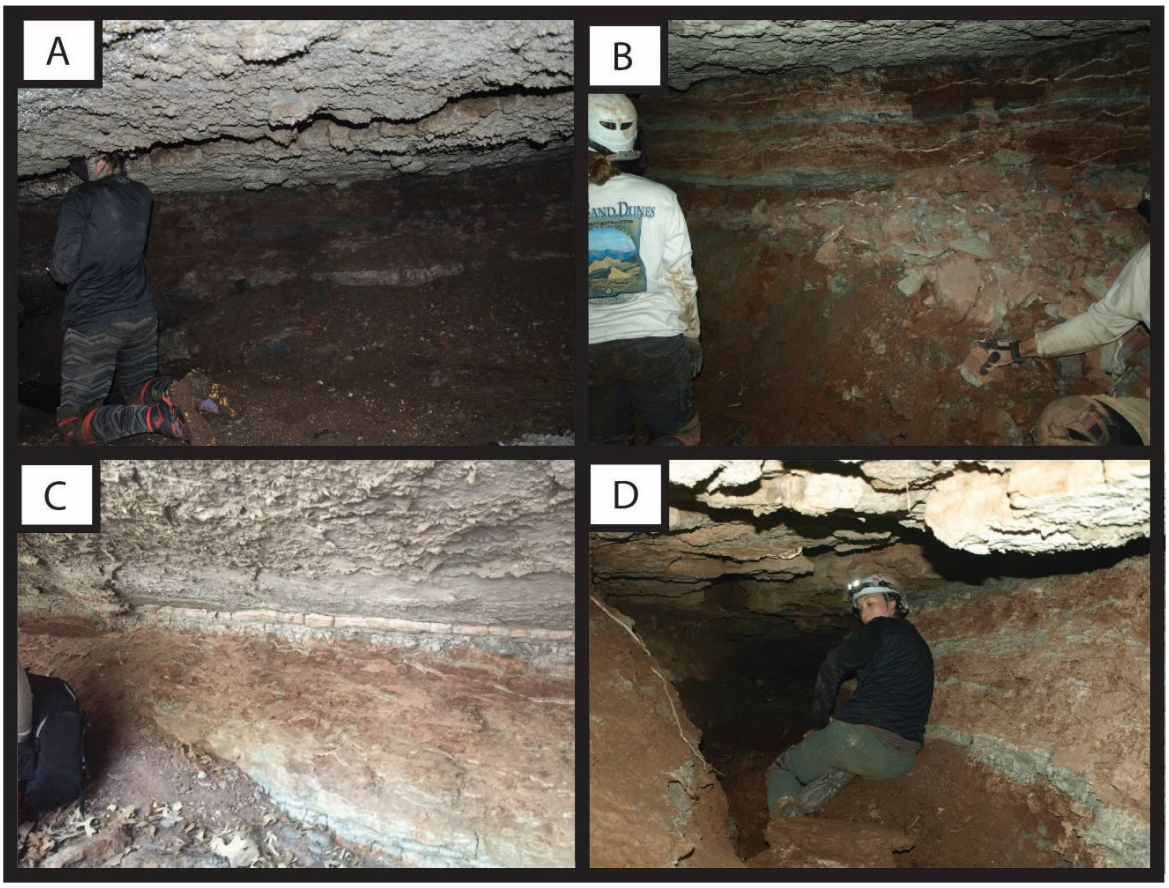

Figure 40. Cave passage entrenchment into the underlying shale unit. A) Dugout Cave. The ceiling is composed of gypsum grading into carbonate. The cave walls are composed of highly friable red shale. B) Colossus Cave. The ceiling is composed of carbonate. The cave walls are composed of red shale with multiple gypsum stringers and selenite crystals. C) Dead Tree Cave. The ceiling is composed of gypsum. A resistant carbonate ledge is sandwiched between the ceiling unit and the underlying shale unit. D) Vole Cave. The ceiling is composed of gypsum and grades into a resistant carbonate ledge. The underlying shale contains abundant satin spar stringer and selenite crystals.

In Monkey Cave, the same cave passage morphology is observed. The exposed thickness of the Flowerpot Shale is greater (one to three feet). The Flowerpot Shale is entrenched so that the cave walls are slightly straight, resembling a square passage

(Figure 14B). The cave walls contain abundant satin spar stringers that can be dissolved away leaving friable shale behind. It is common for cave floors containing sediment banks of satin spar gypsum, selenite gypsum, and clasts of shale. The remaining shale in the cave walls are mechanically eroded out, which further entrenches the cave. This widening by mechanical erosion produces the square passage shape.

In Vole Cave, the exposed thickness of the Flowerpot Shale is substantially larger (3 feet) (Figure 14B). Again, the same passage morphologies are observed, and the Flowerpot Shale is considerably entrenched (Figure 40D). This cave is a through cave, where an insurgence point (sinkhole) connects one end of the cave to the entrance near the wall of a canyon. The cave morphology seen in Vole Cave represents and end member of speleogenesis progression in the area. Any further entrenchment creates unstable cave conditions leading to collapse.

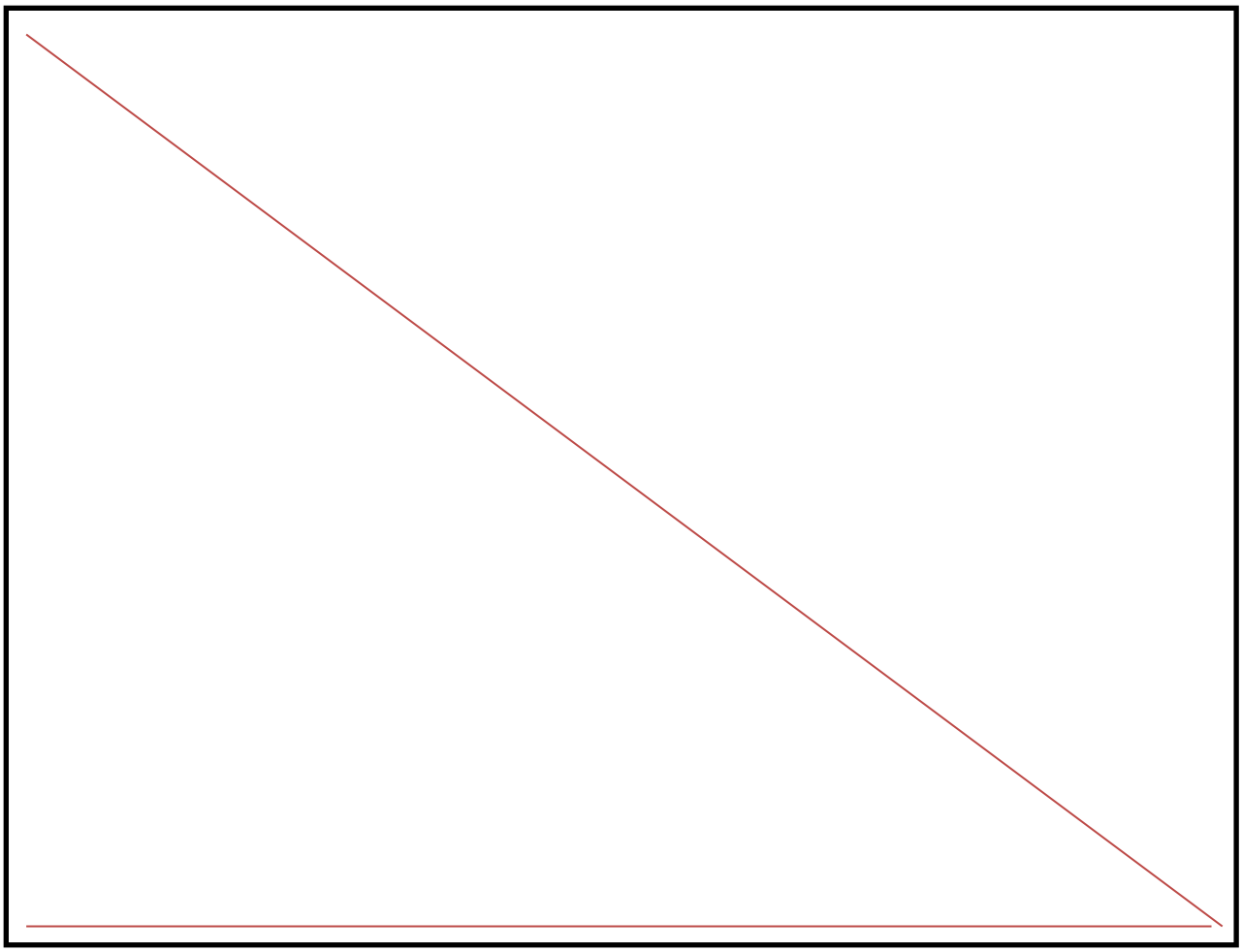

6.5 Other Features

Remnant caves, or shelter caves, border most erosional valleys, are relatively small, and contain the same geologic contact relationship as solutional caves. These caves are interpreted to represent larger caves that have been lost to cliff retreat. This process is evident by the large boulders found on the valley floors that are composed of Medicine Lodge Gypsum (Figure 42). Property One contains several shelter caves along erosional valleys where insurgences and caves are located upstream (Figure 24).

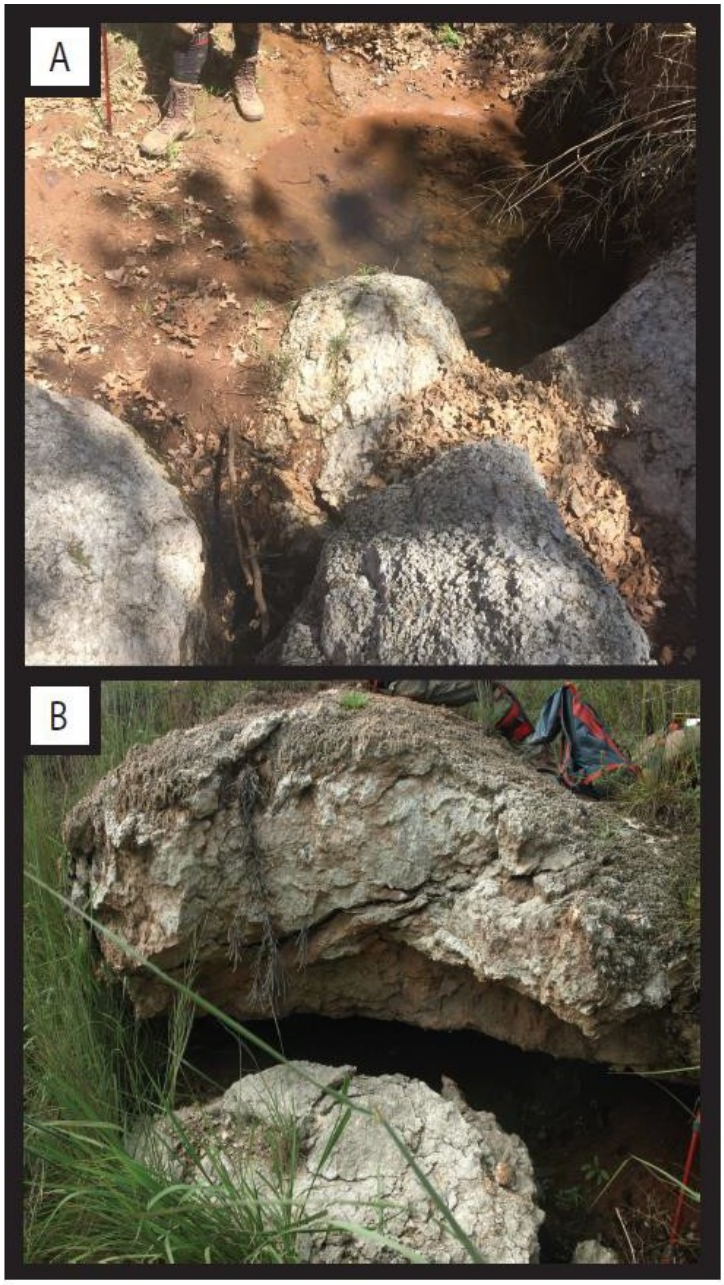

Figure 42. Evidence for cliff retreat. A) Large boulders composed of Medicine Lodge Gypsum at the bottom of a canyon. Boulders are surrounding a spring. B) Shelter cave found along the canyon wall.

Many of the stream beds located at the bottom of the canyons are intermittent, insurgences and resurgences commonly dot the stream bed. Several caves are found within incised meanders at the bottom of canyons. These caves have morphologies and relationships to streams that are interpreted to represent the cut off of meander bends as a karstic bypass of the meanders developed in the gypsum canyon wall.

Other karst features observed on exposed bedrock are rillenkarren, microkarst features, collapsed caves, and pseudokarst. Rillenkarren are observed where gypsum bedrock is exposed without overlying mantled material and where there exists a steep hydraulic gradient for rills to form (Figures 43A, B). Microkarst features were found atop the buttes and mesas where the gypsum is exposed. These features are categorized by small (< two inches up to six inches in diameter), nearly round conduits that may be observed with surface fractures (Figures 43C, F). Some of these features are interpreted as expansion blisters caused by the dehydration of gypsum (Figure 43F). Collapsed caves are commonly found near the bottom of erosional valleys where surface denudation has breached the cave. These caves retain the same features as other caves in the area; however, they are not enterable due to safety concerns (Figures 43D, G). Pseudokarst are found in the gypsiferous soil and occasionally in the overlying sandstone units (known as tafoni caves) (Figure 43E).

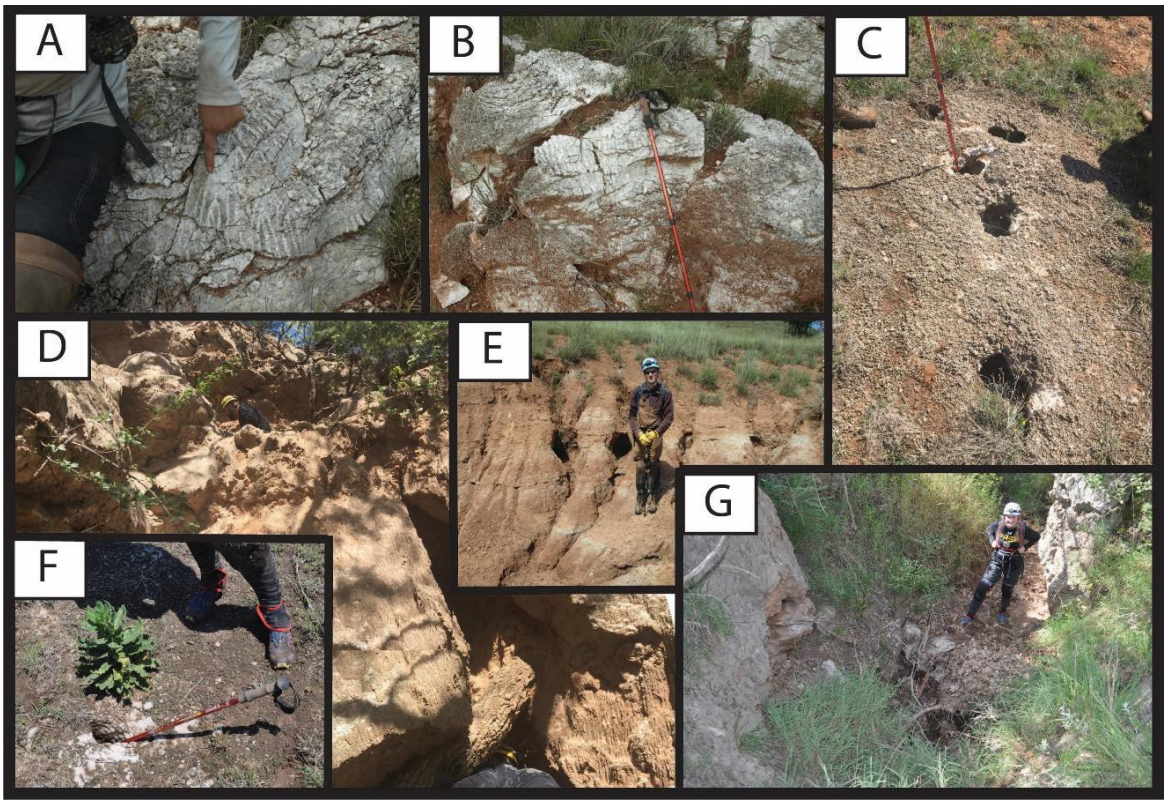

Figure 43. Other Karst Features. A) and B) Rillenkarren on gypsum bedrock. C) Microkarst feature on gypsum bedrock with little to no mantled material. D) Collapsed cave possibly associated with Second Oppurtunity Cave. E) Pseudokarst features in the gypsiferous mantled material. F) Microkarst feature with associated surficial fracture. G) Collapsed cave entrance near the bottom of an erosional valley. This cave is associated with the major sinkhole complex on Property One.

6.6 Differences between Study Locations

Property Two is noticeably different than Property One with respect to the amount of mantled material and the expression of sinkholes. The abundance of mantled material in Property Two appears to lead to less surface expression of caves. Instead, Property Two contains far more sinkholes than Property One. The sinkholes on Property Two appear to be related to cover collapse conditions of the thicker mantled material that is undercut by cave conduits, eventually leading to collapse that reaches the surface.

The Gypsum Hills are marked by slump structures from the dissolution of underlying halite that warp overlying beds (Benison et al., 2015). Future studies should investigate the overall structural relationship between cave formation and regional slump structures to determine if these factors control passage orientations. These slump structures may also alter the local dip and groundwater flow that may also influence karst development.

CHAPTER VIII

CONCLUSIONS

This survey of caves and karst landforms adds significantly to the basic knowledge of the geology of the Gypsum Hills. Field observations indicate cave formation is dependent on (1) the geologic contact between the Permian Blaine Formation and the underlying Flowerpot Shale, (2) the amount and type of surficial mantle material, and (3) fractures in the bedrock for subsurface flow.

Fractures pirate surface water into joints or insurgences. Solutionally enlarged joints are necessary for enlargement of solutional sinks or conduits. Proto-conduits form at the base of the Medicine Lodge Gypsum and entrench into the underlying carbonate layer. Resistant carbonate ledges underlying the Medicine Lodge Gypsum were determined to be the Cedar Springs Dolomite as described by Fay (1964). Further entrenchment into the underlying Flowerpot Shale widens the passage by mechanical erosion and dissolution of satin spar gypsum stringers.

Various sinkhole morphologies, formed by the amount and type surficial mantle material, were identified on the two properties studied. Property One has slightly mantled bedrock with a thin, clay loam, whereas Property Two has highly mantled bedrock with a thicker sandy loam. Sinkhole complexes are found in the exposed gypsum bedrock near the top of valleys and are commonly associated with cave entrances. Similar complexes are not found on Property Two, likely due to the thicker mantled material burying these complexes.

Petrologic and XRD observation confirm the presence of dolomite and inclusions of gypsum within the carbonate ledge layer. This carbonate ledge layer, which is found in every cave, was interpreted to be the Cedar Springs Dolomite as described by Fay (1964). Ooids and *Microcodium* structures were not observed as described by Fay (1964) and Benison et al. (2015), respectively. This dolomite layer marks the change in passage morphology and appears to play a key role in speleogenesis in the area.

The distribution of karst features is controlled by stratigraphy and surface denudation. Insurgent cave entrances are found where bedrock is thinly mantled and are often associated with sinkhole complexes that remove mantled material. Resurgent cave entrances occur in valley walls. Caves preferentially form at the geologic contact between the Medicine Lodge Gypsum and Flowerpot Shale and contain similar passage morphologies (i.e. proto-conduits, carbonate ledges, widened cave wall). Stratigraphy is difficult to determine due to the fast rate of erosion of gypsum and shale beds; however, the presence of cave features at this geologic contact is a new tool to help when determining stratigraphy in the region. These cave features may be also found in core as paleokarst surfaces.

Property Two has far more land than Property One. This study primarily explores cave development on Property One, and sinkhole development on Property Two. Further cave exploration on Property Two is necessary. More caves and karst features are needed to delineate the region's karst development, develop predictive karst models, and begin to develop karst management systems.

This study of the caves and karst of Barber County is a valuable addition to the limited literature in this region and also that it can act as a foundation for much needed further investigation. Future research including dye tracing, shallow geophysical exploration, sinkhole distribution, structural features, and petrographic controls on speleogenesis will be built upon this research.

LITERATURE CITED

Access, K.D. (2011). Support Center. State of Kansas GIS Data Access & Support Center.

Audra, P. and Palmer, A. (2011). The pattern of caves: Controls of epigenic speleogenesis. Géomorphologie : relief, processus, environnement. p 359-378. doi:10.4000/geomorphologie.9571.

Auler, A. and Smart, P. (2003). The influence of bedrock-derived acidity in the development of surface and underground karst: Evidence from the Precambrian carbonates of semi-arid northeastern Brazil. Earth Surface Processes and Landforms. v. 28. p. 157 - 168. Doi: 10.1002/esp.443.

Baars, D.L. (1990). Permian chronostratigraphy in Kansas. Geology 18, p. 687–690

Bachman, G. O., and Johnson, R. B. (1973). Stability of salt in the Permian Salt Basin of Kansas, Oklahoma, Texas and New Mexico: U.S. Geol. Survey, Open File Report 73-14, 66 p.

Benison, K.C. (1997a). Field descriptions of sedimentary and diagenetic features in red beds and evaporites of the Nippewalla Group (middle Permian), Kansas and Oklahoma: Kansas Geological Survey, Open File Report 97-21, 62 p.

Benison, K.C. (1997b). Acid lake and groundwater deposition and diagenesis in Permian red bed-hosted evaporites, midcontinent, U.S.A. [unpublished Ph.D. dissertation]: The University of Kansas, Lawrence, KS, 480 p.

Benison, K.C. (2013). Acid saline fluid inclusions: examples from modern and Permian extreme lake systems: Geofluids, v. 13, p. 579-593.

Benison, K.C., and Goldstein, R.H. (2000). Sedimentology of ancient saline pans: an example from the Permian Opeche Shale, Williston Basin, North Dakota, USA: Journal of Sedimentary Research, v. 70, p. 159-169.

Benison, K.C., and Goldstein, R.H. (2001). Evaporites and siliciclastics of the Permian Nippewalla Group of Kansas, USA: a case for non-marine deposition in saline lakes and saline pans: Sedimentology, v. 48, p. 165-188.

Benison, K.C., and Goldstein, R.H. (2002). Recognizing acid lakes and groundwater in the rock record: Sedimentary Geology v. 151, p. 177-185.

Benison, K.C., Goldstein, R.H., Wopenka, B., Burruss, R.C., and Pasteris, J.D. (1998). Extremely acid Permian lakes and groundwaters in North America: Nature, v. 392, p. 911-914.

Benison, K.C., Zambito, J.J., Soreghan, G.S., Soreghan, M.J., Foster, T.M., and Kane, M.J. (2013). Permian red beds and evaporites of the Amoko Rebecca K. Bounds core, Greely County, Kansas: implications for science and industry, in Dubois, M.K., Watney, W.L., and Tollefson, J., eds., Mid-Continent Core Workshop: from Source to Reservoir to Seal: Mid-Continent Section American Association of Petroleum Geologists, Kansas Geological Survey, Wichita, Kansas, p. 9-14.

Benison, K.C., Zambito, J.J., and Knapp, J. (2015). Contrasting Siliciclastic-Evaporite Strata in Subsurface and Outcrop: An Example from the Permian Nippewalla Group of Kansas, U.S.A., Journal of Sedimentary Research, doi:10.2110/jsr.2015.43.

Blount, C. W. and Dickson F. W. (1973). Gypsum-Anhydrite equilibria in systems CaSO,- H2O and CaSO,--NaCI-H,O. Am. Mineral. 58, 3233331.

Bozeman, S. (1987).The D.C. Jester Cave system: Central Oklahoma Grotto, Oklahoma City, Oklahoma Underground, v. 14, 56 p.

Bozeman, J. and Bozeman, S. (2002). Carbonates Evaporites v. 17: 107 p.

Calaforra, J.M. (1998). Karstologia de yesos: Ciencia y Techologica Monografia 3, Instituto de Estudios Amerienses, Univ. of Almeria, Spain, p. 384.

Campbell, C. L. (1963). Permian evaporites between the Blaine and Stone Corral Formations: Unpub. M.S. thesis, Univ. Kansas, 73 p.

Compass. (2018). Compass, http://fountainware.com/compass/ Accessed 5/9/2018.

Cragin, F. W. (1896). The Permian System in Kansas: Colorado College Studies, v. 6, p. 1-48.

Dasher, G. R. (1994). On Station. Huntsville, Alabama 35810-4431, USA: National Speleology Society, Inc.

Dickson, John. (1966). Carbonate Identification and Genesis as Revealed by Staining. Journal of Sedimentary Research - J SEDIMENT RES. 36. doi:10.1306/74D714F6-2B21-11D7-8648000102C1865D.

Evans, Noel (1931). Stratigraphy of Permian beds in northwestern Oklahoma: Am. Assoc. Petroleum Geologists Bull., vol. 15, pp. 405-439.

Fay, R. O. (1964) The Blaine and related formations of northwestern Oklahoma and southern Kansas: Oklahoma Geol. Survey, Bull. 98, 238 p.

Ford, D.C., and Williams, P.W. (1989). Karst Geomorphology and Hydrology. Academic Division of Unwin Hyman Ltd, London. p. 601.

Foster, T.M. Soreghan, G.S., Soreghan, M.J., Benison, K.C., and Elmore, R.D. (2014). Climatic and palaeogeographic significance of aeolian sediment in the Middle Permian Dog Creek Shale (Midcontinent U.S.A.): Palaeogeography, Palaeoclimatology, Palaeoecology, v. 402, p. 12-29.

Glennie, K.W. (1987). Desert sedimentary environments, present and past: a summary: Sedimentary Geology, v. 50, p. 135–165.

Golonka, J., Ross, M.I. and Scotese, C.R. (1994). Phanerozoic paleogeographic and paleoclimatic modeling maps. In: Pangea: Global Environments and Resources (Eds A.F. Embry, B. Beauchamp and D.J. Glass), Can. Soc. Petrol. Geol. Mem., v. 17, p. 1-47.

Golonka, J., and Ford, D. (2000). Pangean (Late Carboniferous–Middle Jurassic) paleoenvironment and lithofacies: Palaeogeography, Palaeoclimatology, Palaeoecology, v. 161, p. 1–34.

Gould, C. N. (1905). Geology and water resources of Oklahoma: U. S. Geol. Survey, Water-Supply Paper 148, p. 1-178.

Gunn, J. (1983). Point-recharge of limestone aquifers—A model from New Zealand karst: Journal of Hydrology, v. 61, p. 19–29.

Gustavson, T.C., Finley, R.J., and McGillis, K.A. (1980). Regional dissolution of Permian salt in the Anadarko, Dalhart, and Palo Duro basins of the Texas

Panhandle: Texas Bureau of Economic Geology Report of Investigations 106, 40 p.

Gutiérrez, F., and Cooper, A.H. (2013). Dealing with Gypsum Karst Problems: Hazards, Environmental Issues, and Planning. 10.1016/B978-0-12-374739-6.00106-8.

Ham, W. E. (1960). Middle Permian evaporites in southwestern Oklahoma: Internat. Geol. Congress, 21 St., Norden, Rept. Pt. 12, p. 138-151.

Hill, C.A. (1996). Geology of the Delaware Basin, Guadalupe, Apache and Glass Mountains: New Mexico and West Texas. Permian Basin Section – SEPM, Midland, TX, 480 p

Hills, J. M. (1942). Rhythm of Permian seas--a paleogeographic study: Am. Assoc. Petrol. Geologists, Bull., v. 26, p. 217-255.

Holdoway, K.A. (1978). Deposition of evaporites and red beds of the Nippewalla Group, Permian, western Kansas: Kansas Geological Survey, Bulletin 215, 43 p.

Hovorka, S.D., and Granger, A. (1988). Subsurface to surface correlation of Permian evaporites – San Andres – Blaine _ Flowerpot relationships, Texas Panhandle. In: MORGAN, W.A., & BABCOCK, J.A. (eds) Permian Rocks of the Midcontinent. Society of Economic Paleontologists and Mineralogists, Special Paper, v. 1, p. 137-159.

Johnson, K.S. (1967). Stratigraphy of the Permian Blaine Formation and associated strata in southwestern Oklahoma [PhD dissertation]. Champaign (IL): University of Illinois. 247 p.

Johnson, K.S., and Neal, J.T., (2003). Evaporite Karst and Engineering/ Environmental Problems in the United States. Oklahoma Geological Survey Circular, vol. 109. p. 353.

Johnson, K.S. (1972). Northwest Oklahoma; Book 2 of Guidebook for geologic field trips in Oklahoma. Oklahoma Geological Survey, Educational Publication 3. 42 p.

Johnson, K.S. (1981). Dissolution of salt on the east flank of the Permian Basin in the Southwestern U.S.A.: Journal of Hydrology, v. 54, p. 75–93.

Johnson, K.S. (1986). Hydrogeology and Recharge of a Gypsum - Dolomite Karst Aquifer in Southwestern Oklahoma, U.S.A.

Johnson, K.S. (1990a). Hydrogeology and karst of the Blaine gypsum-dolomite aquifer, southwestern Oklahoma.

Johnson, K.S. (1990b). Standard outcrop section of the Blaine Formation and associated strata in southwestern Oklahoma. Oklahoma Geology Notes. v. 50. p. 144-168.

Johnson, K.S. (1991). Guidebook for Geologic Field Trips in Oklahoma: Northwest Oklahoma: Oklahoma Geological Survey, Educational Publications, v. 3, 42 p.

Johnson KS. (1992). Evaporite karst in the Permian Blaine Formation and associated strata in western Oklahoma, USA. In: (Back W., Herman, J.S., & Paloc H., eds.): Hydrogeology of selected karst regions. International Association Hydrogeologists, 13, Verlag Heinz Heisse Publishing Co., Hannover, Germany, 405-420.

Johnson, K.S. (1996). Gypsum karst in the United States. International Journal of Speleology. 25. doi:10.5038/1827-806X.25.3.13.

Johnson, K.S. (2002). Karst in evaporite rocks of the United States. Carbonates and Evaporites. v. 17. p. 90-97. doi:10.1007/BF03176473.

Johnson, K.S. (2003). Evaporite karst in the Permian Blaine Formation and associated strata of western Oklahoma. Oklahoma Geological Survey, Circular 109. 41-55.

Johnson, K.S. (2011). Alabaster Caverns State Park---gypsum karst. Shale Shaker. 62. 108-112.

Jordan, L., and Vosburg, D.L. (1963) Permian Salt and Associated Evaporites in the Anadarko Basin of the Western Oklahoma–Texas Panhandle Region: Oklahoma Geological Survey, Bulletin 102, 76 p.

Kansas Geological Survey. (1997). Physiographic Map. Retrieved from http://www.kgs.ku.edu/Physio/redhills.html.

Kastning, E. H. (1977) Faults as positive and negative influences on ground-water flow and conduit enlargement, in Dilamarter, R. R. and Csallany, S. C., eds., Hydrologic Problems in Karst Regions: Bowling Green, Western Kentucky University, p. 193-201.

Klimchouk, A.B. (1996b). The typology of gypsum karst according to its geological and geomorphological evolution. In: Klimchouk, A., Lowe, D., Cooper, A., Sauro, U. (Eds.), Gypsum Karst of the World: Int. J. Speleology, 25, pp. 49–60.

Klimchouk, A.B. (2005). Conceptualization of speleogenesis in multistory artesian systems: a model of transverse speleogenesis. Int. J. Speleol. 34, 45–64.

Klimchouk, Alexander and D. Aksem, S. (2005). Hydrochemistry and solution rates in gypsum karst: Case study from the Western Ukraine. Environmental Geology. 48. 307-319. doi:10.1007/s00254-005-1277-3.

Klimchouk, A.B. (2007). Hypogene speleogenesis: hydrogeological and morphogenetic perspective. Special Paper, 1. National Cave and Karst Research Institute, Carlsbad, NM. 106 pp. Klimchouk, A.B., 2009. Principal characteristics of hypogene speleogenesis. In: Stafford, K., Land, L., Veni, G. (Eds.), Advances in Hypogene Karst Studies. Symposium, 1. National Cave and Karst Research Institute, Carlsbad, NM, pp. 1–11.

Kulstad, R. O., Fairchild, P., and McGregor, D. (1956). Gypsum in Kansas: Kansas Geol. Survey. Bull. 113, 110 P.

Lee, W., and Merriam, D. F. (1954b) Cross sections in eastern Kansas: Kansas Geol. Survey, Oil and Gas Inv. 12, p. 1-8.

Lowe, D. and Waltham, T. (2002). Dictionary of karst and caves. British Cave Research Association Cave Studies, 10, 1–40.

Maher, J. C., and Collins, J. B. (1948). Hugoton Embayment of Anadarko Basin in southwestern Kansas, southeastern Colorado, and Oklahoma Panhandle: Am. Assoc. Petroleum Geologists, Bull., v. 32, p. 813-816.

Malone, D. J. (1962) Stratigraphic relations and structural significance of the Blaine Formation in the subsurface of southwestern Kansas: Unpub. M.S. thesis, Univ. Wichita, 72 p.

Maughan, E. K. (1966) Environment of deposition of Permian salt in the Williston and Alliance basins, in Rau, J. L., ed., Second Symposium on Salt: N. Ohio Geol. Soc., Cleveland, Ohio, p. 35-47.

McGregor, D.R., Pendry, E.C., and McGregor, D.L. (1963) Solution caves in gypsum, north-central Texas: Journal of Geology, v. 71, p. 108-115.

McKee, E. D., Oriel, S. S., and others. (1967a). Paleotectonic investigations of the Permian System of the United States: U.S. Geol. Survey, Prof. Paper 515, 271 p.

McKee, E. D., Oriel, S. S., and others. (1967b). Paleotectonic maps of the Permian System: U.S. Geol. Survey, Misc. Geol. Inv. Map I-450.

McLaughlin, T. G. (1942). Geology and ground-water resources of Morton County, Kansas: Kansas Geol. Survey, Bull. 40, p. 1-126.

Merriam, D. F. (1958b). Preliminary regional structural contour map on top of the Stone Corral Formation (Permian) in Kansas: Kansas Geol. Survey, Oil and Gas Inv. 17, map.

Merriam, D. F. (1955). Jurassic rocks in Kansas: Am. Assoc. Petroleum Geologists, Bull., v. 39, p, 31-46.

Merriam, D. F. (1957). Subsurface correlation and stratigraphic relation of rocks of Mesozoic age in Kansas: Kansas Geol. Survey, Oil and Gas Inves. 14, p. 1-25.

Merriam, D. F. (1962b). History of Precambrian studies in Kansas: Kansas Acad. Sci., Trans., v. 65, no. 4, p. 433-447.

Merriam, D. F., and Mann, C. J. (1957). Sinkholes and related geologic features in Kansas: Kansas Acad. Sci., Trans., v. 60, no. 3, p. 207-243.

Merriam, D. F. (1963). Triassic rocks of Kansas: The Compass, v. 40, no. 2, p. 122-127.

Monroe, W. H. (1970). A glossary of karst terminology. Washington: U.S. Gov. Print. Off.

Moore, R. C., and others (1951). The Kansas rock column: Kansas Geol. Survey, Bull. 89, p. 1-132.

Moore, R. C. (1951). The Kansas rock column: Kansas Geol. Survey, Bull. 89, p. 1-132.

Mudge, M.R. (1967). Central Midcontinent region, in McKee, E.D., and Oriel, S.S., eds., Paleotectonic Investigations of the Permian System in the United States: U.S. Geological Survey, Professional Paper 515, p. 97–128.

Myers, A.J., Gibson, A.M., Glass, B.P., and Patrick, C.R. (1969). Guide to Alabaster Cavern and Woodward County, Oklahoma: Oklahoma Geological Survey-Guidebook 15, p. 38.

Nance, H.S. (1988). Interfingering of evaporites and red beds: an example from the Queen/Grayburg Formation, Texas: Sedimentary Geology, v. 56, p. 357–381.

Navas, A. (1990). The Effect of Hydrochemical Factors on the Dissolution Rate of Gypsiferous Rocks in Flowing Water. Earth Surface Processes and Landforms, vol. 15, no. 8, p. 709–715, doi: 10.1002/esp.3290150805.

Norton, G.H. (1939). Permian red beds of Kansas: American Association of Petroleum Geologists, Bulletin, v. 23, p. 1751–1819.

Palmer, A., and Palmer, M.V. (2004). Sulfate-carbonate interactions in the development of karst. Northeastern Geology and Environmental Sciences. 26. p. 93-106.

Palmer, A. (1991). Origin and morphology of limestone caves. Geol Soc Am Bull 103: 1-21. Geological Society of America Bulletin - GEOL SOC AMER BULL. 103. p. 1-21. doi:10.1130/0016.

Palmer, A. N. (2007a).Cave geology. Dayton, OH: Cave Books.

Palmer, Arthur. (2011). Distinction between epigenic and hypogenic caves. Geomorphology. v. 134. p. 9-22. doi:10.1016/j.geomorph.2011.03.014.

Quinlan, J.F., Smith, R.A., & Johnson, K.S. (1986). Gypsum karst and salt karst of the United States of America. In: Atti symposio international sul carsismo nelle evaporiti. Le Grotte d'Italia, 4. XIII.. 73-92.

Rascoe, Bailey, Jr. (1968). Permian System in the western Mid-Continent: The Mountain Geologist, v. 5, p. 127-138.

Rascoe, Bailey, Jr., and Baars, D. L. (1972). The Permian System, in Geologic Atlas of the Rocky Mountain Region: Rocky Mt. Assoc. of Geologists, Denver, Colo., p. 143-165.

Roscher, M., and Schneider, J.W. (2006). Permo-Carboniferous climate: early Pennslyvanian to Late Permian climate development of central Europe in a regional and global context, in Lucas, S.G., Cassinis, G., and Schneider, J.W., eds. Non-Marine Permian Biostratigraphy and Biochronology: Geological Society of London, Special Publication 265, p. 95-136.

Runkle, D.L and Johnson, K.S. (1988). Hydrogeologic study of a gypsum-dolomite karst aquifer in western Oklahoma and adjacent parts of Texas, U.S.A., in Karst

Hydrogeology and Karst Environment Protection, Proceedings of the International Association of Hydrologists 21st Congress, v, 21,p. 400-405.

Sawyer, R.W. (1924). Am. Assoc. Petroleum Geologists Bull., v. 8, no. 3, p. 312-320, map.

Schneider, C. A.; Rasband, W. S. & Eliceiri, K. W. (2012). "NIH Image to ImageJ: 25 years of image analysis", Nature methods 9(7): 671-675, PMID 22930834 (on Google Scholar).

Schumaker, R. D. (1966). Regional study of Kansas Permian evaporite formations: Unpub. M.S. thesis, Wichita State Univ., 87 p.

Strong, R.M. (1960). Subsurface Geology of Barber County, Kansas: Unpub. M.S. thesis, Kansas State University.

Sweet, A.C., Soreghan, G.S., Sweet, D.E., Soreghan, M.J., and Madden, A.S. (2013) .Permian dust in Oklahoma: source and origin for Middle Permian (Flowerpot–Blaine) red beds in western tropical Pangaea: Sedimentary Geology, v. 284–285, p. 181–196.

Swineford, A., (1955). Petrography of Upper Permian rocks in south-central Kansas: Kansas Geol. Survey, Bull., 111, 179 p.

Tomlinson, C.W. (1916). The origin of red beds: a study of the conditions of origin of the Permo-Carboniferous and Triassic red beds of the western United States: Journal of Geology, v. 24, p. 28–253.

Turner, P. (1980). Continental Red Beds: New York, Elsevier, Developments in Sedimentology 29, 562 p.

Plas, L. V., and Tobi, A. C. (1965). A chart for judging the reliability of point counting results. American Journal of Science, 263(1), 87-90. doi:10.2475/ajs.263.1.87.

Walker, T.R. (1967). Formation of red beds in modern and ancient deserts: Geological Society of America, Bulletin, v. 78, p. 353–368.

Weary, D.J., and Doctor, D.H. (2014) Karst in the United States: A digital map compilation and database: U.S. Geological Survey Open-File Report 2014–1156, 23 p., https://dx.doi.org/10.3133/ofr20141156.

White, W.B. (1988). Geomorphology and Hydrology of Karst Terrains, New York, Oxford University Press, p. 464.

Young, J., and Beard, J. (1993). Caves in Kansas, Kansas Geological Survey, Educational Series 9.

Zharkov, M.A., and Chumakov, N.M. (2001). Paleogeography and sedimentation settings during Permian–Triassic reorganizations in biosphere: Stratigraphy and Geological Correlation, v. 9, p. 340–363.

TABLES

Table 1. Cave dimensions.

Cave Name	Elevation (ft)	Total Length (ft)	Area (ft^2)	Volume (ft^3)
Acorn	1811.02	106	1546.37	2,584.30
Birthday	1801.18	50	722.129	421.3
Clover	1847.11	43	319	1,665.20
Colossus	1847.11	1232	3620.81	3456.7
Connection	1860	56	166	225.7
Dead Tree	1866.8	40	428.92	71.5
Dugout	1860.24	82	816.03	2,965.60
Four by Four	1866.8	45	102.283	98
Gary's Tube	1840.55	32	127	138.8
Goose	1817.59	46	176.474	426.7
Misery Pit	1891	55	202	979.8
Monkey	1824.15	132	2238.94	3755.9
Mountain Lion	1860	83	2694	1014.2
Rocky Road	1924	17	37	152.2
Second Opportunity	1879.92	100	1296	5,566.30
Vole	1922.57	946	1051.08	1466

Table 2. Cave Biota.

Cave	**Biota**
Second Opportunity	Little Brown Myotis
Acorn	Little Brown Myotis
Colossus	Camel Cricket, Funnelweb Spider, Townsend's Big-eared bat
Misery Pit	Funnel Spider, Tarantula Hawk, Camel Cricket
Mountain Lion	Coyote, Yellow Garden Spider, Funnelweb Spider
Monkey	Camel Cricket, Little Brown Myotis, Porcupine
Dugout	Barred Tiger Salamander
Vole	Little Brown Myotis, Striped skunk, Plains Pocket Mouse, Plains harvest mouse, Tarantula

Table 3. Cave classification.

Cave Name	Dominant Features	Cross-sectional View	Other Features	Morphologies
Acorn	Phreatic with vadose entrenchment overprinting	Elliptical	Perennial Stream	Ceiling fractures, proto-conduit, perennial stream
Birthday	Incised meander cave	Elliptical	Soda Straw	Ceiling fractures/Upper passage, gypsum breakdown blocks/ceiling collapse
Clover	Through cave	Square	Soda Straw	Ceiling fracture, gypsum breakdown blocks/ ceiling collapse
Colossus	Through cave	Square	Sinkhole	Joint set intersection with dissolution along
Connection	Phreatic tube	Tube	Sinkhole	Tube-shaped passage
Dead tree	Incised Meander cave	Square	Spring	Ceiling fracture, gypsum breakdown blocks/ ceiling collapse
Dugout	Phreatic with vadose entrenchment overprinting	Square	Perennial Stream	Ceiling fracture, gypsum breakdown blocks/ ceiling collapse
Four-by-four	Phreatic tube	Tube	Sinkhole	Ceiling fracture, tube-shaped passage
Garys	Collapsed reroute	Tube	Sinkhole	Tube-shaped passage
Goose	Meander bypass	Tube	Spring	Tube-shaped passage
Misery Pit	Phreatic tube	Tube to Bell-shape	Sinkhole Vadose Shaft	Tube-shaped passage
Monkey	Phreatic with vadose entrenchment overprinting	Tube to Keyhole	Perennial Stream	Ceiling fractures/ intersecting joint sets, proto-conduit
Mountain Lion	Phreatic with vadose entrenchment overprinting	Bell-shape	Sinkhole Vadose Shaft	Ceiling fracture/ intersecting joint sets, proto-conduit
Rocky Road	Phreatic tube	Tube	Sinkhole	Tube-shaped passage
Second Opportunity	Phreatic with vadose entrenchment overprinting	Square	Sinkhole Perennial Stream	Ceiling fracture/intersecting joint sets
Vole	Through cave/Phreatic with vadose entrenchment overprinting	Keyhole to Square	Sinkhole	Ceiling fracture/ proto-conduit

APPENDIX A

DESCRIPTIONS OF THE CAVES OF BARBER COUNTY, KANSAS

Acorn Cave

The cave is located near the top of a canyon. There are three cave entrances, two nearest the main passage, and one entrance in an upper passage. This upper passage is accessible along a fracture that extends vertically. The fracture runs approximately N30ºE. A small stream runs from the back of the cave wall towards the main entrance.

Birthday Cave

This cave is located near the top of a canyon with a possible sinkhole nearest the eastern entrance. The drip line is very long (approximately 50 feet) with a large breakdown block (approximately 20 feet long) near the drip line. This breakdown block represents ceiling collapse. This cave is through the Medicine Lodge Gypsum, carbonate layer, and Flowerpot Shale. The perimeter is lined with a sediment bank that progrades from the ceiling. The sediment mound is composed of large selenite blocks (up to 6 inches) and red-brown shale. A large fracture is visible in the ceiling. Soda straws (less than one inch long) are found along the fracture.

Clover Cave

This cave is a “through cave” with a small stream running from the northeast to the southwest. Water seeps through the geologic contact between the carbonate and Flowerpot Shale. Sediment banks are composed of selenite blocks, satin spar gypsum, and red-brown shale. There are two fractures in the cave that intersect. A large

breakdown block that is composed of the Medicine Lodge Gypsum and the carbonate layer is located at this intersection, representing a ceiling collapse. Soda straws (less than one inch long) are found along the ceiling nearest the eastern entrance.

Colossus Cave

This cave is the largest "through cave" found on Property One. The western entrance includes a large ceiling block (~ 20 feet wide and ~40 feet long) that had collapsed, leaving a short (~ one foot tall) and wide (~20 feet) entrance. The collapsed ceiling block extends into the cave creating a three foot ceiling height. The ceiling height increases to six feet beyond the collapsed ceiling block. The passage morphology is rectangular in shape, and the ceiling is composed of carbonate and the cave wall is composed of the Flowerpot Shale. Sediment banks line the back wall and are composed of satin spar gypsum, selenite blocks, and shale.

Ceiling fractures trend N70E and N86W. Ceiling fractures that intersect extend vertically to other passages; however, whole ceiling blocks have since collapsed. Surface runoff flows into the cave through a solutionally enlarged joint set as evidence by scallop features. A standing pool of water is also found near the joint.

Connection Cave

The cave entrance is found in a large sinkhole complex. Passage morphology is tube-shaped and is formed within the Medicine Lodge Gypsum. The cave is choked with sediment.

Dead Tree Cave

The cave entrance is found in the bottom of a canyon with an insurgence near the entrance (~5 feet away). The dripline is very long (~30 feet) with a large breakdown boulder (>5 feet) blocking the entrance. The cave ceiling is composed of the Medicine Lodge Gypsum, the resistant carbonate ledge protrudes out of the ceiling, and the Flowerpot Shale forms the cave wall. A sediment bank near the cave entrance is composed of satin spar gypsum blocks, selenite gypsum, and Flowerpot Shale. The cave ceiling includes a joint set with one solutionally enlarged joint that is wide enough to view the surface.

Dug out Cave

The cave entrance is located nearest the top of a large canyon. The first cave room, nearest the entrance (< 10 feet in), was initially choked with sediment and breakdown blocks, but was cleared to reveal a larger cave room. Solutionally enlarged joint sets that intersect extend vertically up to 14 feet. The cave is formed in the Medicine Lodge Gypsum, carbonate layer, and the Flowerpot Shale. Sediment banks are common and are composed of selenite gypsum, satin spar gypsum blocks, and fragments of Flowerpot Shale. A small stream flows from the back of the cave towards the entrance. This stream flows from a fracture in the Medicine Lodge Gypsum and carbonate layer and has gouged out a “stair-step” pattern in the Flowerpot Shale. A standing pool of water is found where the stream empties from the fracture.

Four-by-Four Cave

This cave is located in a fracture in the Medicine Lodge Gypsum Member and is associated with a sinkhole. The passages are spherical in shape and defined as a phreatic tube. There is a pool of standing water nearest the back of the cave. The passage continues toward the east and is too tight to survey.

Gary's Cave

The cave entrance is found at the top of a canyon, in a sinkhole. This cave is a phreatic tube that is through the Medicine Lodge Gypsum, carbonate layer, and Flowerpot Shale. The cave is choked with soil with no noticeable wind direction.

Goose Cave

The cave entrance is found near the bottom of a canyon nearest a resurgence spring. The entrance includes a joint that extends toward the top wall of the canyon. The ceiling of the cave is composed of the Medicine Lodge Gypsum and the carbonate layer. The cave wall is composed of the Flowerpot Shale.

Misery Pit

A large sinkhole complex atop the valley floor reveals multiple caves. This cave entrance is found in one of these sinkholes. The cave is spherical in shape and is composed mainly of the Medicine Lodge Gypsum, carbonate layer, and the Flowerpot Shale. A ceiling fracture in the Medicine Lodge Gypsum runs nearly parallel with the cave passage. A 15 foot deep shaft is located in the center of the cave with a diameter of approximately 10

feet. The cave continues in the direction of the fracture and becomes sediment choked with no noticeable wind direction.

Monkey Cave

The cave entrance is located near the top of a canyon wall and is associated with an insurgence. The insurgence is located on the stream bed and includes a standing pool of water that is fed by storm water exiting the cave. Rills can be observed in the sediment below the cave entrance. The ceiling of the cave is composed of the Medicine Lodge Gypsum and the carbonate layer, and the cave walls are composed of the Flowerpot Shale. A ceiling fracture differentiates two ceiling heights in the cave, where the one-foot tall ceiling height passage dog-legs to the northwest. A standing pool of water is found nearest the back of the cave where a joint set intersects in the ceiling. The standing pool of water is associated with a small stream that flows toward the cave entrance. This stream likely flows toward the entrance of the cave during storm events as evidenced by the slack water marks in sediment banks near the cave floor. There is a large sinkhole complex just northwest from cave entrance.

Mountain Lion Cave

The cave entrance is found in a sinkhole complex that is associated with rocky road cave, connection cave, and misery pit cave. The ceiling of the cave is composed of the Medicine Lodge Gypsum and the carbonate layer. The ceiling is slightly bell shaped with the carbonate layer protruding out into the passage. Scallops are found in the Medicine Lodge Gypsum indicating storm water flowing towards the sinkhole complex (to the southwest). The cave walls are composed of the Flowerpot Shale. The cave ceiling height

averages two feet and contains a fracture. A vadose shaft is found near the center of the cave and curves northwest to northeast. Scallops are found in the shaft, indicating surface water flow. Vocal connection for the shaft was established with a nearby vadose shaft located on the valley floor near the sinkhole complex. The cave become sediment choked by a sediment bank, but opens to a three foot high passage. This passage becomes very narrow and continues down the dip of the Flowerpot Shale. Wind direction indicates the passage likely continues.

Rocky Road Cave

This cave is also associated with Connection cave, Misery Pit cave, and Mountain Lion cave in the sinkhole complex. The cave entrance is found in the walls of the sinkhole in the Medicine Lodge Gypsum, and the cave passages are tube-shaped. The cave becomes choked with sediment with no noticeable wind direction.

Second Opportunity Cave

There are multiple cave entrances near the base of a sinkhole. The cave ceiling is flat and is composed of the Medicine Lodge Gypsum, and the carbonate layer. The cave walls are composed of the Flowerpot Shale. A stream runs from the back of the cave and flows near the perimeter of the cave toward the northwest entrance. The stream has down cut the Flowerpot Shale forming a V-shaped cave floor. Water seeps through the geologic contact between the carbonate layer and Flowerpot Shale. A solutionally enlarged fracture near the back of the cave extends vertically for eight feet. A small passage extends beyond the fracture and sunlight is visible.

Vole Cave

This cave is a through cave where the cave entrance is located near the top of a canyon wall, and the exit located in a sinkhole. The ceiling of the cave is composed of the Medicine Lodge Gypsum and is tube shaped. The more resistant carbonate layer protrudes out into the cave passage. A notch is formed below the carbonate layer and the friable Flowerpot Shale. The cave walls are composed of the Flowerpot Shale. The overall passage shape is rectangular. Ceiling fractures are observed in the Medicine Lodge Gypsum and might influence passage direction.

APPENDIX B

MAPS OF THE CAVES OF BARBER COUNTY, KANSAS

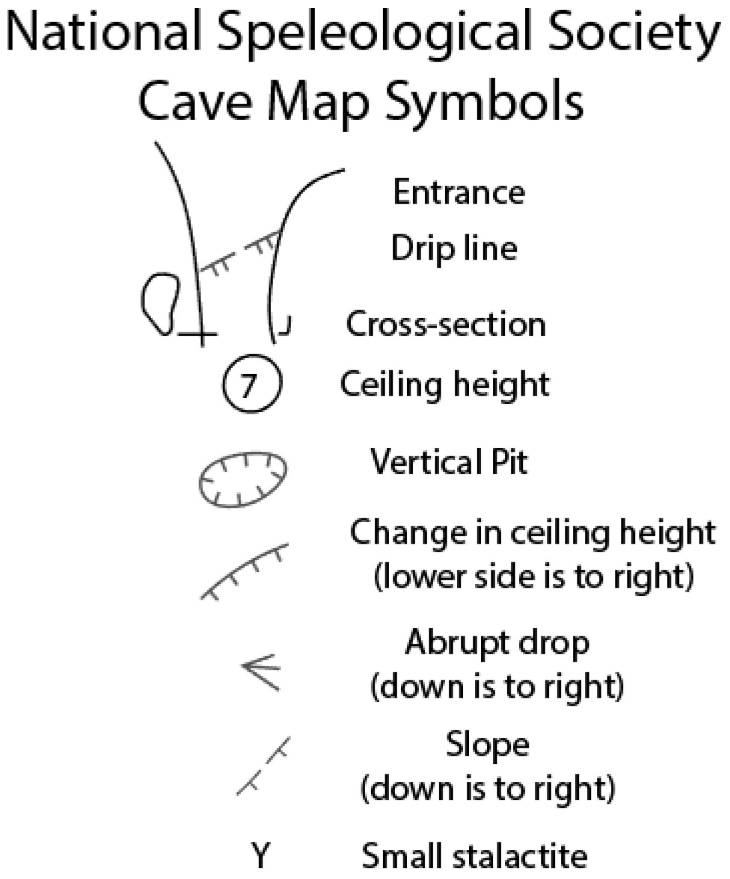

Cave Map Symbol Explanation (modified from Dasher, 1994).

Acorn Cave
Property One

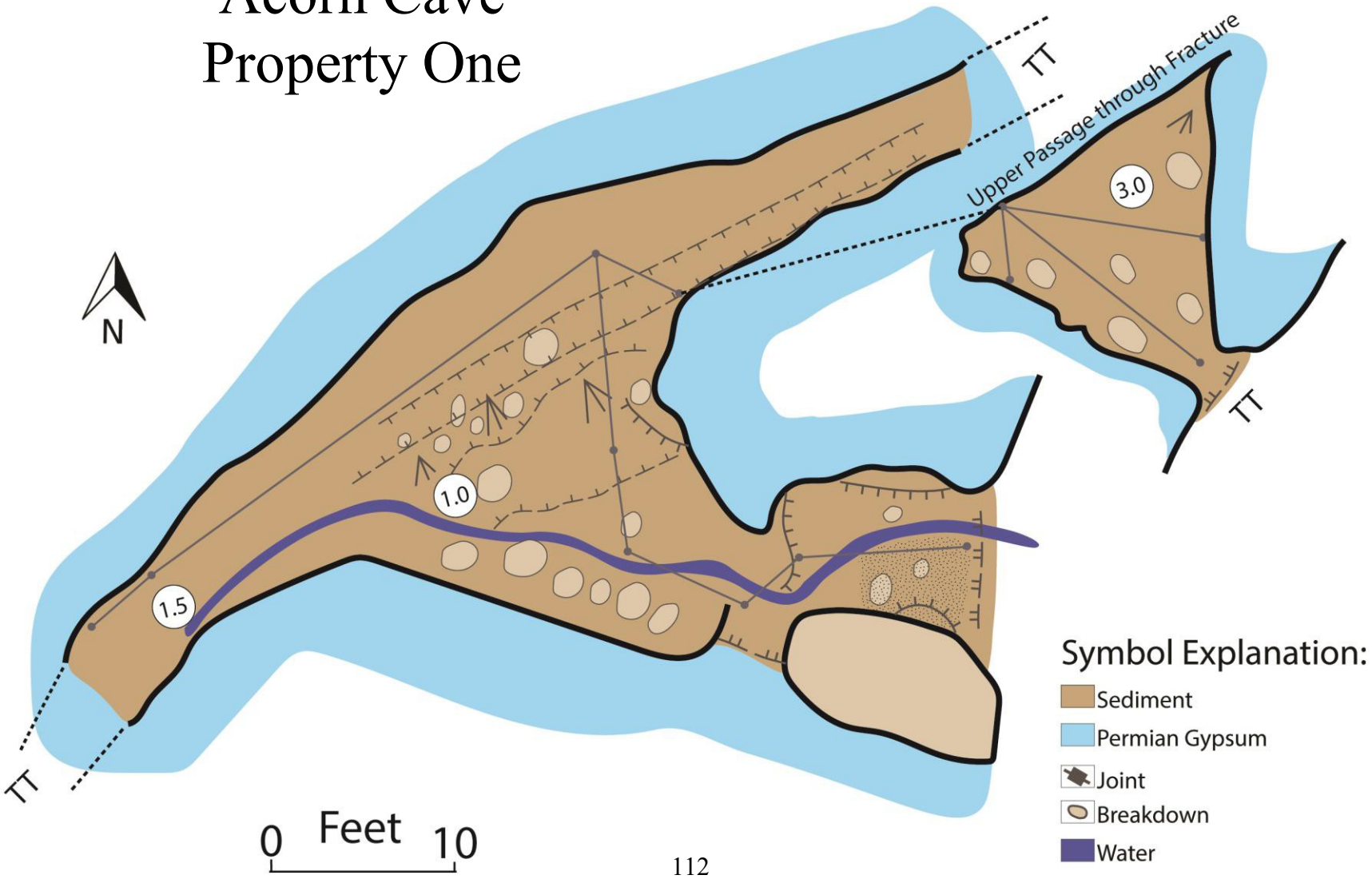

Birthday Cave
Property One

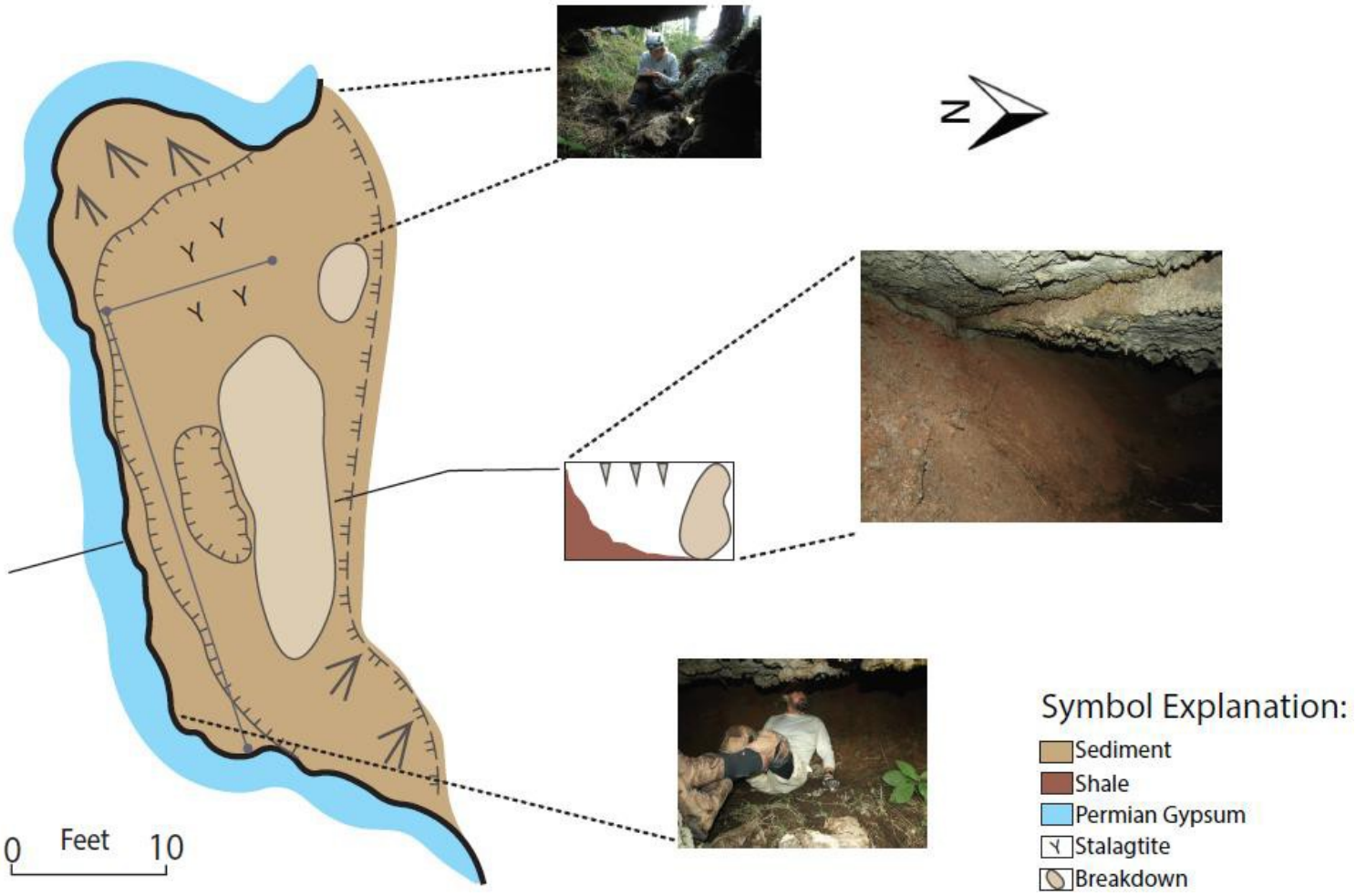

Clover Cave
Property One

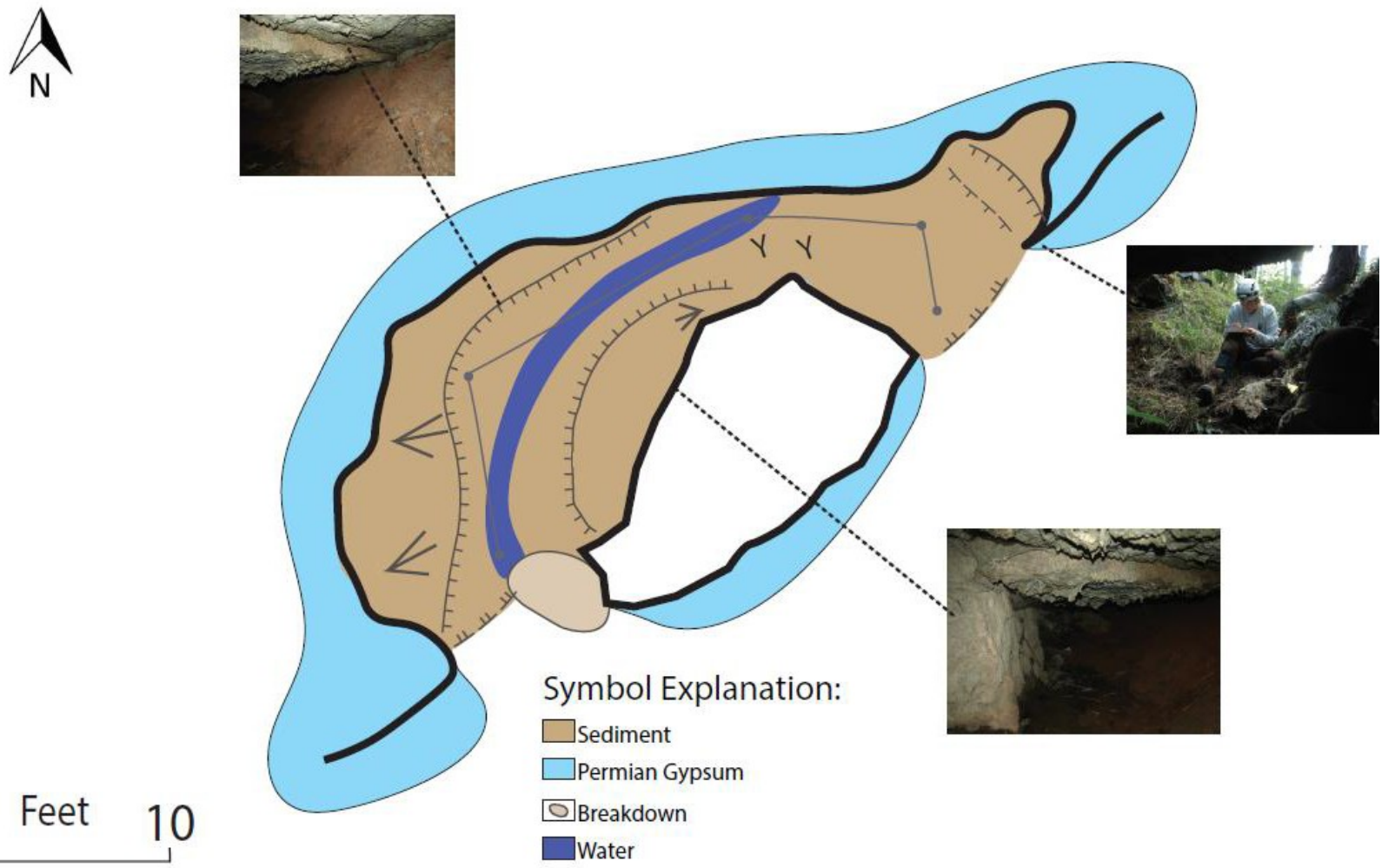

Colossus Cave
Property One

Connection Cave
Property One

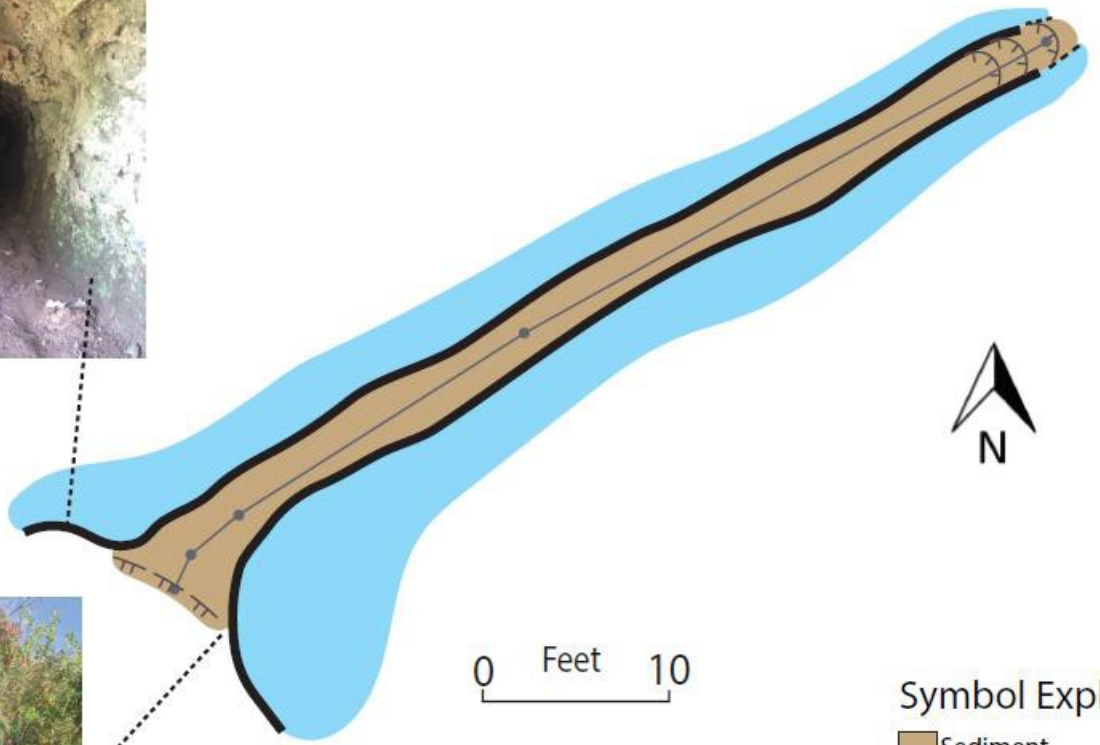

Symbol Explanation:

Sediment

Permian Gypsum

Dead Tree Cave

Dead Tree Cave

Property One

Area One

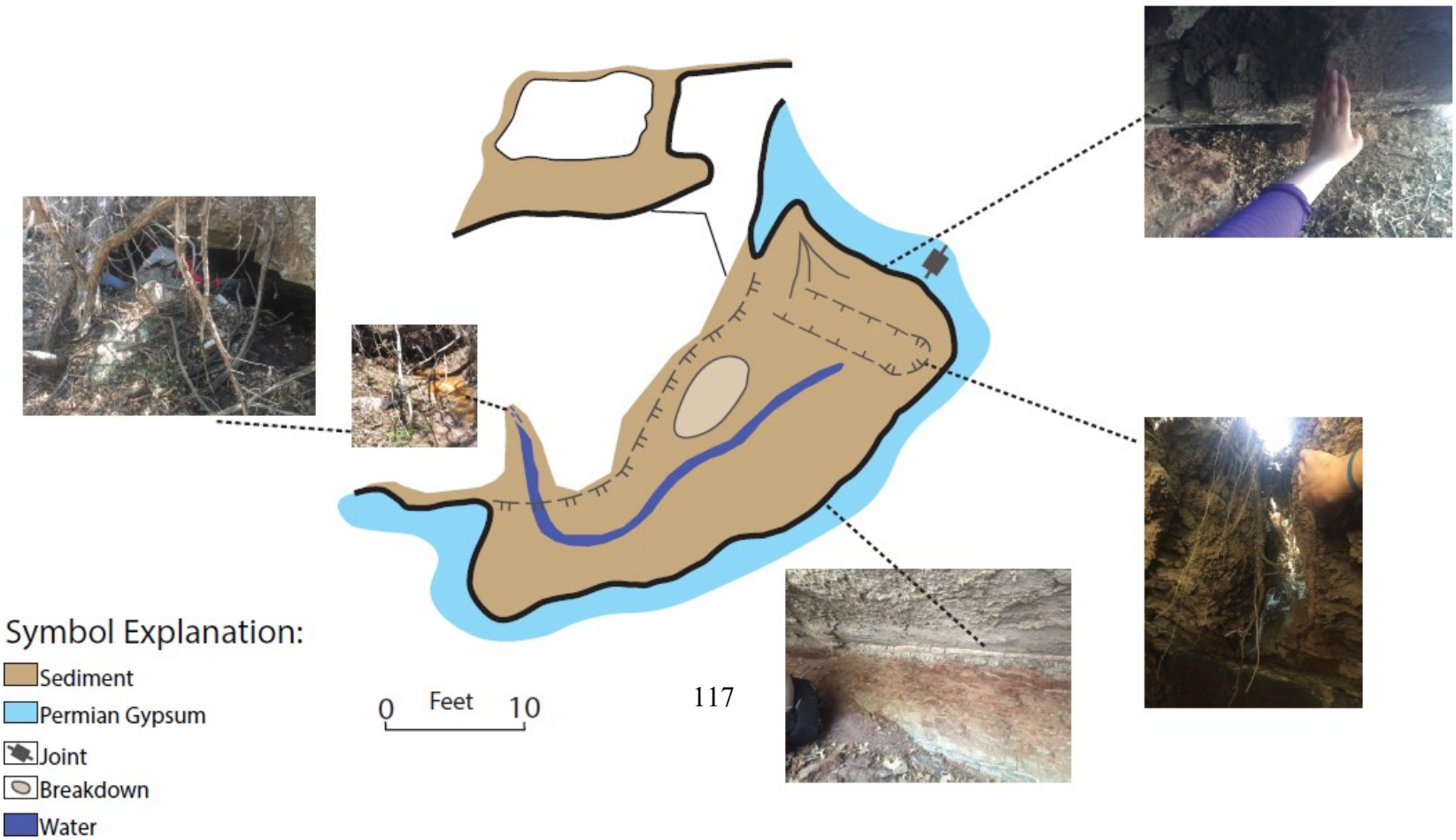

Dugout Cave
Property One

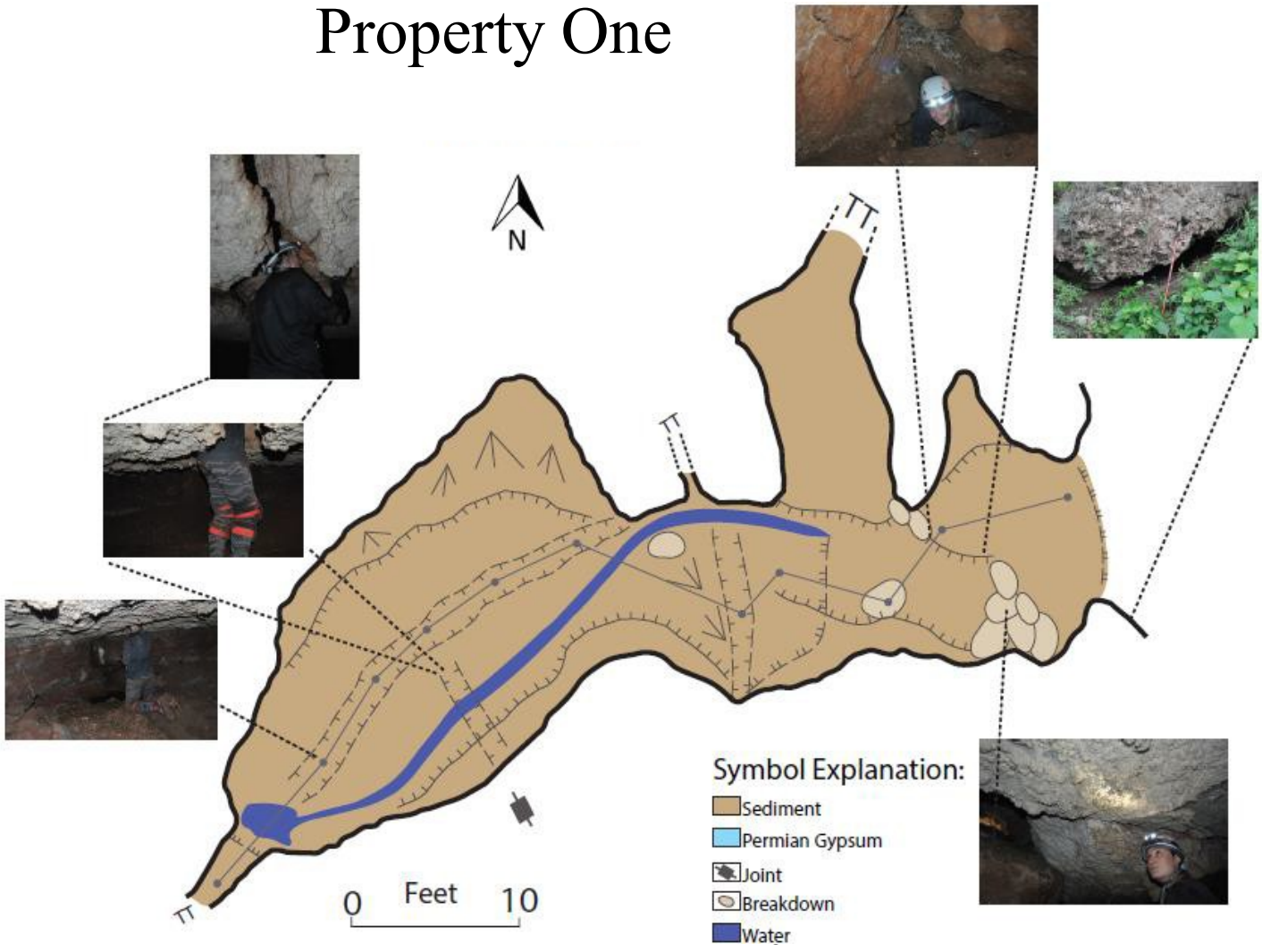

Four-by-four Cave

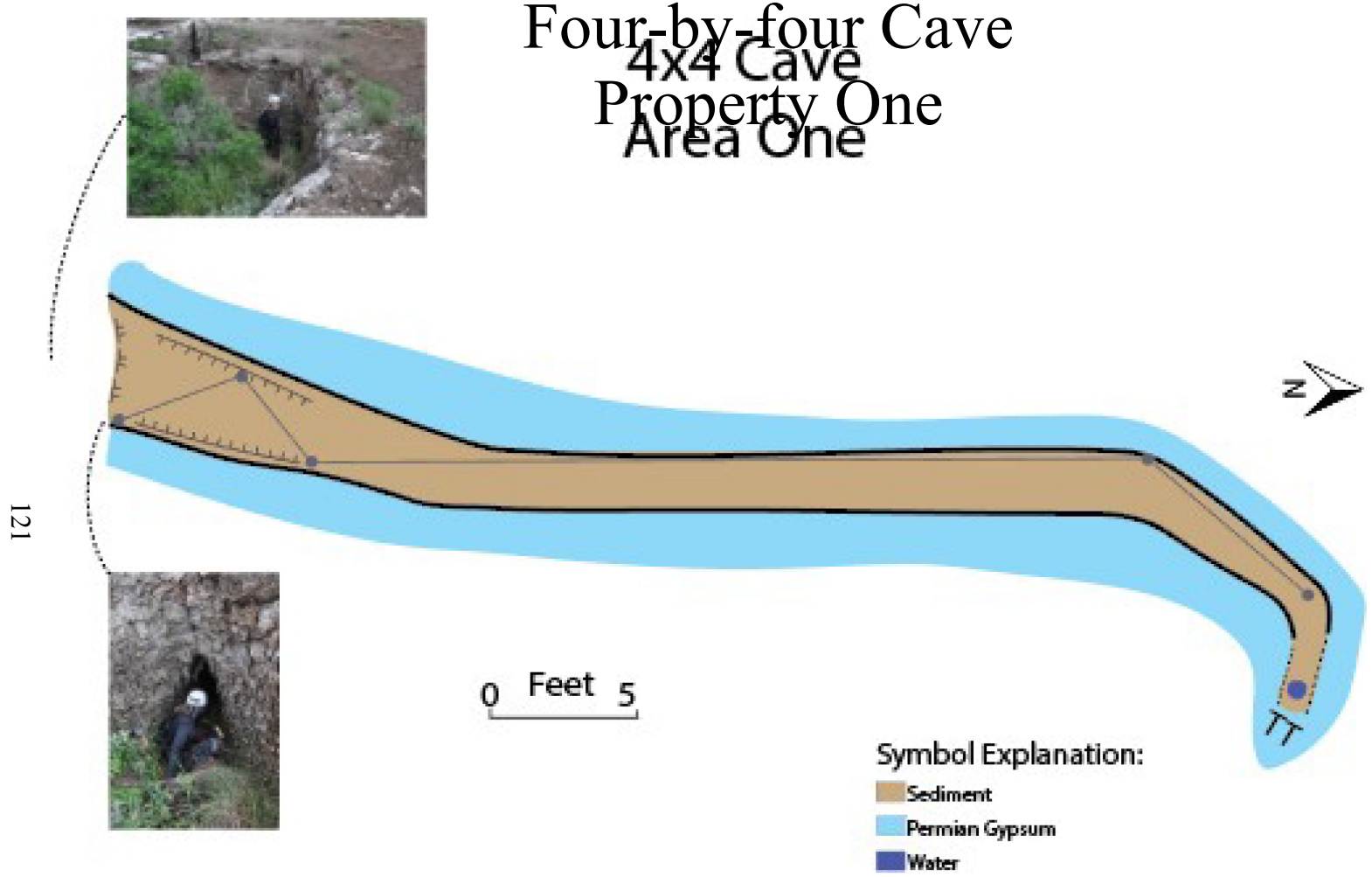

121

Gary's Cave
Property One

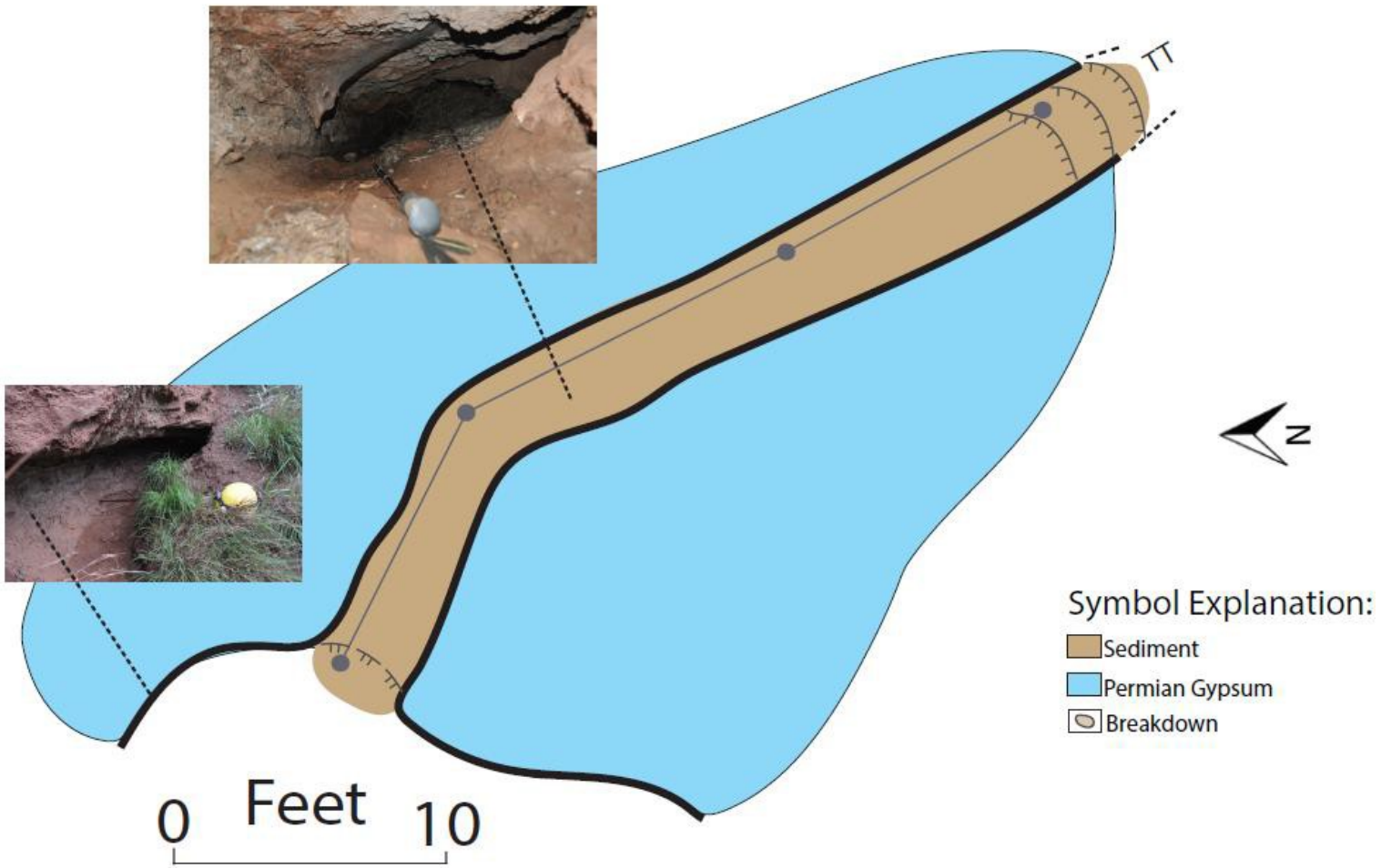

Goose Cave
Property One

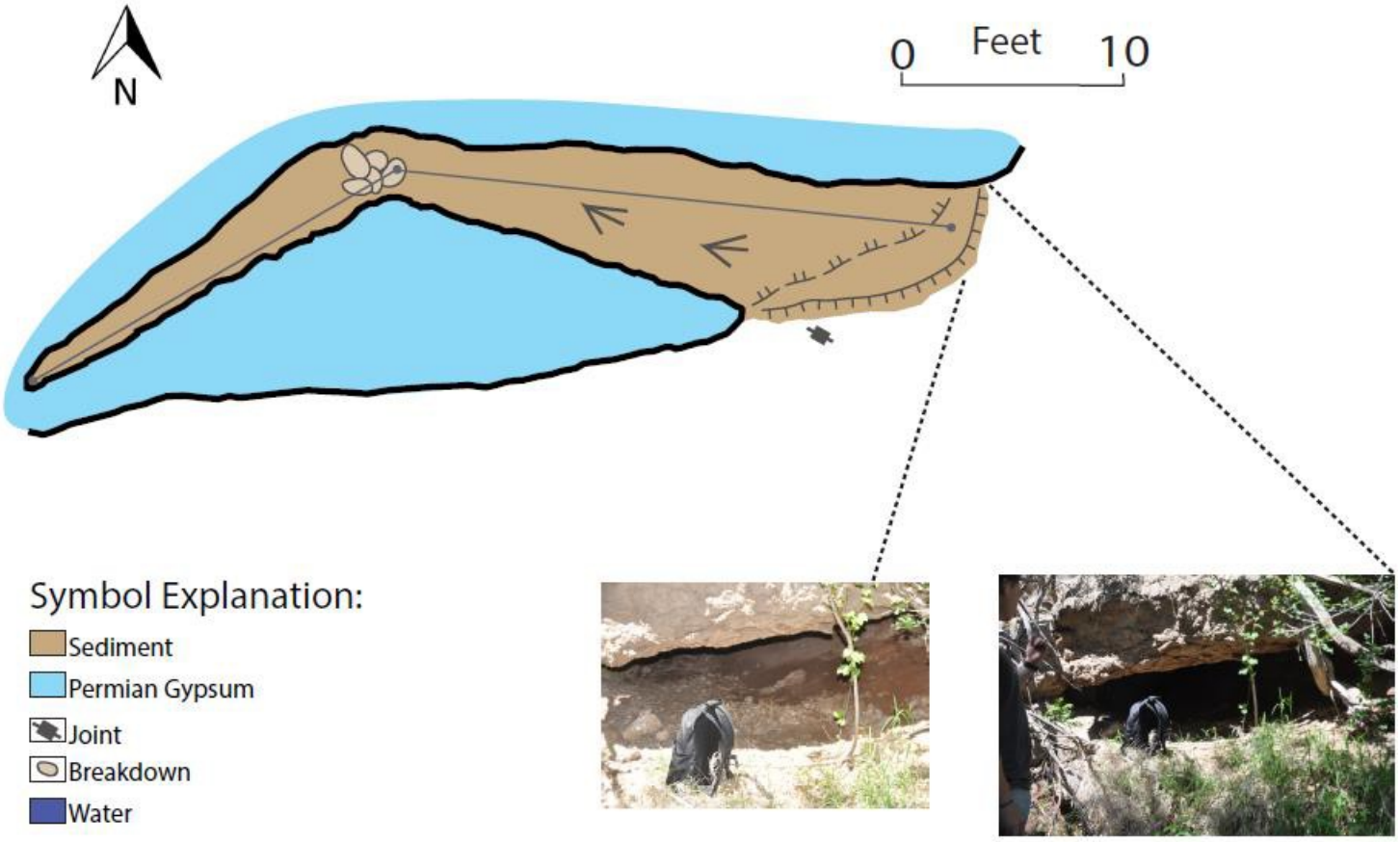

Misery Pit Cave
Property One

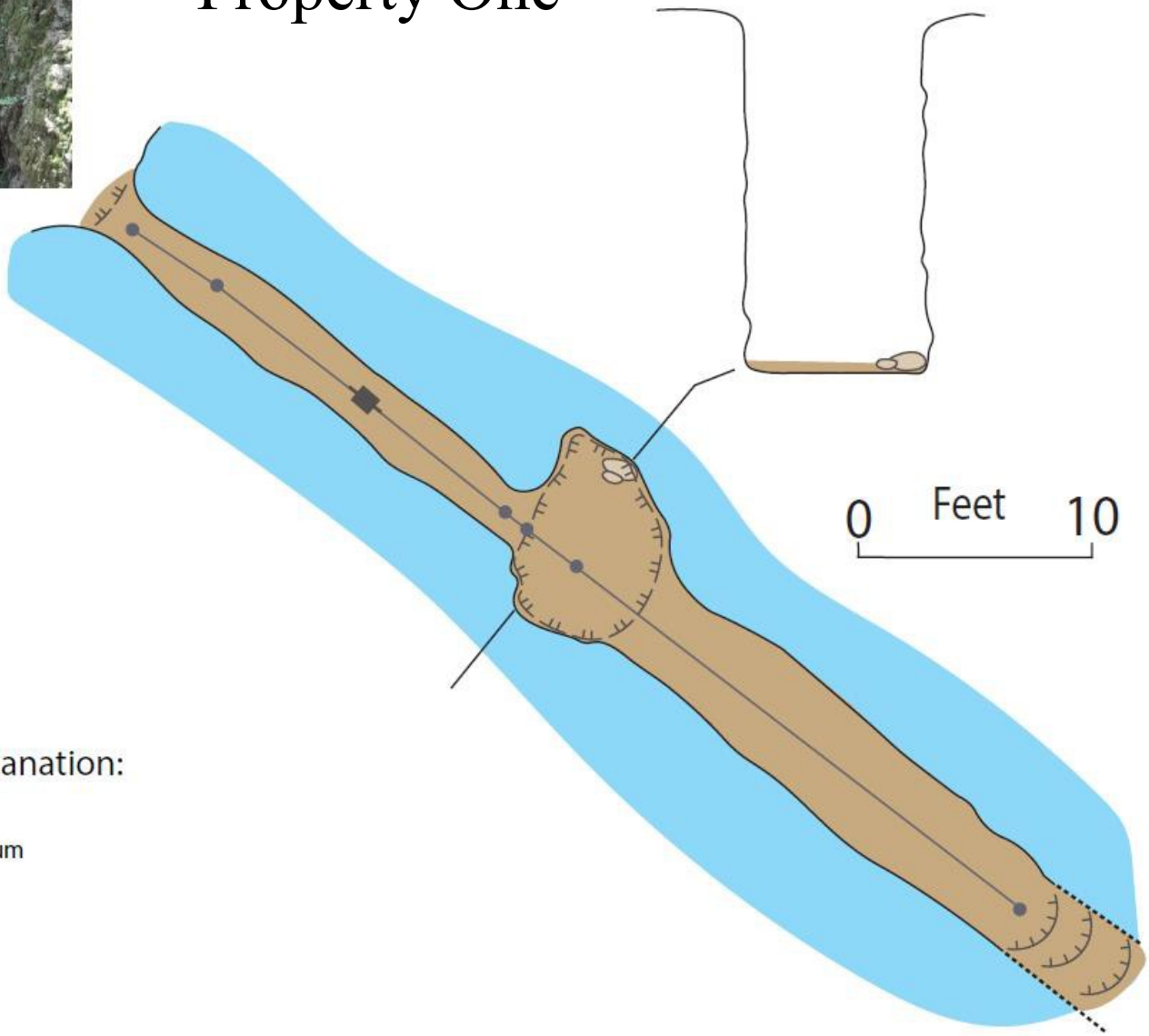

Monkey Cave
Property One

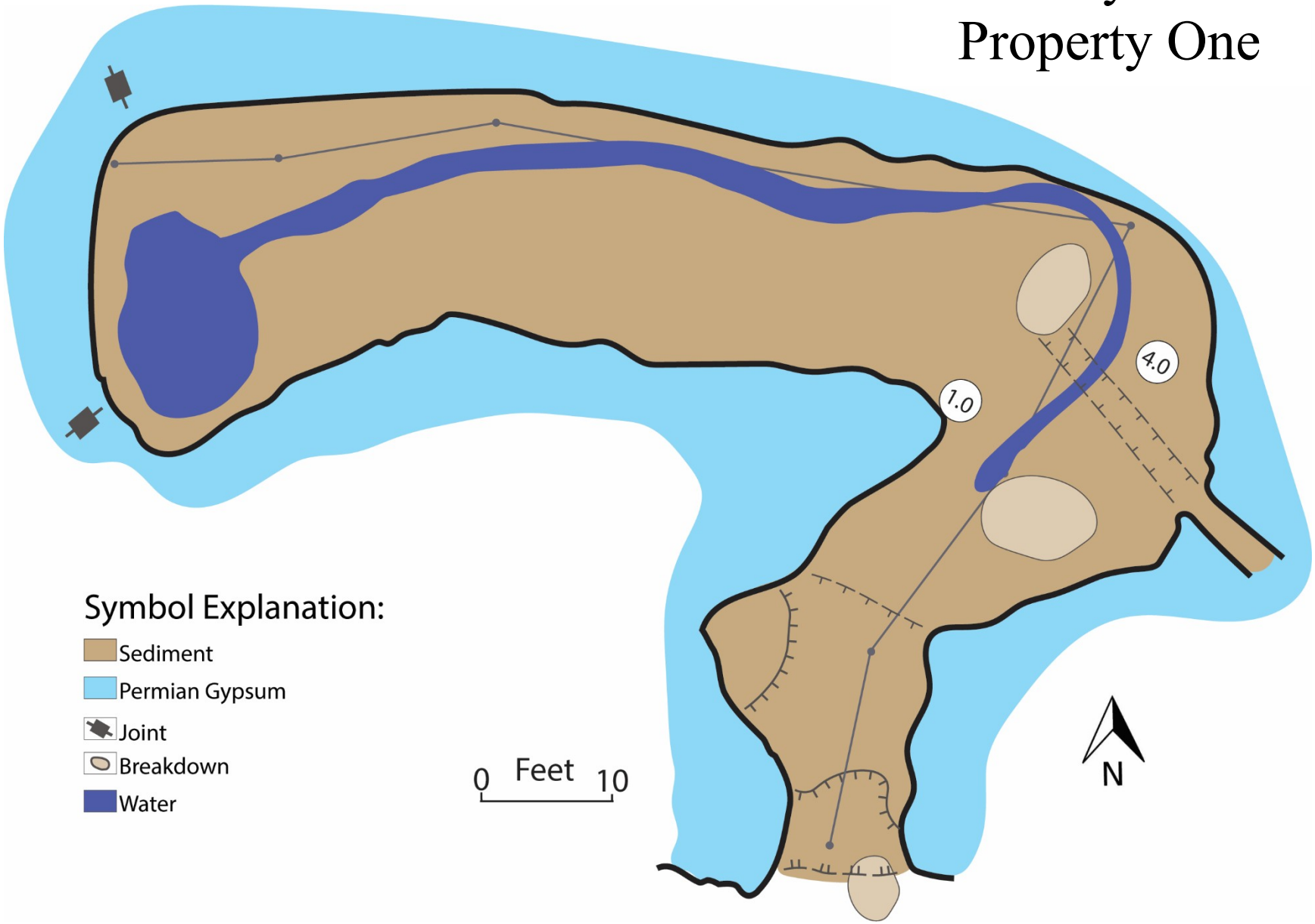

Mountain Lion Cave
Property One

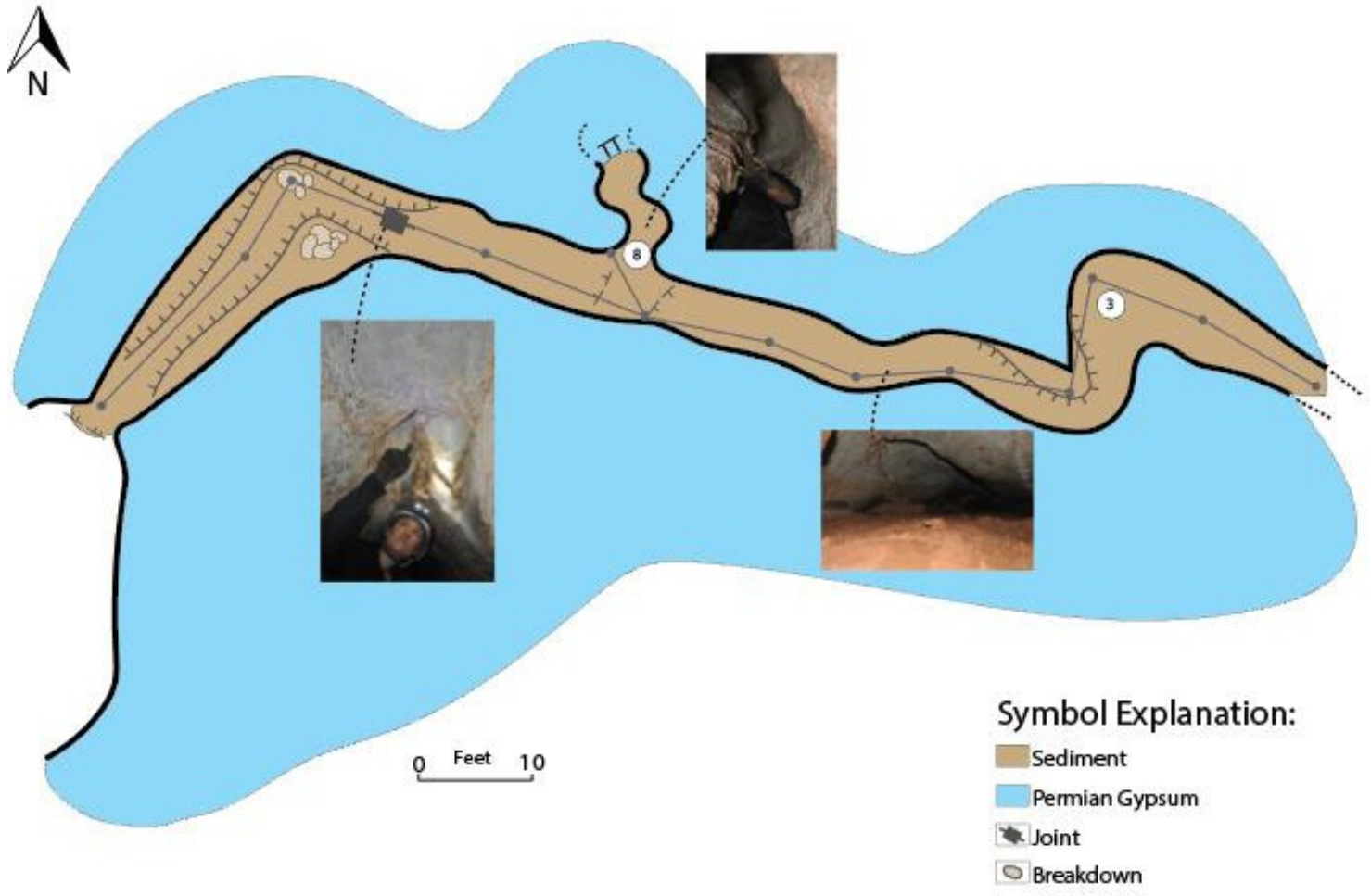

Rocky Road Cave
Property One

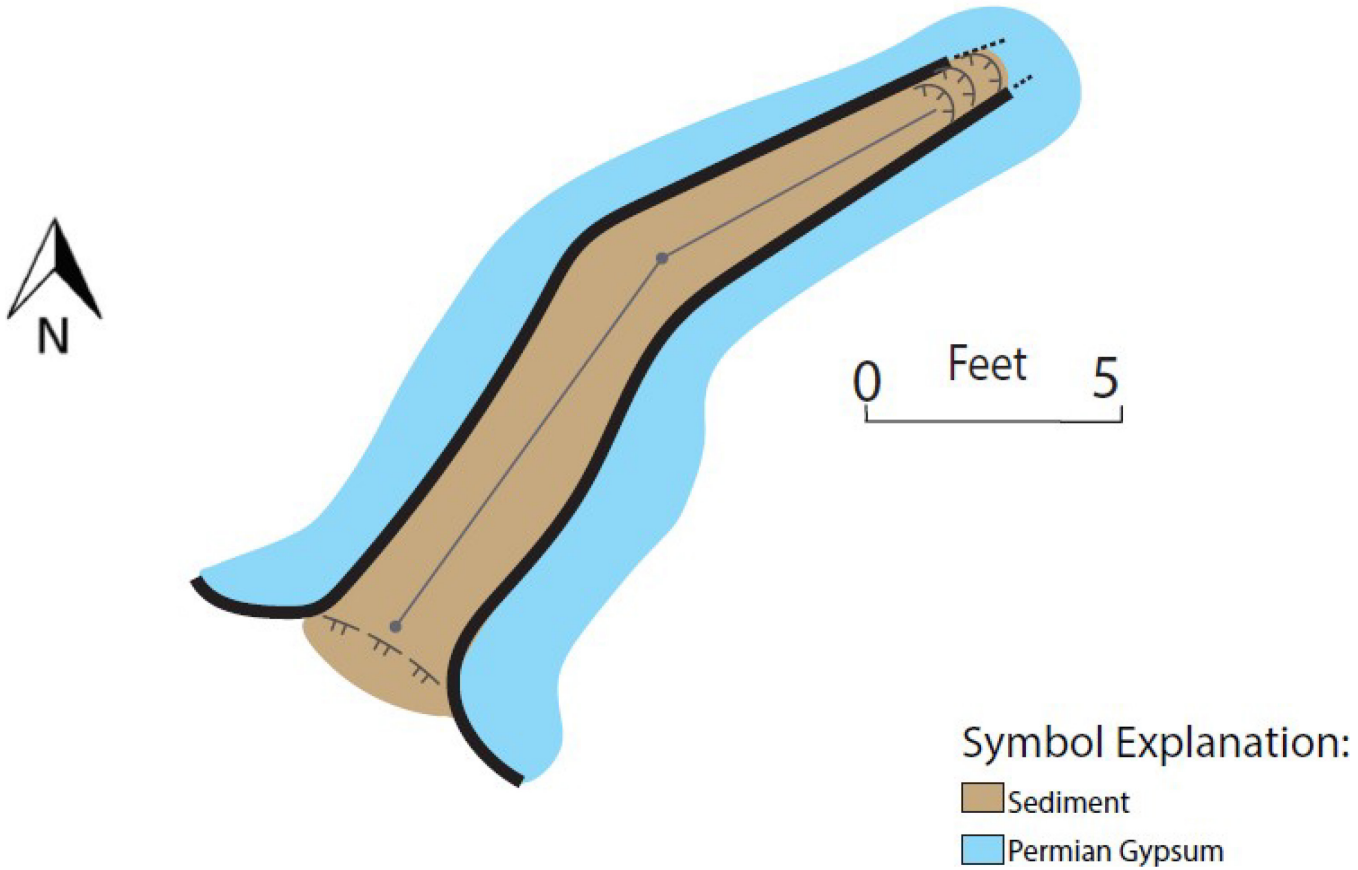

Second Opportunity Cave
Property One

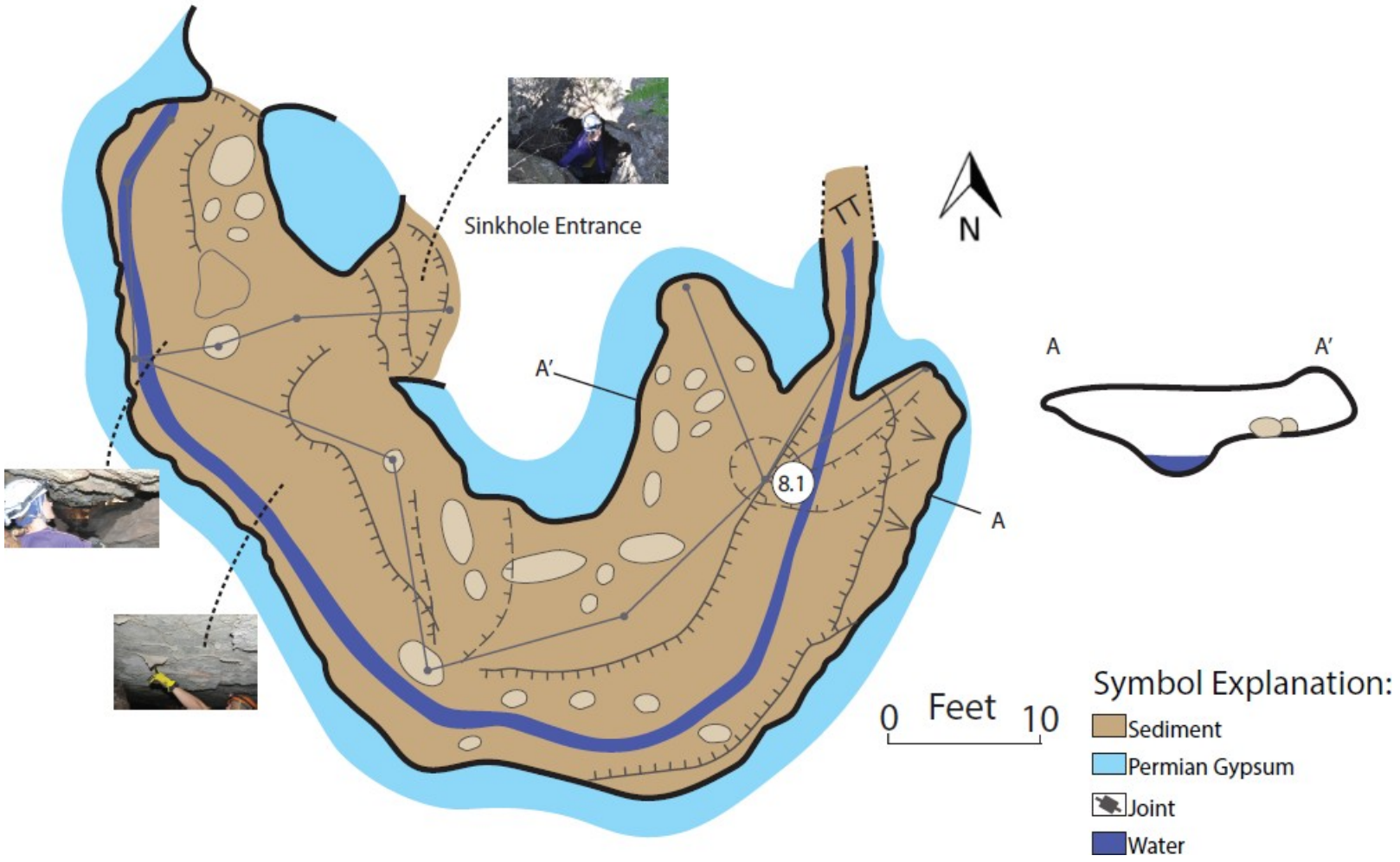

Vole Cave
Property One

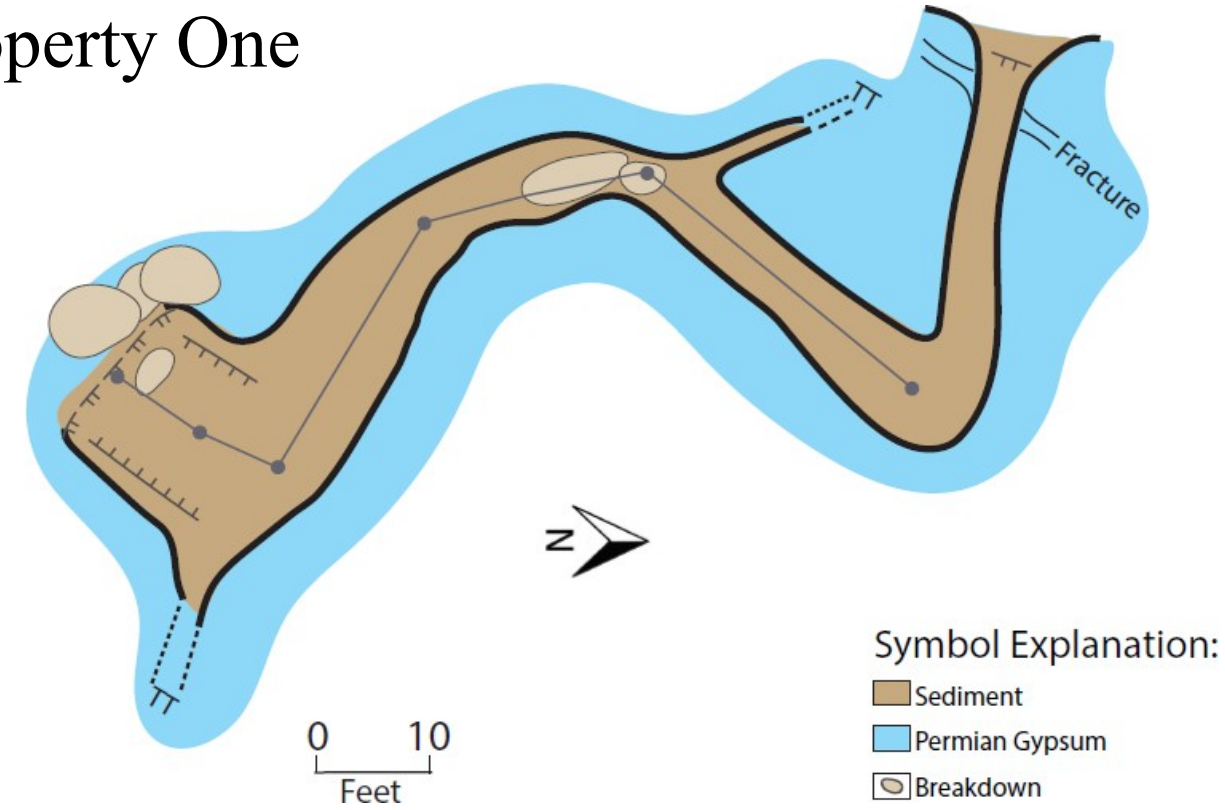

APPENDIX C

KARST FEATURES OF BARBER COUNTY, KANSAS

Feature		Property
1	Spring	1
2	Spring	1
3	Spring	1
4	Spring	1
5	Spring	1
6	Spring	1
7	Spring	1
8	Spring	1
9	Spring	1
10	Spring	1
11	Spring	1
12	Spring	1
13	Sink	1
14	Sink	1
15	Sink	1
16	Sink	1
17	Sink	1
18	First Cave	1
19	Acorn Cave	1

20	Second Opportunity	1
21	Monkey Cave	1
22	Fracture Cave	1
23	Goose Cave	1
24	Dead Tree Cave	1
25	Potential Cave	1
26	Sinkhole Cave	1
27	Garys Cave	1
28	Birthday Cave	1
29	Four-by-four Cave	1
30	Dugout Cave	1
31	Clover Cave	1
32	Mountain Lion Cave	1
33	Scaredy Cave	1
34	Vole Cave	1
35	Colossus Cave	1
36	Bone Cave	2
37	Rocky Road Cave	1
38	Connection Cave	1
39	Misery Pit	1
40	Sinkhole	2
41	Sinkhole	2

64	Vadose Shaft	1
65	Sinkhole	2
66	Microkarst	1
67	Microkarst	1
68	Microkarst	1
69	Microkarst	1
71	Microkarst	1
72	Microkarst	1
73	Microkarst	1
74	Microkarst	1
75	Meander Cave	1
76	Bypass Cave	1
77	Two-spring Cave	1
78	Collapse Cave	1
79	Collapse Cave	1
80	Collapse Cave	1

Fort Hays State University
FHSU Scholars Repository
Non-Exclusive License Author Agreement

I hereby grant Fort Hays State University an irrevocable, non-exclusive, perpetual license to include my thesis ("the Thesis") in *FHSU Scholars Repository,* FHSU's institutional repository ("the Repository").

I hold the copyright to this document and agree to permit this document to be posted in the Repository, and made available to the public in any format in perpetuity.

I warrant that the posting of the Thesis does not infringe any copyright, nor violate any proprietary rights, nor contains any libelous matter, nor invade the privacy of any person or third party, nor otherwise violate FHSU Scholars Repository policies.

I agree that Fort Hays State University may translate the Thesis to any medium or format for the purpose of preservation and access. In addition, I agree that Fort Hays State University may keep more than one copy of the Thesis for purposes of security, back-up, and preservation.

I agree that authorized readers of the Thesis have the right to use the Thesis for non-commercial, academic purposes, as defined by the "fair use" doctrine of U.S. copyright law, so long as all attributions and copyright statements are retained.

To the fullest extent permitted by law, both during and after the term of this Agreement, I agree to indemnify, defend, and hold harmless Fort Hays State University and its directors, officers, faculty, employees, affiliates, and agents, past or present, against all losses, claims, demands, actions, causes of action, suits, liabilities, damages, expenses, fees and costs (including but not limited to reasonable attorney's fees) arising out of or relating to any actual or alleged misrepresentation or breach of any warranty contained in this Agreement, or any infringement of the Thesis on any third party's patent, trademark, copyright or trade secret.

I understand that once deposited in the Repository, the Thesis may not be removed.

Thesis: Gypsum karst speleogenesis of southcentral Kansas of the Permian Blaine Formation

Author: Kaitlyn Gauvey

Signature: Kaitlyn Gs

Date: 5/13/2019